STUDY OF RAREFIED GAS FLOWS
BY THE DISCRETE ORDINATE METHOD

A THESIS

Presented to

The Faculty of the Graduate Division

by

Don Peyton Giddens

In Partial Fulfillment

of the Requirements for the Degree

Doctor of Philosophy

in the School of Aerospace Engineering

Georgia Institute of Technology

July, 1966

STUDY OF RAREFIED GAS FLOWS

BY THE DISCRETE ORDINATE METHOD

Approved:

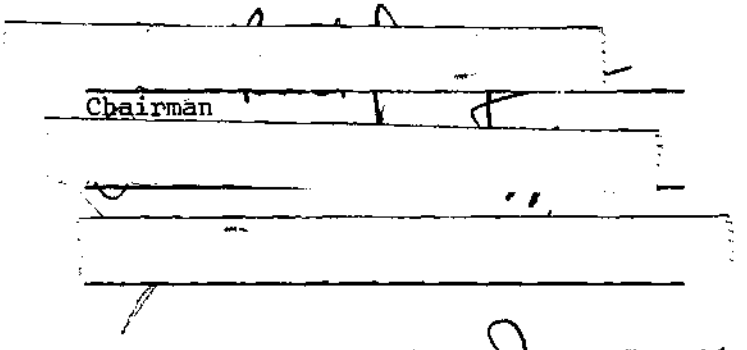

Chairman

Date approved by Chairman: July 27, 1966

ACKNOWLEDGMENTS

I would like to express my appreciation to Dr. A. Ben Huang for his suggestion of the thesis topic and for his guidance, advice, and cooperation during the research endeavor. Dr. Arnold L. Ducoffe and Dr. James Wu, who served on the reading committee, are gratefully thanked for their encouragements and for their patient examination of the manuscript.

The advice and cooperation of several of my fellow graduate students must not go unnoticed. I thank Dr. Robert L. Stoy and Mr. Joseph D. Stewart for their frequent discussions on the kinetic theory aspects of this thesis. Also, I received invaluable advice from Mr. Kenton D. Whitehead and Mr. Jerry A. Sills on various numerical and computational aspects of the problem. In addition, Major Charles W. Bagnal carried out much of the computational work reported in Chapter V. Also, I thank Miss Mary Dale for typing the rough draft of this thesis.

I sincerely appreciate the financial aid of an NDEA fellowship and of Ford Foundation loans for easing my financial situation during the graduate work.

Finally, I want to thank my children, Karen, Donny, and Kimberly, and particularly my wife Ann for her patience, understanding, and encouragement during my entire stay at this institution.

TABLE OF CONTENTS

LIST OF TABLES

LIST OF ILLUSTRATIONS

LIST OF SYMBOLS

A	parameter in the function F(A)
$\vec{c}$	nondimensional velocity, $\beta\vec{v}$
d	distance between plates in Couette and channel flow
$F(A)$	a function defined as $\int_0^\infty \exp(-\Omega^2 - A/\Omega)d\Omega$
f	velocity distribution function
f_{eq}	Maxwellian equilibrium distribution function
f_o	Maxwellian distribution function for constant density, isothermal flow
$H_i, \bar{H}_i$	weighting coefficients for the Gauss-Hermite and modified Gauss quadratures
K	Knudsen number, the ratio of mean free path to a characteristic length
k	Boltzmann constant
k_1	multiple of the mean free path
m	molecular mass
N	integer representing the number of discrete ordinates used in the interval o to ∞ for the Gaussian quadratures
n	number density of the gas
n_o	number density for constant density flow
n'	perturbation in the number density
P_{xz}	shear stress in the yz plane
$P_{xz_{f.m.}}$	value of P_{xz} in the free molecular limit
p_j	roots of the characteristic equation (39) for a given value of d/μ, $p_j = \frac{d}{\mu}\sqrt{n_j}$

$Q,\bar{Q}$	volume flow rate and nondimensionalized volume flow rate, $\bar{Q} = 2\frac{\mu}{d}\frac{Q}{\bar{\eta}}$
$\vec{q}$	macroscopic velocity nondimensionalized by the most probable molecular velocity, $\vec{q} = \beta\vec{u}$
T	temperature of the gas
T_o	temperature for isothermal flow
T'	perturbation in the temperature
t	time
$\vec{u}$	macroscopic velocity vector
$\vec{v}$	microscopic velocity vector
x	space coordinate normal to the surfaces
$\bar{x}$	ratio of actual distance to mean free path, $\bar{x} = x/\mu$
$\bar{x}_l$	ratio of actual distance to a multiple of the mean free path, $\bar{x}_l = x/k_l$
$\vec{x}$	space position vector, $\vec{x} = x\vec{i} + y\vec{j} + z\vec{k}$
z	space coordinate parallel with the flow
$\alpha_i,\bar{\alpha}_i$	discrete ordinates for the Gauss-Hermite and modified Gaussian quadratures
β	inverse of the most probable molecular velocity, $\beta = (m/2kT)^{1/2}$
β_o	inverse of the most probable molecular velocity corresponding to isothermal flow, $\beta_o = (m/2kT_o)^{1/2}$
δ	inverse Knudsen number, $\delta = d/\mu$
$\bar{\eta}$	a parameter in the channel flow problem, proportional to the pressure gradient times the mean free path, $\bar{\eta} = \bar{\kappa}\mu$
η_j	the roots of the characteristic equation (38)
$\bar{\kappa}$	a constant which is proportional to the pressure gradient in channel flow

μ mean free path for the BGK collision model

ξ nondimensional coordinate normal to the surfaces in Couette and channel flow, $\xi = x/d$

$\bar{\xi}$ transformed coordinate normal to the surface in Rayleigh flow, $\bar{\xi} = 1 - e^{-\bar{x}}$

$\bar{\xi}_1$ transformed coordinate normal to the surface in Rayleigh flow, $\bar{\xi}_1 = 1 - e^{-\bar{x}_1}$

σ collision time

σ_1 fraction of incident molecules which are diffusely reflected from a surface

τ ratio of true time to the average time required for a molecule to cross from one plate to another in Couette flow, $\tau = t/\beta d$

τ_1 parameter with dimension of distance, $\tau_1 = t/\beta$

$\bar{\tau}$ ratio of true time to collision time, $\bar{\tau} = t/\beta\mu$

$\bar{\tau}_1$ ratio of true time to a multiple of the collision time, $\bar{\tau}_1 = t/\beta k_1$

$\Phi^{\pm}(x,\vec{c},t)$ perturbed distribution function defined by $f^{\pm} = f_o[1 + \Phi^{\pm}(x,\vec{c},t)]$

$\Psi^{\pm}(x,c_x,t)$ perturbed distribution function defined by $f^{\pm} = f_o[1 + c_z \Psi^{\pm}(x,c_x,t)]$

$\Psi^{\pm}_{\kappa}$ represents the function $\Psi^{\pm}$ evaluated at the discrete velocity point $c_x = {}^{\pm}\alpha_{\kappa}$

Ω variable of integration in the function F(A)

Superscript

$^{\pm}$ indicates the positive and negative direction of c_x

Subscript

o	indicates reference condition which does not vary with time or space

SUMMARY

In this work, the method of discrete ordinates as applied to the solution of the linearized Boltzmann equation with BGK collision model is established on a rigorous, fundamental basis. The method consists of replacing the integrations over velocity space of the perturbed distribution function by an appropriate quadrature. This requires approximating the velocity dependence of this function by a set of functions, each evaluated at appropriate discrete points in velocity space. Thus, rather than solving an integro-differential equation for a function depending upon space, time, and velocity, the problem is transformed into the solution of a linear system of first order partial differential equations in a set of functions which are continuous in space and time, but are point-functions in velocity space. This set of equations is then solved simultaneously as an approximation (only in the sense of numerical truncations) to the true perturbed distribution function. An interesting and useful feature of applying the quadrature method to the velocity dependence of the distribution function is that the macroscopic quantities of interest are all formed by taking velocity moments of this function. Hence, these moment integrations are evaluated using the same quadrature by which the distribution function is originally solved, resulting in an extremely convenient form for calculations.

After developing the discrete ordinate method for the unsteady, multi-dimensional linearized gas dynamic problems, the technique is applied to several flow situations in order to establish the accuracy

and utility of the method. First, the case of steady Couette flow between two infinite parallel plates is considered. This problem has been previously solved numerically over all flow regimes from free molecular to continuum. Several analytical methods have also been applied to the problem, two of which are the iteration method of Willis and the half-range moment method of Gross, Jackson, and Ziering.

The discrete ordinate method using the Gauss-Hermite quadrature was compared to these other methods. It gave results for the flow velocity and shear stress which compared favorably with the accurate numerical solution in the transition and slip flow regimes and led to the proper solution in the continuum limit. In an effort to improve the results in the near free molecular flow regime, a new half-range Gauss quadrature was developed. With this modified quadrature excellent results were obtained from near free molecular flow to the continuum regime. One of the important features of the discrete ordinate method is that general solutions are readily obtained for arbitrary orders of approximation, so that higher approximations are easily found if a computer is available to solve a linear system of algebraic equations. This feature does not appear to occur with the half-range moment method, so that the discrete ordinate technique yields superior solutions to this problem for a given amount of computational effort.

The next problem examined was the case of the volume flow rate of a one-dimensional flow in an infinite channel. Again, an accurate numerical solution by Cercignani and Daneri was available with which to compare the results; and the half-range moment method had previously been applied to this problem by Huang and Stoy. The discrete ordinate

method gave excellent agreement with the numerical solution up to the near free molecular flow regime when the new modified Gauss quadrature was used, and also proved to be superior again to the half-range moment method for a given amount of computational effort.

In order to examine the method for time dependent problems, the cases of the transient development of Couette flow and of the Rayleigh flow problem of accelerating an infinite plate in its own plane were next considered. The technique led to a system of linear partial differential equations, and these were attacked with the numerical method of finite differences. Cases of impulsive plate acceleration and of accelerating from rest to a given final velocity over a period of time were examined. These problems yielded quite interesting results in describing the transient behavior of the perturbed distribution function. The results for extremely small and extremely large times agreed well with analytical expressions for these asymptotic conditions. Also, the problems involved in applying the finite difference method to a nearly free molecular flow are discussed.

The results of the investigation may be summarized in the following conclusions:

1. The discrete ordinate method has been shown to give accurate solutions over a wider range of Knudsen numbers for a given amount of computational effort than any other existing analytic method applied to the linearized BGK Boltzmann equation.

2. Much of the success of the method is due to the development of the modified quadrature. However, the Gauss-Hermite quadrature may be used with good success for values of $d/\mu > 1$.

3. The difference scheme presented for the time dependent system of partial differential equations is stable and converges to the steady state solution for the transient Couette flow problem investigated and to the appropriate asymptotic solution for the Rayleigh flow problem.

4. Difficulties in the application of a finite difference method to an initial value problem have been pointed out, with emphasis being placed on discussing the effects of the relation of grid spacing to mean free path.

5. For physically realistic initial value problems the finite difference scheme applied in conjunction with the discrete ordinate method will give excellent results, even to a scale quite small compared to the mean free path of the gas.

6. The primary weakness in the discrete ordinate method is in the very near free molecular flow regime (Knudsen numbers greater than 100) where it is necessary to take large values of N to obtain accurate results. This weakness is not in the solution for the perturbed distribution function, but rather in applying a quadrature to form the velocity moments from this solution.

CHAPTER I

INTRODUCTION

Background and Review of Recent Literature

The field of gasdynamics can be roughly divided into several regimes depending rather arbitrarily upon a parameter known as the Knudsen number, K. This parameter represents the ratio of the mean free path of the gas to some characteristic length of the problem at hand, such as a body dimension or shock wave thickness. Hence, if the gas is particularly dense for a given situation, or the characteristic length is quite large, the Knudsen number is much less than unity and the flow characteristics are determined primarily by intermolecular collisions within the gas. This type of flow is in the continuum regime and the gas may be treated as a continuous medium rather than as being composed of individual molecules. The Navier-Stokes equations which govern the phenomena in this regime have been well substantiated by numerous experiments and applications. At the other extreme is the case of free molecular and near free molecular flow where the gas is quite rarefied or the characteristic length is extremely small. The Knudsen number is much larger than one so that the intermolecular collisions are negligible and the collisions between the gas molecules and the surface become important. Flow phenomena in the strictly free molecular regime where there are no molecular collisions away from the boundaries of the flow are determined by the freestream velocity

distribution function and by the gas-surface interaction. Analysis is made strictly from a microscopic viewpoint in which molecules travel in straight line paths away from the boundaries.

In the cases where the Knudsen number has a value intermediate between these extremes, two other regimes have been suggested: the transition regime (K greater than unity but not extremely large) and the slip flow regime (K less than unity but not extremely small). In transition flow both gas-gas and gas-surface collisions have essentially equivalent importance in governing the flow characteristics. In slip flow the gas-surface collisions control the phenomena which occur within several mean free paths from a surface, but in the main portion of the flow the gas behaves much the same as it does in the continuum regime. Analytically, the slip flow regime was frequently attacked by use of the Navier-Stokes equations with boundary conditions which had been modified to account for velocity slip and temperature jump at the surfaces. Also, attempts have been made to describe such flows using higher order macroscopic equations such as the Burnette or Grad thirteen moment equations; however, the mathematics involved in these higher order equations is extremely complex, and there is little evidence that they yield results significantly better than those obtained by use of the Navier-Stokes equations with modified boundary conditions. For example, Sherman [1] performed an experimental investigation on shock waves in low density flows and found that the Navier-Stokes equations gave an equally good comparison between theory and experiment as did the higher order equations. Also, these macroscopic equations cannot be extended into the transition and near free molecular regimes without appreciable error as

is evidenced by the work of Yang and Lees [2], who applied Grad's thirteen moment equations to the Rayleigh problem of a plate set impulsively in motion in its own plane. Significant differences between the free molecular limit found using the Boltzmann transport equation and the results for the Grad's equations were pointed out by Yang and Lees [3] in a later paper, thus indicating that the higher order macroscopic equations lose their validity as the gas becomes more and more rarefied.

In the near free molecular flow regime the most useful analytic method, both from the standpoint of accuracy and ease of application, is the iteration method developed by Willis [4] in 1958. This technique consists of an iteration on the velocity distribution function with the zeroth iteration usually being taken as the free molecular or collisionless solution. The accuracy thus decreases as the Knudsen number decreases, and the method is generally not applied well into the transition regime since iterations of higher order than the first are extremely difficult to obtain. Also, convergence of the iteration scheme has not been demonstrated for any problem other than that of linearized Couette flow. It should be pointed out that if an approximate solution is known for transition Knudsen numbers, the iteration technique can be applied to this solution rather than to the free molecular results. This has been done by Stoy [5] and Huang and Stoy [6] for the case of channel flow between two parallel plates in which the zeroth iteration is taken as a low order solution using the velocity moment method (which is discussed below). In the near free molecular and transition regions,

results after one iteration gave good agreement with the numerical solution given by Cercignani and Daneri [7]. However, in the region of slip flow the first iteration gave no change from the zeroth, so that convergence to the correct solution appears to be extremely slow in this region, if it exists at all for this problem. However, despite the fact that it is usually impractical to extend the iteration well into the transition and slip flow regimes, there is no other known method which can give such good results in the near free molecular regime for the same amount of work.

Another technique, the velocity moment method, is available for solution of the linearized Boltzmann equation and is based on an expansion of the velocity distribution function as a series of orthogonal polynomials in velocity space. This method was applied to the linearized problem of shear flow and heat transfer between parallel plates by Mott-Smith [8] and by Wang-Chang and Uhlenbeck [9], [10], and [11]. The infinite series of orthogonal polynomials must be truncated after a finite number of terms, and Reference [10] indicates that the convergence of these solutions for large Knudsen numbers is poor. Gross, Jackson, and Ziering [12] have improved greatly upon this technique by expressing the distribution function as one which possesses a two-stream character, that is, by distinguishing between particles which are traveling toward a surface and those moving away from it. This improvement is based upon the fact that the velocity distribution function is discontinuous at a surface with respect to the velocity component normal to that surface. Further, this condition holds within a distance on the order of a mean free path from the surface regardless of the Knudsen number so that it

provides a boundary condition for all flow regimes. However, even this modification does not allow the moment method to yield accurate solutions in the near free molecular and early transition regimes with a reasonable amount of effort.

Thus, to this date there is no single analytical method which, when applied to the governing equations of gas dynamics, will yield solutions over the entire range of Knudsen numbers with a reasonable amount of work, even for the simplest linearized problems.

Discussion of the Method

The method of discrete ordinates has long been known in the field of radiative transfer (i.e. Chandrasekhar [13] and Kourganoff [14]) and, in fact, was suggested as a possible analytic approach to the Boltzmann equation by Krook [15] in 1955 and again by Gross, et al. [12] in 1957. This technique consists of replacing the integration over velocity space of the perturbed distribution function in the linearized Boltzmann equation by an appropriate quadrature. This requires approximating the velocity dependence of the perturbed distribution function by a set of functions, each evaluated at appropriate discrete points in velocity space. Thus, rather than solving an integro-differential equation for a function of space, time, and velocity, the problem is transformed into the solution of a linear system of first order partial differential equations in a set of functions which are continuous in space and time but are point-functions in velocity space. This set is then solved simultaneously as an approximation (only in the sense of numerical truncations) to the true distribution function. An interesting and use-

ful feature of applying the quadrature method to the velocity dependence of the distribution function is that the macroscopic properties of interest are all formed by taking velocity moments of this function. Hence, these moment integrations are evaluated using the same quadrature by which the distribution function is originally solved, resulting in an extremely convenient form for calculation.

There have been two previous papers on the discrete ordinate method--the first by Broadwell [16] and the second by Hamel and Wachman [17]--both of which appeared in 1964. Broadwell used an interesting physical argument based on a hard spheres collision model to evaluate the collision integral of the Boltzmann equation. This, mathematically, was equivalent to the use of a first order quadrature formula. Although these results give a good qualitative picture of the flow phenomena for the problems of Couette and Rayleigh flow investigated by Broadwell, they are not very accurate from the quantitative viewpoint; and such an approximation would most probably be incapable of describing the flow characteristics in any wide class of gasdynamic problems.

The paper by Hamel and Wachman was an improvement over Broadwell's work in that the quadrature technique was explored from a mathematical rather than a physical point of view and then applied to the hard sphere model for the case of steady Couette flow to a higher degree of approximation. However, from several standpoints there are portions of that work which might need further investigation. First is that both Gauss-Laguerre and Gauss-Hermite quadratures were used and weighted in an arbitrary fashion depending upon the inverse Knudsen number, δ. The precise manner of weighting these two forms is difficult to establish

without knowing the results a priori. Second, the mathematical method used resulted in the inability to calculate macroscopic flow properties on their digital computer in the slip and continuum flow regimes for the steady Couette flow case investigated. This occurred because the technique used for solving the resulting set of simultaneous differential equations leads to a series form which causes numerical difficulties for δ greater than two. Finally, and most important, the functional form proposed as the solution to the Couette problem does not possess a character which yields the proper velocity profile in the continuum limit ($\delta \to \infty$). Although the macroscopic velocities at the boundaries and at the centerline are forced to have the proper values by applying the boundary conditions and the symmetry of the problem, the continuum limit requires a linear variation across the space between the plates; and this is not achieved with the strictly exponential solution obtained by Hamel and Wachman. Hence, even if no numerical difficulties for δ greater than two were encountered, the results for the slip and continuum flow regions should be incorrect.

Purpose of the Research

Since the Navier-Stokes and other higher order macroscopic equations may be obtained as special forms of the Boltzmann transport equation, there has been considerable interest in the possibility of solving many gasdynamic problems for all flow regimes, from free molecular to continuum, using this equation. The capability of solving a given problem for all values of Knudsen number from a single equation and using a single technique is not only of academic interest, but also

of significant practical importance.

It is the purpose of this research to develop the method of discrete ordinates for the solution of the linearized Boltzmann equation in an effort to determine the accuracy and practicability of using the technique for solving flow problems over as wide a range of Knudsen numbers as possible. The only other papers dealing with the discrete ordinate method either represent a crude approximation with few contributions to the mathematical development of the quadrature method or cannot be applied to a wide range of flow regimes due to the incompleteness of the solution.

This investigation was conducted from the point of view that the method must be established on a sound, rigorous, and fundamental base; and an effort was made to keep the mathematics as simple--but as complete and useful--as possible. In this work the method of discrete ordinates as applied to the linearized Boltzmann equation with the Bhatnager-Gross-Krook [18] model for the collision integral is established over a much wider range of Knudsen numbers than any other single method (some discussion on these aspects has also been presented in two papers by Huang and Giddens [19] and [20]). The technique is applied to several one-dimensional steady and unsteady problems and the results compared with those of other investigators where such information is available.

CHAPTER II

DEVELOPMENT OF THE DISCRETE ORDINATE METHOD

Discussion of the Kinetic Theory Approach to Gasdynamics

The Liouville equation of statistical mechanics can be reduced, under the assumptions of molecular chaos and binary collisions of a single component gas, to the Boltzmann transport equation [21]

$$\frac{\partial f}{\partial t} + \vec{v}\cdot\nabla_{\vec{x}} f + (\vec{F}_{ext}/m)\cdot\nabla_{\vec{v}} f = (\delta f/\delta t)_c \qquad (1)$$

where $f = f(\vec{x},\vec{v},t)$ is the velocity distribution function which depends upon space, velocity, and time. Here $\vec{x}$ and $\vec{v}$ are the space and velocity vectors, $\nabla_{\vec{x}}$ and $\nabla_{\vec{v}}$ are the gradient operators in physical space and velocity space, respectively, $\vec{F}_{ext}$ is the external force vector applied to the gas of molecular mass, m, and $(\delta f/\delta t)_c$ is the total time rate of change of the distribution function due to collisions of the molecules. For problems of interest in this research it will be assumed that there are no external forces acting on the particles of the gas. Further, since one of the prime objectives of this investigation is to establish the method of discrete ordinates upon a sound mathematical foundation and to retain analytical expressions as much as possible, the Bhatnager-Gross-Krook model developed in Reference [18] will be used for the collision integral. Not only is this perhaps the simplest model available, but it is also one of the most accurate for several gases. For example,

Stoy [5] found that the BGK model gave good agreement with experiment for the cases of flow of hydrogen, helium, and carbon dioxide in an infinite channel.

Using this BGK model the Boltzmann equation takes the form

$$\frac{\partial f}{\partial t} + \vec{v}\cdot\nabla_{\vec{x}} f = \frac{n}{\sigma}(f_{eq}-f) \tag{2}$$

where n is the number density of the gas, σ is the collision time, and f_{eq} is the local Maxwellian equilibrium distribution function given by

$$f_{eq} = \frac{n\beta^3}{\pi^{3/2}} e^{-\beta^2|\vec{v}-\vec{u}|^2} \tag{3}$$

where β is the inverse of the most probable molecular velocity, i.e. $\beta = (m/2kT)^{1/2}$, and $\vec{u}$ is the flow velocity.

Although the BGK collision model has been applied, Equation (2) governs a very wide class of gasdynamic problems so long as the assumptions of a single component gas with binary collisions, of molecular chaos, and of no external force fields hold for the particular situation. For example, Equation (2) may be used to solve many high speed flow problems such as the shock wave structure or hypersonic flow over a flat plate in addition to some of the more classical problems of lower speed flows suggested in the subsequent sections of this dissertation.

Development of the Linearized Boltzmann Equation

It will be assumed that the problems to be dealt with in the present investigation are such that the true distribution function is

perturbed only slightly from a reference equilibrium condition which is independent of position and time. In particular, it is assumed that

$$f = \beta_o^3 f_o[1 + \Phi(\vec{x},\vec{c},t)] \tag{4}$$

where $f_o = n_o \pi^{-3/2} e^{-c^2}$ is the reference equilibrium distribution function corresponding to $\beta_o = (m/2kT_o)^{1/2}$ with T_o being the reference temperature. Here, $\vec{c} = \beta_o \vec{v}$ is the nondimensional microscopic velocity and Φ, the perturbed distribution function, depends upon space, velocity, and time and is considered small in magnitude compared to unity. Further, it follows that

$$n = n_o(1 + n') \tag{5}$$

and

$$T = T_o(1 + T') \tag{6}$$

so that

$$n' = \frac{1}{n_o} \iiint f_o \Phi d^3c \tag{7}$$

The nondimensional macroscopic velocity in the i-direction is then given by

$$q_i = \frac{1}{n} \iiint f_o \Phi c_i d^3c \tag{8}$$

where $q_i = \beta u_i$.

Thus, the equilibrium distribution function, f_{eq}, may be expressed as

$$f_{eq} = n_o(1+n')\pi^{-3/2}\left[\frac{m}{2kT_o(1+T')}\right]^{3/2} e^{-\frac{m}{2kT_o(1+T')}|\vec{v}-\vec{u}|^2} \tag{9}$$

If the problems are such that n', T', and $\vec{q} \ll 1$, then the following linearized expression for the equilibrium distribution function can be obtained:

$$f_{eq} \cong f_o[1 + n' + 2\vec{c}\cdot\vec{q} + (c^2-3/2)T'] \tag{10}$$

Thus, there may be only small density, temperature, and velocity gradients and small velocities relative to the thermal velocity of the molecules. The linearized equation is then

$$\beta \frac{\partial \Phi}{\partial t} + \vec{c}\cdot\nabla_{\vec{x}}\Phi = \frac{n\beta}{\sigma}[-\Phi + n' + 2\vec{c}\cdot\vec{q} + (c^2 - 3/2)T'] \tag{11}$$

The validity of this relation requires that

$$\frac{\partial \Phi}{\partial v_i} \ll \frac{1}{f_o}\frac{\partial f_o}{\partial v_i}$$

Equation (11) governs the calculation of the distribution function for problems which satisfy the conditions required for its derivation.

Application of the Method of Discrete Ordinates

It is the purpose of this research to develop the discrete ordinate method from a fundamental viewpoint so that it will be

established rigorously for basic gasdynamic problems. For this reason the problems considered are such that there are no temperature or density gradients so that n' and T' vanish. Further, it has been found by previous investigators, i.e. Gross, et al. [12], that to adequately describe conditions within a mean free path of a surface the distribution function must be expressed as one which possesses a stream-wise character; that is, a distinction must be made between molecules which are moving toward or away from a surface. Therefore, at this point Equation (11) is characterized to the case where the variation of f depends upon a two-stream character in the microscopic velocity direction c_x.

One dimensional classical problems, such as plane Couette flow and Rayleigh flow, were chosen for discussion in the interest of simplicity; however, the success of these applications indicates that the method could, in principle, be extended to flow problems with higher dimensions.

For the Couette and Rayleigh flow problems, the x-direction is taken to be normal to the plane of the bounding surfaces as shown in Figure 1. Using Equation (8) and this two-stream description, Equation (11) may be separated into two equations as follows:

$$\beta \frac{\partial \Phi^+}{\partial t} + c_x \frac{\partial \Phi^+}{\partial x} = \frac{n}{\sigma} \beta \{ - \Phi^+ + \frac{2}{\pi^{3/2}} c_z \iint_{-\infty}^{\infty} \left[\int_0^{\infty} \Phi^+ e^{-c_x^2} dc_x + \int_{-\infty}^{0} \Phi^- e^{-c_x^2} dc_x \right] \cdot c_z e^{-(c_y^2 + c_z^2)} dc_y dc_z \} \tag{12}$$

Couette Flow

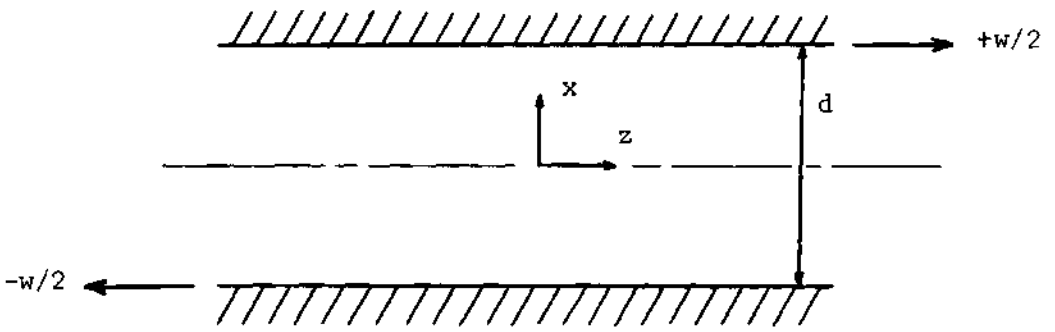

Note: w/2 and w are the actual plate velocities nondimensionalized by the most probable molecular velocity, β^{-1}.

Rayleigh Flow

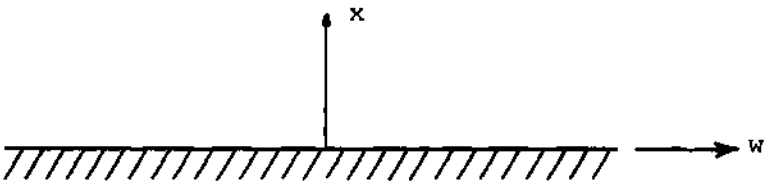

Figure 1. Geometries and Coordinate Systems for the Couette and Rayleigh Flow Problems.

and

$$\beta \frac{\partial \Phi^-}{\partial t} + c_x \frac{\partial \Phi^-}{\partial x} = \tag{13}$$

$$\frac{n}{\sigma} \beta \{ - \Phi^- + \frac{2}{\pi^{3/2}} c_z \int_{-\infty}^{\infty} \int [\int_{0}^{\infty} \Phi^+ e^{-c_x^2} dc_x + \int_{-\infty}^{0} \Phi^- e^{-c_x^2} dc_x]$$

$$\cdot c_z e^{-(c_y^2 + c_z^2)} dc_y dc_z \}$$

Note that Φ has been re-defined according to the relation

$$\Phi(\vec{x},\vec{c},t) = \begin{cases} \Phi^+(x,\vec{c},t) & \text{for } c_x > 0 \\ \\ \Phi^-(x,\vec{c},t) & \text{for } c_x < 0 \end{cases} \tag{14}$$

In order to solve the above equations it is proposed that the integrals in the integro-differential equation be approximated by an appropriate quadrature. The Gauss quadrature technique for evaluating an integral of the form

$$\int_a^b w(u)f(u)du \quad ,$$

where w(u) is a weighting function, involves the approximation

$$\int_a^b w(u)f(u)du \tilde{=} \sum_{i=1}^{N} H_i f(\alpha_i) \tag{15}$$

The H_i are weighting coefficients, and the α_i are discrete points at which the function f is evaluated. These quantities depend upon a, b, and w(u); and the method for their determination will be discussed in detail in Chapter III.

Since the integrals of Equations (12) and (13) contain a weighting function of the form e^{-c^2} and the limits of integration are from 0 to ∞ and $-\infty$ to 0, the Gauss-Hermite quadrature may be applied to the right-hand side of these equations. This results in a system of linear partial differential equations of the form

$$\beta \frac{\partial \Phi^{\pm}_{\kappa\nu\varepsilon}}{\partial t} \pm \alpha_\kappa \frac{\partial \Phi^{\pm}_{\kappa\nu\varepsilon}}{\partial x} = \frac{\eta}{\sigma} \beta \{ - \Phi^{\pm}_{\kappa\nu\varepsilon} \tag{16}$$

$$+ \frac{2}{\pi^{3/2}} \gamma_\varepsilon \sum_{k=1}^{2L} \sum_{j=1}^{2M} \sum_{i=1}^{N} \gamma_k H_i H_j H_k [\Phi^{+}_{ijk} + \Phi^{-}_{ijk}] \}$$

where $\kappa = 1,2,\ldots,N$; $\nu = 1,2,\ldots,2M$; and $\varepsilon = 1,2,\ldots,2L$. Here the $\Phi^{\pm}_{\kappa\nu\varepsilon}$ are functions of position and time and, for example, $\Phi^{+}_{\kappa\nu\varepsilon}$ represents the function $\Phi(x,\vec{c},t)$ evaluated at the discrete velocity points $c_x = + \alpha_\kappa$, $c_y = \zeta_\nu$, and $c_z = \gamma_\varepsilon$. The values of α_κ are the positive roots of the Hermite polynomial of degree 2N, the ζ_ν are the roots of that polynomial of degree 2M, and the γ_ε are those for degree 2L. The H_κ, H_ν, and H_ε are the corresponding weighting coefficients of the Gauss-Hermite quadrature. Thus, the integro-differential Equations (12) and (13) have been approximated by a linear system of partial differential equations.

For the BGK collision model it can be shown that the summations over j and k are independent of each other so that the actual working

form for Equation (16) is

$$\beta \frac{\partial \Psi_\kappa^\pm}{\partial t} \pm \alpha_\kappa \frac{\partial \Psi_\kappa^\pm}{\partial x} = \frac{\eta\beta}{\sigma} \left[- \Psi_\kappa^\pm + \frac{1}{\sqrt{\pi}} \sum_{i=1}^{N} H_i (\Psi_i^+ + \Psi_i^-) \right] \tag{17}$$

where the solution for $\Phi^\pm$ has been expressed by the form

$$\Phi^\pm(x,\vec{c},t) = c_z \Psi^\pm(x,c_x,t) \tag{18}$$

which exactly satisfies the linearized Boltzmann equation. This means that the complete distribution function has been expressed as

$$f^\pm(x,\vec{c},t) = \beta_o^3 f_o [1 + c_z \Psi^\pm(x,c_x,t)] \tag{19}$$

Note that this form for the distribution function indeed gives the results that number density, n, and temperature, T, are constant as may be seen by forming the appropriate velocity moments using the kinetic theory definition of these two quantities.

Equation (17) represents a system of 2N linear partial differential equations in the unknowns $\Psi_\kappa^+(x,t)$ and $\Psi_\kappa^-(x,t)$ for $\kappa = 1,2,\ldots,N$. Since the macroscopic flow quantities of interest are determined by moment integrations over velocity space of Equation (19), then these integrals may be evaluated using the same quadrature--and hence, the same points in velocity space--as is used originally in solving for the distribution function. For example, the flow velocity in the z-direction may be expressed as

$$q_z(x,t) = \frac{1}{n} \int_{-\infty}^{\infty} \int_{-\infty}^{\infty} \int_{-\infty}^{\infty} v_z \, f(x,\vec{v},t) \, dv_x \, dv_y \, dv_z \tag{20}$$

or, using Equation (19),

$$q_z(x,t) = \frac{1}{2\sqrt{\pi}} \int_{-\infty}^{\infty} e^{-c_x^2} \Psi(c_x,x) dc_x \tag{21}$$

The Gauss-Hermite quadrature is then applied to this integral to give

$$q_z(x,t) = \frac{1}{2\sqrt{\pi}} \sum_{i=1}^{N} H_i [\Psi_i^+(x,t) + \Psi_i^-(x,t)] \tag{22}$$

Other macroscopic quantities may be determined in a similar manner. For example, the shear stress in the y-z plane is given by

$$P_{xz}(x,t) = \frac{1}{2\sqrt{\pi}} \sum_{i=1}^{N} H_i \alpha_i [\Psi_i^+(x,t) - \Psi_i^-(x,t)] \tag{23}$$

Thus, once the $\Psi_\kappa^\pm$ functions have been determined from Equation (17) with appropriate boundary conditions, the flow characteristics may be evaluated from these convenient summations.

CHAPTER III

DEVELOPMENT OF AN APPROPRIATE QUADRATURE

The Gauss-Hermite Quadrature

In the first application of the discrete ordinate method to the problem of steady Couette flow the Gauss-Hermite quadrature was used since the various values of α_κ and H_κ are tabulated up to 2N = 20 in several mathematical tables and texts, i.e. Kopal [22]. This particular quadrature was developed for integrals of the form

$$\int_{-\infty}^{\infty} e^{-\Omega^2} g(\Omega)\, d\Omega$$

Hence, in order to apply it to the half-range integrations over c_x it is necessary to break up the integration into

$$\int_{-\infty}^{\infty} e^{-\Omega^2} g(\Omega) d\Omega = \int_{-\infty}^{\infty} e^{-\Omega^2} [g^+(\Omega)+g^-(\Omega)]d = \sum_{i=1}^{N} H_i g^+(\alpha_i) + \sum_{i=1}^{N} H_i g^- (-\alpha_i) \quad (24)$$

where

$$g^+(\Omega) = 0 \quad \text{for} \quad \Omega < 0 \quad (25)$$

$$g^-(\Omega) = 0 \quad \text{for} \quad \Omega > 0$$

The α_i are the positive roots of the Hermite polynomial of degree 2N, and the H_i are the corresponding weighting coefficients. This separation of the intervals of integration is possible due to the fact that

the 2N roots are symmetrically distributed about zero (for instance, see Huang [23]). The detailed results obtained in applying the Gauss-Hermite quadrature to steady Couette flow and to the flow in an infinite channel will be discussed in a subsequent chapter.

The Modified Gauss Quadrature

Equations (12) and (13) in Chapter II indicate that the integrals of interest in the linearized Boltzmann equation with BGK model are the half-range integrals

$$\int_{-\infty}^{0} \Phi^{-} e^{-c_x^2} \, dc_x \quad \text{and} \quad \int_{0}^{\infty} \Phi^{+} e^{-c_x^2} \, dc_x$$

Rather than adapting the Gauss-Hermite quadrature to these forms, a much more direct approach in applying the discrete ordinate method is to develop a new quadrature specifically for the above integrals. Further, there is good physical justification for such an approach. Due to the two-stream character of the perturbed distribution function, there is a discontinuity between $\Phi^{+}(c_x > 0)$ and $\Phi^{-}(c_x < 0)$ at the velocity point $c_x = 0$. The discontinuity, which is quite important in near free molecular flow, can be well described by the half-range quadrature whereas the full-range or Gauss-Hermite method cannot do this. Thus, it is expected that the results for near free molecular flow will be greatly improved if each of the integrals is approximated by a half-range quadrature with new roots and weighting coefficients generated specifically for the intervals $(-\infty,0)$ and $(0,\infty)$. More detailed discussion on this feature is given in a paper by Huang and Giddens [24].

Since

$$\int_{-\infty}^{0} e^{-\Omega^2} g(\Omega)d\Omega = \int_{0}^{\infty} e^{-\bar{\Omega}^2} g(\bar{\Omega})d\bar{\Omega} \tag{26}$$

if $\bar{\Omega} = -\Omega$, the half-range quadrature appropriate to the interval $(-\infty,0)$ may be obtained from that generated for the interval $(0,\infty)$. Hence, it is only necessary to derive the roots, $\bar{\alpha}_i$, and weighting coefficients, $\bar{H}_i$, such that

$$\int_{0}^{\infty} e^{-\Omega^2} g(\Omega)d\Omega = \sum_{i=1}^{N} \bar{H}_i g(\bar{\alpha}_i) \tag{27}$$

Then, from Equation (26), it follows that

$$\int_{-\infty}^{0} e^{-\Omega^2} g(\Omega)d\Omega = \sum_{i=1}^{N} \bar{H}_i g(-\bar{\alpha}_i) \tag{28}$$

The method for determining the new quadrature values is now considered. It is desired to find the values $\bar{\alpha}_i$ and $\bar{H}_i$ such that Equations (27) and (28) are satisfied. The requirement of Gauss is that these equations are exact if $g(\Omega)$ is a polynomial of degree 2N-1 or less. If $g(\Omega)$ is not such a polynomial, then these expressions represent approximations to the true values of the integrals.

Thus, define

$$\omega_k = \int_{0}^{\infty} e^{-\Omega^2} \Omega^k \, d\Omega \quad (k = 0,1,\ldots,2N-1) \tag{29}$$

which, according to Equation (27), may be written as

$$\omega_k = \sum_{i=1}^{N} \bar{H}_i \, \bar{\alpha}_i^k \tag{30}$$

Since the ω_k may be obtained from (29) by analytic integration, Equation (30) represents a system of 2N equations in the 2N unknowns $\bar{\alpha}_i$ and $\bar{H}_i$ for i = 1,2,...,N. However, this is a non-linear system and for large values of N is not readily solvable.

Following Kopal [22] the array of 2N equations of the form of Equation (30) is divided into N sets of N + 1 equations each, with the form given by

$$\omega_{j+k} = \sum_{i=1}^{N} \bar{H}_i \, \bar{\alpha}_i^{j+k} \tag{31}$$

for j = 0,1,...,N-1 and k = 0,1,...,N. A set of N constants, c_k, is defined as the solution of the simultaneous linear system

$$\omega_{j+N} + \sum_{k=0}^{N-1} c_k \omega_{j+k} = 0 \tag{32}$$

Inserting Equation (31) into Equation (32) gives

$$\sum_{i=1}^{N} \bar{H}_i \, \bar{\alpha}_i^j [\bar{\alpha}_i^N + \sum_{k=0}^{N-1} c_k \, \bar{\alpha}_i^k] = 0 \tag{33}$$

In order for (33) to be true for non-trivial values of $\bar{\alpha}_i$ and $\bar{H}_i$, it is sufficient that the terms in the bracket of (33) be equal to zero. Thus, the $\bar{\alpha}_i$ for i = 1,2,...,N are the roots of the algebraic polynomial of degree N,

$$x^N + \sum_{k=0}^{N-1} c_k x^k = 0 \tag{34}$$

where the c_k are obtained by the solution of Equations (29) and (32). Then, knowing the $\bar{\alpha}_i$ by solving (34), it is possible to substitute the results into Equation (30) in order to determine the $\bar{H}_i$ from a linear system. Thus, the new quadrature roots and coefficients may be obtained by solving two linear algebraic systems of N equations each along with determining the roots of an Nth degree polynomial.

The above equations were solved on a Burroughs B5500 digital computer for cases up to N = 8. These results are presented in Table 1. Although nine significant digits are reported for each case, no claim can be made to an accuracy greater than eight decimal places due to the accumulation of round-off error in the computer.

This new modified quadrature was applied to the Couette and channel flow problems. As indicated in greater detail in Chapters IV and V, the improvement in the results over the Gauss-Hermite quadrature is remarkable. In fact, it is the development of this modified quadrature which enables the discrete ordinate method to give accurate answers over such a wide range of Knudsen numbers. In the near free molecular flow regime this is directly related to the evaluation of the integral (see Huang and Giddens [24])

$$F(A) = \int_0^\infty e^{-\Omega^2 - A/\Omega} d\Omega \tag{35}$$

This integral occurs as the solution for the perturbed distribution

Table 1. Roots and Weighting Coefficients for the Modified Gauss Quadrature for N = 1 to 8

N	Roots, α_j	Weighting Coefficients, H_j
1	0.564189584	0.886226925
2	0.300193931	0.640529180
	1.252421045	0.245697746
3	0.190554150	0.446029770
	0.848251867	0.396468267
	1.799776578	0.437288880
4	0.133776447	0.325302999
	0.624324689	0.421107102
	1.342537825	0.133442501
	2.262664477	$0.637432347 \times 10^{-2}$
5	0.100242151	0.248406139
	0.482813937	0.392331068
	1.060949843	0.211418215
	1.779729480	$0.332466497 \times 10^{-1}$
	2.669760263	$0.824853772 \times 10^{-3}$
6	$0.786006456 \times 10^{-1}$	0.196849206
	0.386739236	0.349155692
	0.866431154	0.257257962
	1.465691545	$0.760135170 \times 10^{-1}$
	2.172716470	$0.685210492 \times 10^{-2}$
	3.036815972	$0.984442006 \times 10^{-4}$
7	$0.637163079 \times 10^{-1}$	0.160614533
	0.318193583	0.306303720
	0.724183347	0.275545914
	1.238085494	0.120624443
	1.838440401	$0.218895217 \times 10^{-1}$
	2.531553434	$0.123780543 \times 10^{-2}$
	3.373437976	$0.109889525 \times 10^{-4}$
8	$0.529778530 \times 10^{-1}$	0.134163250
	0.267409313	0.268130722
	0.616160988	0.276228985
	1.064704717	0.157293957
	1.587766508	$0.448128001 \times 10^{-1}$
	2.185429830	$0.540120585 \times 10^{-2}$
	2.862054102	$0.194398570 \times 10^{-3}$
	3.686276823	$0.160745515 \times 10^{-5}$

function in near free molecular flow using the Willis iteration method if c_x is substituted for Ω and A is taken to be proportional to the inverse Knudsen number. Thus, the accuracy with which a given quadrature can approximate F(A) for small A will serve as an indication as to whether that quadrature may be used to solve rarefied gasdynamic problems in the near free molecular flow regime.

The function F(A) has been evaluated numerically by Chahine and Narasimha [25] who estimate that their computations are accurate to eight decimal places. Willis [26] also evaluates this integral using a series expansion and reports values estimated to be accurate to six decimal places. Table 2 gives the evaluation of F(A) by the Gauss-Hermite quadrature (N=10) and by the modified quadrature (N=8) and these are compared with the numerical solution of Chahine and Narasimha. Note that the half-range quadrature gives better numerical results than those of the Gauss-Hermite quadrature over the entire range of values of A; but, in particular, it is far superior for small values. The new modified quadrature must be considered as one of the most important contributions of this research, because it allows the discrete ordinate method to be extended much farther into the near free molecular flow regime.

Table 2. Comparison of the Gauss-Hermite and Modified Gauss Quadratures with the Numerical Evaluation of Chahine and Narasimha [25] for the Integral

$$F(A) = \int_0^\infty \exp(-\Omega^2 - A/\Omega)d\Omega$$

A	F(A) Reference [25]	F(A) Gauss-Hermite Quadrature, N=10	F(A) Modified Gauss Quadrature, N=8
0	.886227	.886227	.886227
.01	.838745	.862867	.847083
.02	.804955	.840303	.812358
.03	.776229	.818508	.781353
.04	.750737	.797450	.753490
.05	.727609	.777102	.728286
.06	.706336	.757438	.705341
.07	.686581	.738432	.684322
.08	.668105	.720058	.664950
.09	.650731	.702294	.646993
.10	.634321	.685116	.630259
.15	.563508	.607283	.560090
.20	.506231	.541158	.504639
.25	.458329	.484736	.458232
.30	.417407	.436372	.418193
.35	.381920	.394718	.383082
.40	.350797	.358662	.352004
.45	.323259	.327293	.324326
.50	.298717	.299859	.299561
.60	.256889	.254426	.257264
.70	.222647	.218586	.222672
.80	.194206	.189744	.194033
.90	.170310	.166105	.170060
1.0	.150046	.146409	.149795
1.5	.083910	.083131	.083898
2.0	.049876	.050036	.049921
2.5	.030899	.031117	.030914
3.0	.019739	.019853	.019734
3.5	.012916	.012953	.012909
4.0	.008619	.008621	.008616
4.5	.005847	.005838	.005846
5.0	.004022	.004013	.004023
6.0	.001972	.001969	.001973
7.0	.001005	.001004	.001005
8.0	.000528	.000528	.000528
9.0	.000285	.000285	.000285
10.0	.000157	.000157	.000157

CHAPTER IV

COUETTE FLOW BETWEEN PARALLEL PLATES

Solution of the Governing Equations for the Case of Couette Flow

General Solution

In this chapter the discrete ordinate method is applied to the solution of a steady Couette flow between two parallel plates. Since this problem has been solved numerically by Willis [26] for inverse Knudsen numbers ranging from 1.0 to 20.0 and analytically for the range of 0.01 to 1.0, it is possible to compare the solution obtained by the discrete ordinate method with these results. Also, Gross, et al. [12] and Lees [27] have presented solutions over portions of this inverse Knudsen number range with which the present method may be compared in order to see which gives the more accurate results.

The geometry for this problem was shown in Figure 1. Note that the top and bottom plates move opposite to each other with nondimensional velocity w. The distance between the plates is d and the x-direction is taken to be normal to the plates. For this case Equation (17) may be reduced to

$$\pm \alpha_\kappa \frac{\mu}{d} \frac{d\Psi_\kappa^\pm}{d\xi} = -\Psi_\kappa^\pm + \frac{1}{\sqrt{\pi}} \sum_{i=1}^{N} H_i(\Psi_i^+ + \Psi_i^-) \qquad (36)$$

$$\kappa = 1,2,\ldots,N$$

where $\mu = \sigma/n\beta$ is the mean free path for BGK model and $\xi = x/d$ is the normalized coordinate between the plates. Note that Equation (36) is a homogeneous linear system of ordinary differential equations and may be solved by the standard method of assuming solutions of the form

$$\psi_\kappa^{\pm} = A_\kappa^{\pm} e^{p\xi}$$

The complete details for solving Equation (36) are given in Appendix A. However, it is important to point out here that both the Gauss-Hermite and the modified quadratures allow the appearance of a degenerate solution for the characteristic equation which determines p. Thus, in addition to the exponential forms, the solution to (36) also possesses a term linear in ξ and a constant. It is this feature which does not occur in the strictly exponential solution given by Hamel and Wachman [17] and hence allows the present method to extend accurate solutions into the continuum flow regime.

The solution to Equation (36) is given by (see Appendix A)

$$\psi_\kappa^{+}(\xi) = \frac{1}{\sqrt{\pi}} \sum_{j=1}^{N-1} \left[C_j \frac{e^{p_j \xi}}{1 + \sqrt{\eta_j}\,\alpha_\kappa} + D_j \frac{e^{-p_j \xi}}{1 - \sqrt{\eta_j}\,\alpha_\kappa} \right] + E\left(\xi - \frac{\mu}{d}\alpha_\kappa\right) - F \qquad (37)$$

and

$$\psi_\kappa^{-}(\xi) = \frac{1}{\sqrt{\pi}} \sum_{j=1}^{N-1} \left[C_j \frac{e^{p_j \xi}}{1 - \sqrt{\eta_j}\,\alpha_\kappa} + D_j \frac{e^{-p_j \xi}}{1 + \sqrt{\eta_j}\,\alpha_\kappa} \right] + E\left(\xi + \frac{\mu}{d}\alpha_\kappa\right) - F \qquad (38)$$

where $\eta_j = (\mu/d\ p_j)^2$ for $j = 1,2,\ldots,N-1$. The η_j and p_j are determined by this relation and by the characteristic equation

$$\sum_{i=1}^{N} H_i \frac{1}{1 - \eta\alpha_i^2} = \frac{\sqrt{\pi}}{2} \tag{39}$$

Note that since $\sum_{i=1}^{N} H_i = \frac{\sqrt{\pi}}{2}$ there is the degenerate solution $\eta = 0$. The C_j, D_j, E, and F in Equations (37) and (38) must be determined by applying the boundary conditions of the problem.

Application of the Appropriate Boundary Conditions

Usually the distribution function at a surface is considered to be composed of two parts: one part is the fraction of incident molecules reflected specularly and the other is the fraction reflected diffusely, denoted by σ_1 the reflection coefficient. Thus

$$f^{\pm}(\xi = \mp \frac{1}{2},\ c_x) = \sigma_1 f_M(\xi = \mp \frac{1}{2}) + (1 - \sigma_1) f^{\mp}(\xi = \mp \frac{1}{2},\ \mp c_x) \tag{40}$$

where $f_M(\xi = \mp \frac{1}{2})$ is the local Maxwellian equilibrium distribution function at the plates. For problems studied in this research it is assumed that $\sigma_1 = 1$ so that the boundary conditions require that the molecules are reflected completely diffusely from the surfaces. This assumption is in agreement with experimental data for molecules impinging upon engineering surfaces under subsonic flow conditions since the reported values of σ_1 are usually above 0.9 (for example, see Estermann [28]). The boundary conditions may then be linearized in keeping with previous assumptions to the form

$$\Psi^{+}(\xi = -\frac{1}{2},\ c_x > 0) = -w$$

$$\Psi^{-}(\xi = +\frac{1}{2},\ c_x < 0) = +w$$

For the discrete ordinate method these conditions must hold for each κ so that the constants in Equations (37) and (38) are determined by applying the 2N relations

$$\Psi_{\kappa}^{\pm}(\xi = \mp\frac{1}{2}) = \mp w \qquad (\kappa = 1,2,\ldots,N) \tag{41}$$

Due to conditions of symmetry of the flow it can be shown that $C_j = -D_j$ and $F = 0$ so that only N of these relations are required and the solution of the Couette problem may be written

$$\Psi_{\kappa}^{+}(\xi) = \frac{1}{\sqrt{\pi}} \sum_{j=1}^{N-1} C_j \left[\frac{e^{p_j \xi}}{1 + \sqrt{\eta_j}\,\alpha_\kappa} - \frac{e^{-p_j \xi}}{1 - \sqrt{\eta_j}\,\alpha_\kappa} \right] + E(\xi - \frac{\mu}{d}\,\alpha_\kappa) \tag{42}$$

and

$$\Psi_{\kappa}^{-}(\xi) = \frac{1}{\sqrt{\pi}} \sum_{j=1}^{N-1} C_j \left[\frac{e^{p_j \xi}}{1 - \sqrt{\eta_j}\,\alpha_\kappa} - \frac{e^{-p_j \xi}}{1 + \sqrt{\eta_j}\,\alpha_\kappa} \right] + E(\xi + \frac{\mu}{d}\,\alpha_\kappa) \tag{43}$$

for $\kappa = 1,2,\ldots,N$. The C_j and E may be determined from the N equations

$$\frac{1}{\sqrt{\pi}} \sum_{j=1}^{N-1} C_j \left[\frac{e^{p_j/2}}{1 - \sqrt{\eta_j}\,\alpha_\kappa} - \frac{e^{-p_j/2}}{1 + \sqrt{\eta_j}\,\alpha_\kappa} \right] + E(\frac{1}{2} + \frac{\mu}{d}\,\alpha_\kappa) = w \tag{44}$$

for $\kappa = 1,2,\ldots,N$. It is possible to solve Equations (42) and (43) for $\Psi_\kappa^{\pm}/(w/2)$ so that the solution need not be repeated for each different velocity w/2 of the plates.

Solution for the Flow Quantities

The flow velocity and shear stress are found from Equations (22) and (23) and may be written as

$$\frac{q_z(\xi)}{(w/2)} = \bar{E}\xi + \frac{4}{\pi} \sum_{i=1}^{N} \sum_{j=1}^{N-1} H_i \bar{C}_j \frac{\sinh(p_j \xi)}{1 - \eta_j \alpha_i^2} \tag{45}$$

and

$$\frac{P_{xz}}{P_{xz_{f.m.}}} = 2\sqrt{\pi} \left[\frac{1}{4} \frac{\mu}{d} \bar{E} + \frac{2}{\pi} \sum_{i=1}^{N} \sum_{j=1}^{N-1} H_i \alpha_i^2 \bar{C}_j \sqrt{\eta_j} \frac{\cosh(p_j \xi)}{1 - \eta_j \alpha_i^2} \right] \tag{46}$$

In these equations $\bar{E} = E/w$, $\bar{C}_j = C_j/w$, and $P_{xz_{f.m.}}$ is the free molecular flow value of the shear stress, $-w/2\sqrt{\pi}$. Note that in all of these equations the α_i and H_i may be either those of the Gauss-Hermite quadrature or those of the modified half-range quadrature.

Computational Procedures

In order to obtain numerical values for the perturbed distribution function and the flow quantities, Equations (42) through (46) were solved on a Burroughs B-5500 digital computer. Since the equations may be programmed quite generally for arbitrary N, the cases of N = 4 and N = 7 were selected for study. Note that this is in sharp contrast with the moment method in which higher order approximations are obtained

only with increasing difficulty. Computations were made for values of inverse Knudsen numbers ranging from 0.01 to 50.0. The programming technique used required the simultaneous solutions of systems of linear algebraic equations, and these were accomplished using matrix inversion and matrix products subroutines. It was also necessary to solve for the roots of the characteristic polynomial of degree N and the Newton-Maehly procedure was used for this. These roots are tabulated in Table 3 for the cases N = 1 to N = 7. The discrete roots and weighting coefficients for the Gauss-Hermite quadrature were taken from page 569 of Kopal [22] while the values for the modified quadrature were generated on the computer using methods described in Chapter III. These generated values were reported in Table 1. Quantities computed were the perturbed distribution function evaluated at the appropriate discrete velocity ordinates, the flow velocity in the z-direction, the velocity derivative at the centerline, and the ratio of shear stress to the free molecular flow value of shear stress.

Results

In this section the results of the discrete ordinate method, using both Gauss-Hermite and the new modified quadratures, are compared with the results obtained by several other techniques. For convenience, each method is assigned a number according to the following key:

Method 1 — Numerical solution for the Couette problem given by Willis [26]

Method 2 — Solution of Gross, Jackson, and Ziering [12] using the second approximation in the half-range moment method

Table 3. Roots of the Characteristic Equation

$$\sum_{i=1}^{N} H_i \frac{1}{1 - \eta\alpha_i^2} = \frac{\sqrt{\pi}}{2}$$

for the Modified Quadrature

N = 1	N = 2	N = 3	N = 4	N = 5	N = 6	N = 7
0	0	0	0	0		0
	3.537247772	0.412285628	0.206557544	0.141743011	0.108614374	0.333652688
		14.334252997	1.040806772	0.380214132	0.223249845	1.030906060
			36.131427706	2.150952309	0.647059691	6.337974506
				72.461401785	3.873895194	202.602348648
					126.798547317	

Method 3 Solution due to Lees [27] using a form of the moment method

Method 4 Discrete ordinate method for N = 4 using the Gauss-Hermite quadrature

Method 5 Discrete ordinate method for N = 7 using the Gauss-Hermite quadrature

Method 6 Discrete ordinate method for N = 4 using the modified quadrature

Method 7 Discrete ordinate method for N = 7 using the modified quadrature.

Table 4 gives a comparison of the slip velocity at the walls using the methods listed above. It can be seen that both the half-range moment and the discrete ordinate methods give good results in the slip and near continuum flow regimes using the numerical solution of Willis as a standard. (Willis actually uses the numerical solution for $d/\mu \geq 1.0$ and the first iteration solution for $d/\mu < 1.0$.) However, in the transition and near free molecular flow regions the discrete ordinate method with modified quadrature gives a much better solution than any of the other analytical methods compared with Method 1. This fact is in clearer evidence when the actual velocity at the wall is considered in Table 5. Note that for $d/\mu = 0.01$ using the half-range moment method, the result is less than half of its appropriate value, whereas the modified quadrature allows the discrete ordinate method to yield a much more accurate result.

Tables 6 and 7 give a comparison of the results for the shear stress ratio. Here there is evidence that the Gauss-Hermite quadrature has a weakness in the near free molecular flow regime since the free molecular value computed by that quadrature is 5.6 per cent too large

Table 4. Comparison of the Results for Normalized Slip Velocity at the Walls,

$$[1 - q_z(\xi=1/2)/(w/2)]$$

d/μ*	METHOD 1	2	3	4	5	6	7
0.01	.9731	.9871		.9893	.9878	.9824	.9787
0.1	.8559	.8844		.9034	.8923	.8609	.8526
1.0	.4962	.4871	.6393	.5116	.5018	.4963	.4963
1.25	.4515	.4422	.5864	.4622	.4553	.4520	.4515
1.50	.4151	.4064	.5416	.4229	.4179	.4156	.4151
1.75	.3846		.5032	.3906	.3870	.3850	.3846
2.0	.3586	.3523	.4698	.3634	.3607	.3590	.3587
2.5	.3165		.4149	.3200	.3182	.3167	.3166
3.0	.2837	.2808	.3714	.2864	.2851	.2838	.2838
3.5	.2572		.3362	.2595	.2585	.2573	.2574
4.0	.2354	.2341	.3070	.2374	.2365	.2355	.2355
5.0	.2015	.2008	.2617	.2030	.2023	.2016	.2016
7.0	.1566	.1564	.2020	.1575	.1571	.1567	.1567
10.0	.1174	.1174	.1506	.1180	.1178	.1175	.1176

*An approximate breakdown of the different flow regimes for the values of d/μ reported in these tables is:

(i) $d/\mu < 0.1$ — near free molecular flow
(ii) $1.0 \leq d/\mu \leq 3.0$ — transition flow
(iii) $d/\mu > 3.0$ — slip flow

Table 5. Comparison of the Results for Normalized Velocity at the Walls,

$[q_z(\xi=1/2)/(w/2)]$

	METHOD					
d/μ	1*	2**	4	5	6	7
0.01	.0269	.0129	.0107	.0122	.0176	.0213
0.1	.1441	.1156	.0966	.1077	.1391	.1474
1.0	.5038	.5129	.4884	.4982	.5037	.5037
1.25	.5485	.5578	.5378	.5447	.5480	.5485
1.50	.5849	.5936	.5771	.5821	.5844	.5849
1.75	.6154		.6094	.6130	.6150	.6154
2.0	.6414	.6477	.6366	.6393	.6410	.6413

*Values for Method 1 for d/μ = 0.01, 0.1, and 1.0 are taken from Willis' analytical results [26].

**Values for Method 2 for d/μ = 0.01, 0.1, 1.25, and 1.5 are taken from a comparison made by Willis [26].

Table 6. Comparison of the Results for Shear Stress Ratio, $P_{xz}/P_{xz_{f.m.}}$

	METHOD						
d/μ	1	2	3	4	5	6	7
0.01	.9913†	.9913	.9944	1.0451	1.0214	.9913	.9913
0.1	.9259	.9215	.9466	.9738	.9512	.9241	.9254
1.0	.6008	.5899	.6393	.6127	.6058	.6010	.6007
1.25	.5517	.5427	.5864	.5603	.5552	.5513	.5511
1.50	.5099	.5025	.5416	.5170	.5130	.5097	.5096
1.75	.4745	.4687	.5032	.4805	.4772	.4743	.4742
2.0	.4440	.4391	.4698	.4490	.4463	.4436	.4436
2.5	.3938	.3904	.4149	.3975	.3955	.3933	.3933
3.0	.3539	.3516	.3714	.3569	.3552	.3535	.3535
4.0	.2946	.2934	.3070	.2967	.2955	.2943	.2943
5.0	.2526	.2517	.2617	.2540	.2531	.2522	.2522
7.0	.1964	.1960	.2020	.1973	.1968	.1963	.1963
10.0	.1474	.1472	.1506	.1479	.1476	.1473	.1473

†This value is reported as .9914 in Willis [48].

Table 7. Comparison of the Results for $[1 - P_{xz}/P_{xz_{f.m.}}]$

	METHOD					
d/μ	1	2	4	5	6	7
0.01	.008719†	.008746	-.0451	-.0214	.008706	.0086719
0.1	.07412	.07846	.0262	.0488	.0759	.07457
1.0	.3992	.4101	.3873	.3942	.3990	.3993
1.25	.4483	.4573	.4397	.4448	.4487	.4489
1.50	.4901	.4975	.4830	.4870	.4903	.4904
1.75	.5255	.5313	.5195	.5228	.5257	.5258
2.0	.5560	.5609	.5510	.5537	.5564	.5564

†This value is reported to be .0086 (rounded off) in Willis [48].

for N = 4 and about 2.9 per cent too large for N = 7. This error may be related to the fact that

$$\frac{P_{xz}}{P_{xz_{f.m.}}} = \frac{1}{w} \sum_{i=1}^{N} H_i \alpha_i (-\Psi_i^+ + \Psi_i^-) \tag{47}$$

which for the free molecular limit yields

$$\frac{P_{xz}}{P_{xz_{f.m.}}} = 2 \sum_{i=1}^{N} H_i \alpha_i \tag{48}$$

since $\Psi_i^+ \rightarrow -w$ and $\Psi_i^- \rightarrow +w$. For finite values of N using the Gauss-Hermite quadrature the above summation is not exactly equal to 1/2. Only in the limit as $N \rightarrow \infty$ does Equation (48) yield the correct result. However, use of the modified quadrature does yield the correct value regardless of the value of N since one of the relations used in generating the quadrature values is that

$$\sum_{i=1}^{N} H_i \alpha_i = \int_0^{\infty} e^{-u^2} u \, du = 1/2 \tag{49}$$

This is another indication of the advantages obtained by using the modified technique.

The velocity slope at the centerline is tabulated in Tables 8 and 9. Again, Methods 6 and 7 indicate much better results than any of the other analytical techniques when compared with the solution of Willis, particularly in the near free molecular flow regime.

Table 8. Comparison of the Results for

$$[1 - 1/2(dq_z/d\xi)_{\xi=0}]$$

	METHOD						
d/μ	1	2	3	4	5	6	7
0.01	.9749	.9871	.9944	.9893	.9878	.9824	.9787
0.1	.8680	.8864	.9468	.9034	.8924	.8619	.8571
1.0	.5556	.5110	.6393	.5231	.5254	.5643	.5565
1.25	.5154	.4768	.5864	.4794	.4881	.5265	.5145
1.50	.4821	.4514	.5416	.4460	.4591	.4923	.4807
1.75	.4537		.5032	.4194	.4353	.4618	.4525
2.0	.4290	.4150	.4698	.3976	.4148	.4347	.4282
2.5	.3881		.4149	.3633	.3801	.3899	.3881
3.0	.3550	.3625	.3714	.3364	.3508	.3547	.3554
3.5	.3275		.3362	.3139	.3253	.3263	.3281
4.0	.3041	.3208	.3070	.2943	.3028	.3027	.3048
5.0	.2664	.2828	.2617	.2610	.2654	.2656	.2670
7.0	.2136	.2244	.2020	.2108	.2122	.2139	.2141
10.0	.1641	.1695	.1506	.1617	.1630	.1649	.1647

Table 9. Comparison of the Results for

$$1/2(dq_z/d\xi)_{\xi=0}$$

	METHOD					
d/μ	1	2	4	5	6	7
0.01	.02509	.01294	.01072	.01222	.01757	.02126
0.1	.1320	.1136	.0966	.1076	.1381	.1429
1.0	.4444	.4890	.4769	.4746	.4357	.4435
1.25	.4846	.5232	.5206	.5119	.4735	.4855
1.5	.5179	.5486	.5540	.5409	.5077	.5193
1.75	.5463		.5806	.5647	.5382	.5475
2.0	.5710	.5850	.6024	.5852	.5653	.5718

The differences in the results of the various methods are illustrated graphically in Figures 2, 3, and 4. Figure 2 compares the percentage difference in slip velocity at the walls for the half-range moment method results of Gross, et al. [12] and for those of the discrete ordinate method using both quadrature forms as compared with the numerical calculations of Willis [26] in the Knudsen number range 0.1 to 1.0 (corresponding to $1.0 \leq d/\mu \leq 10.0$). Note that the accuracy of the discrete ordinate method using the Gauss-Hermite quadrature for the cases N = 4 and N = 7 compares favorably with that for the second approximation for the half-range moment method. Although higher approximations for the half-range moment method should result in greater accuracy, this can only be done at the expense of much more computational effort since each case must be treated separately. On the other hand, the cases for various values of N using the discrete ordinate method were obtained from a single computer program, the only changes involved being different input values for the roots and weighting coefficients for each new value of N.

When the modified quadrature is used, the percentage difference in these results and those of Willis is less than 0.1 per cent over this range of Knudsen numbers. It should be noted that Willis estimates the accuracy of his numerical calculation to be correct to within 0.2 per cent of the exact value, so that within the possible error of those answers the discrete ordinate method with modified quadrature for N = 4 and 7 gives the same results as the numerical solution.

The results of the shear stress ratio are compared in Figure 3. Again, over the range of Knudsen numbers considered the modified quadra-

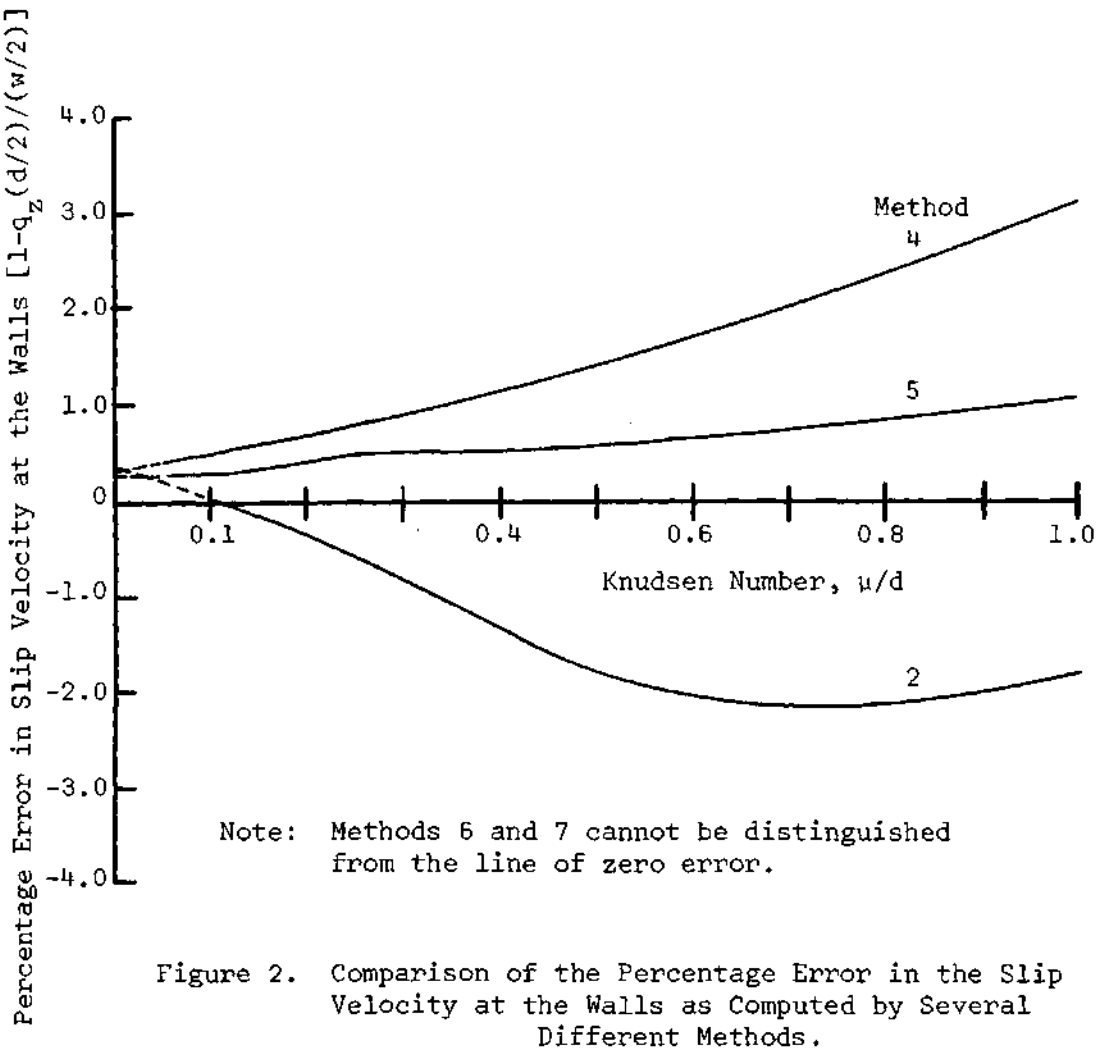

Note: Methods 6 and 7 cannot be distinguished from the line of zero error.

Figure 2. Comparison of the Percentage Error in the Slip Velocity at the Walls as Computed by Several Different Methods.

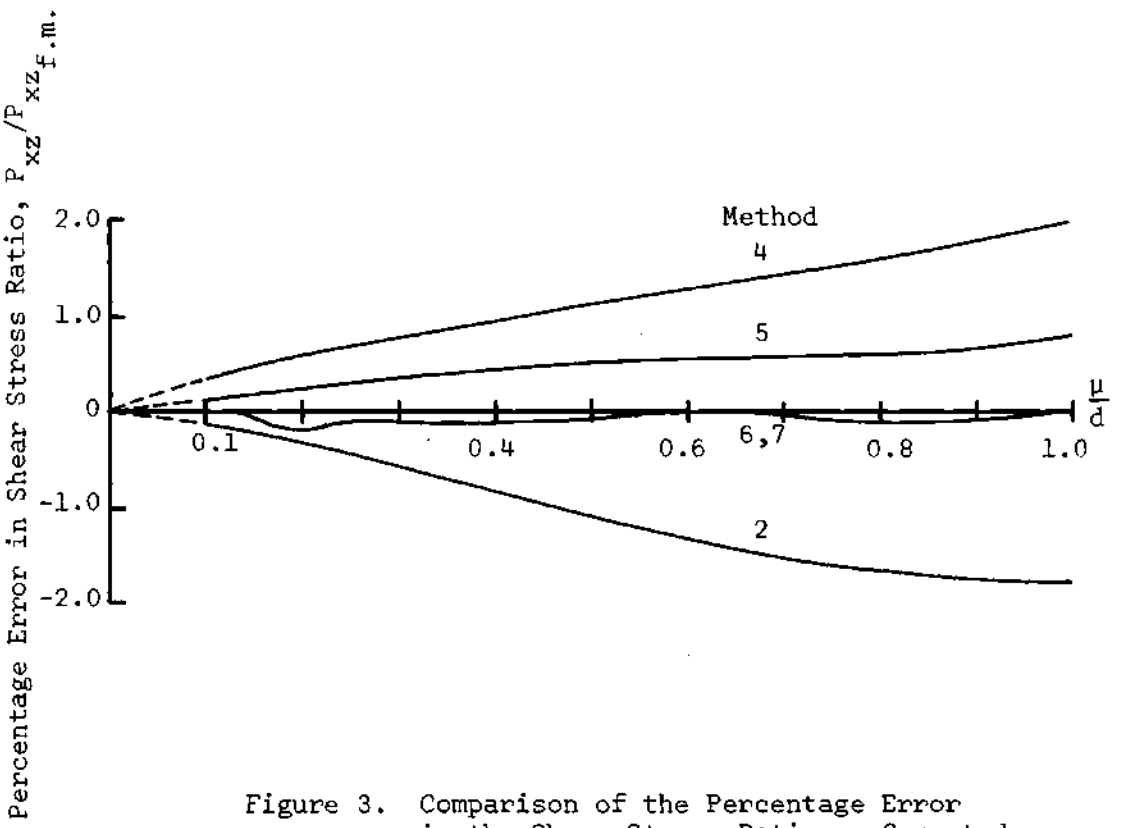

Figure 3. Comparison of the Percentage Error in the Shear Stress Ratio as Computed by Several Different Methods.

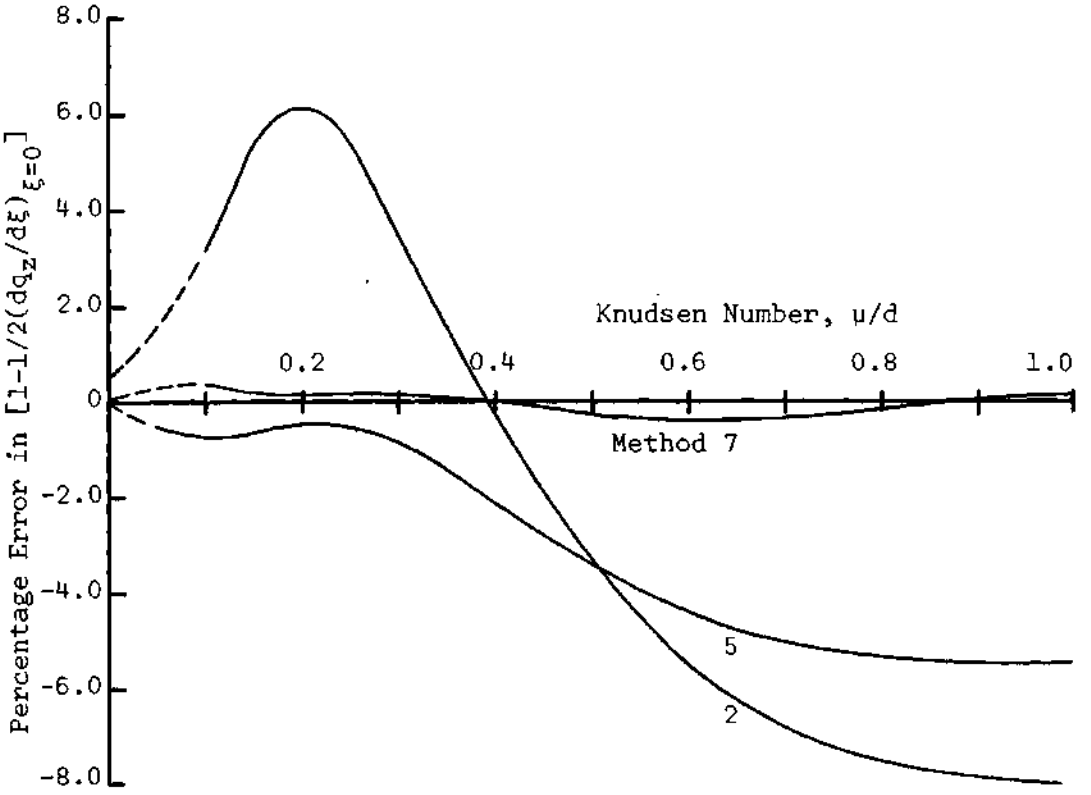

Figure 4. Comparison of the Percentage Error in the Difference Between the Continuum Limit for the Velocity Slope at the Centerline and the Value of this Quantity for Rarefied Gases as Computed by Several Different Methods.

ture yields answers which agree with the numerical solution to within the accuracy estimated by Willis. Figure 4 gives a comparison of the velocity slope at the centerline. Although here the percentage difference is noticeable, the discrete ordinate method when used with the modified quadrature is superior to any of the other analytical methods.

An important point to note is that the results obtained with the discrete ordinate method depart from those of the iteration technique in near free molecular flow. As discussed in Chapter III, this is due to the fact that the perturbed distribution function, after the first iteration on the free molecular solution, depends upon the evaluation of the integral

$$F(A) = \int_0^\infty e^{-\Omega^2 - A/\Omega} d\Omega$$

The near free molecular flow case corresponds to small A and the discrete ordinate method, although giving the exact result in the limit A = 0, has its greatest error over regions of extremely small A. This fact is illustrated in Figures 5 and 6 where the results for F(A) using this method are compared with the numerical solution for small A given by Willis [4]. The improvement of the modified quadrature over the Gauss-Hermite solution is quite evident in these figures.

The solution for the perturbed distribution function itself is illustrated in Figures 7 and 8 where the Ψ^- distribution function is plotted for conditions at the bottom plate and the Ψ^+ functions are plotted for conditions at the centerline for various values of d/μ and

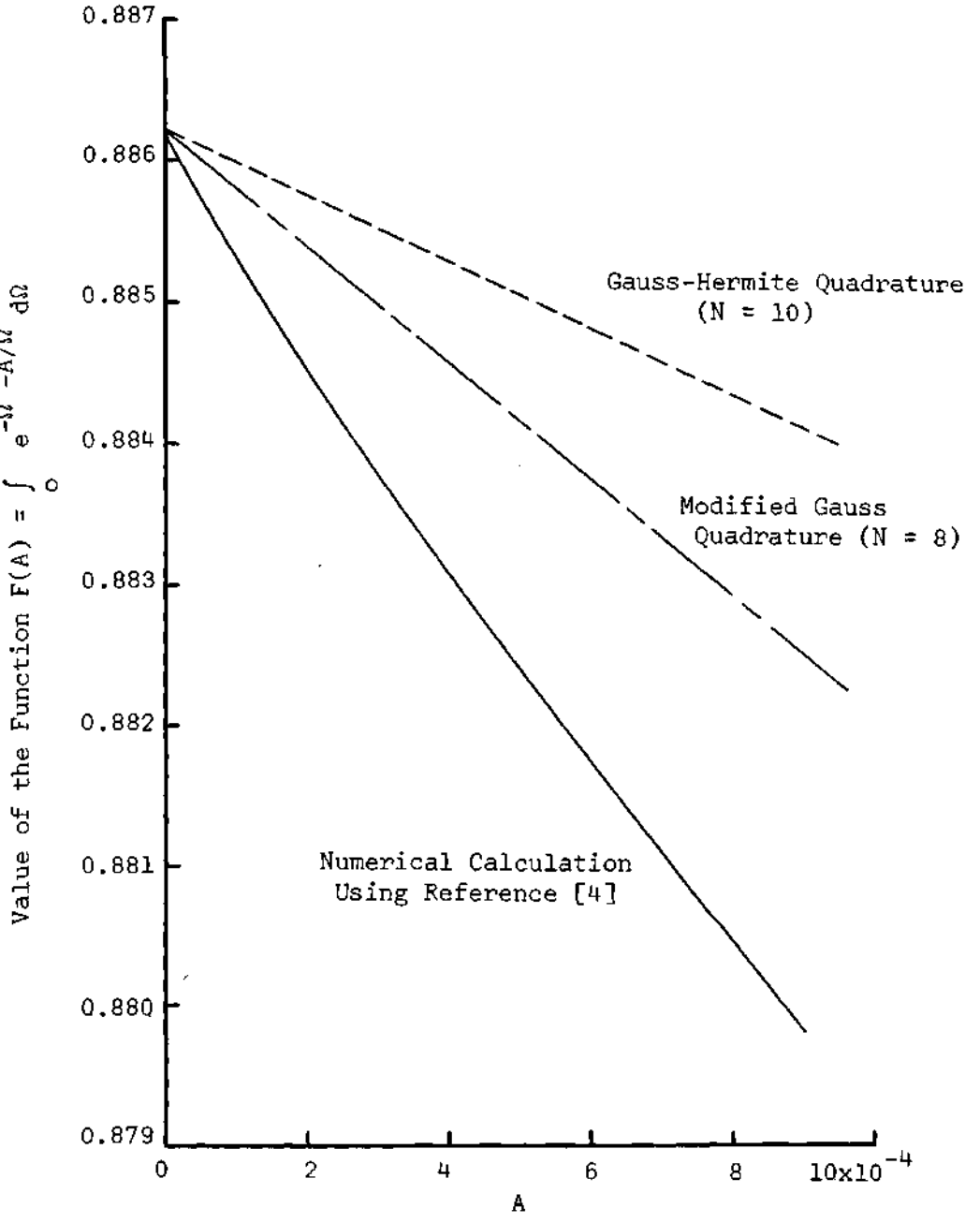

Figure 5. Comparison of the Gauss-Hermite and Modified Quadrature Techniques for the Evaluation of the Function F(A) for Extremely Small Values of A.

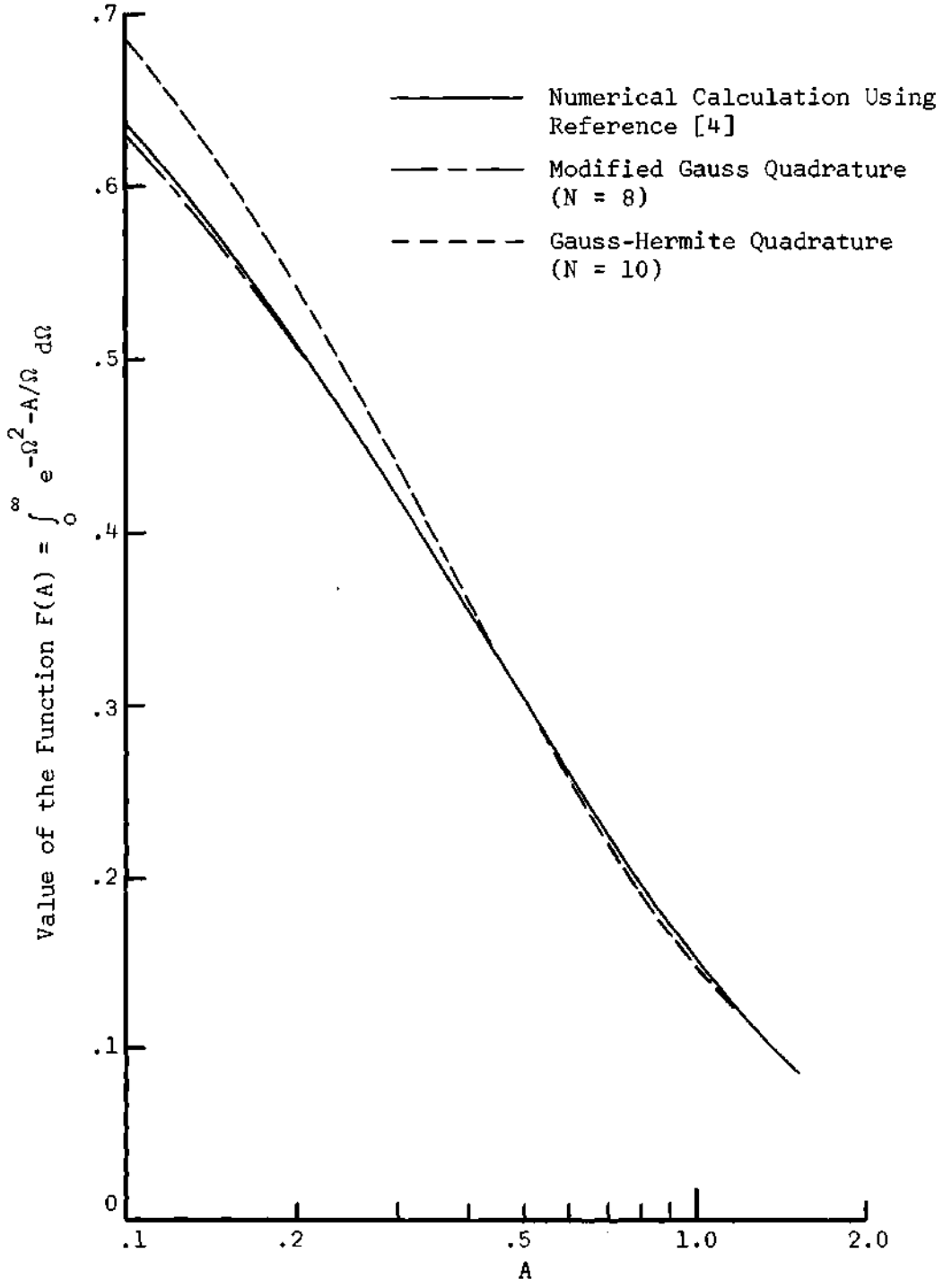

Figure 6. Comparison of the Gauss-Hermite and Modified Quadrature Techniques for the Evaluation of the Function F(A) for Small Values of A.

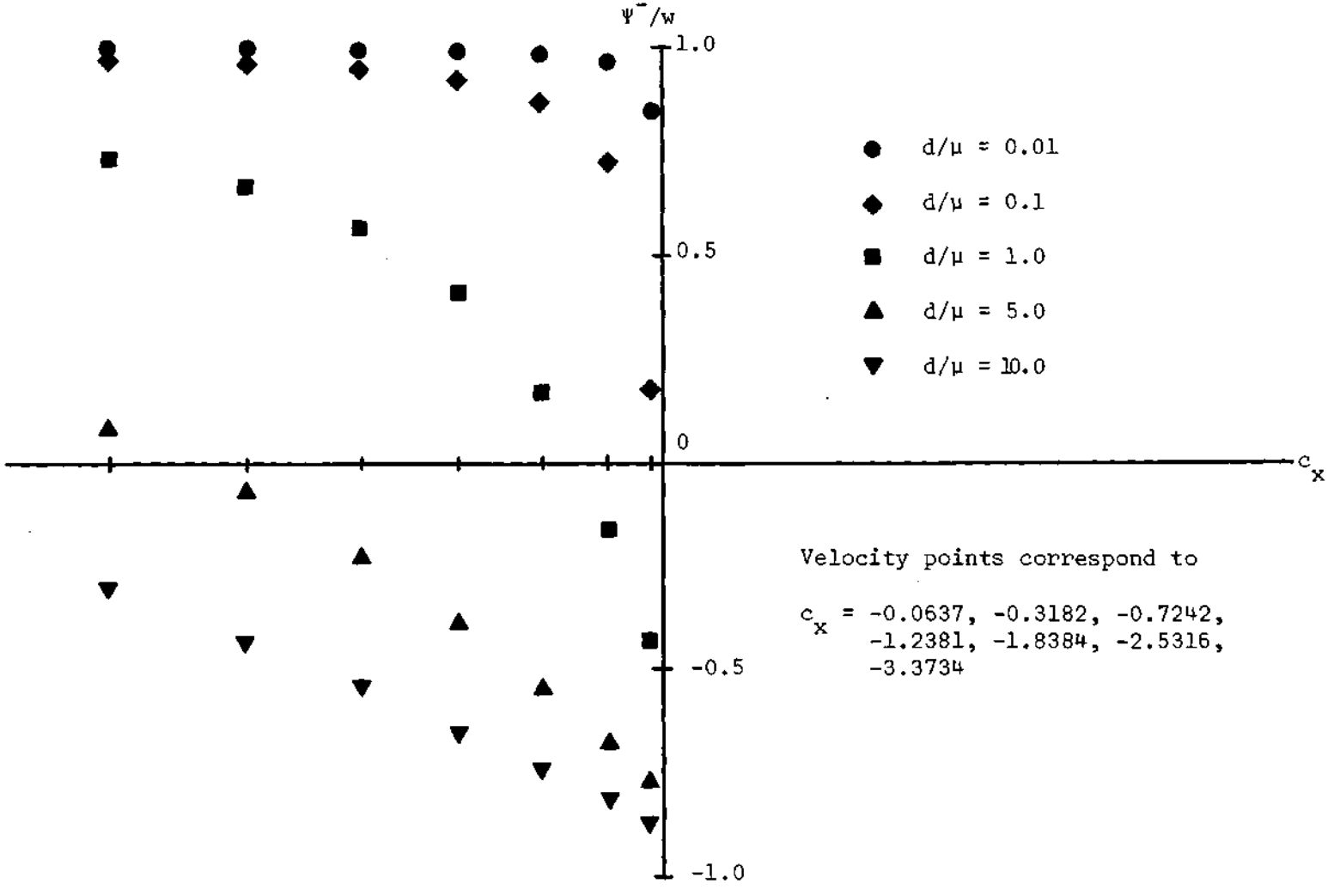

Figure 7. The Point-Function Description of the Perturbed Distribution Function, Ψ^-, at the Bottom Plate as the Inverse Knudsen Number Varies.

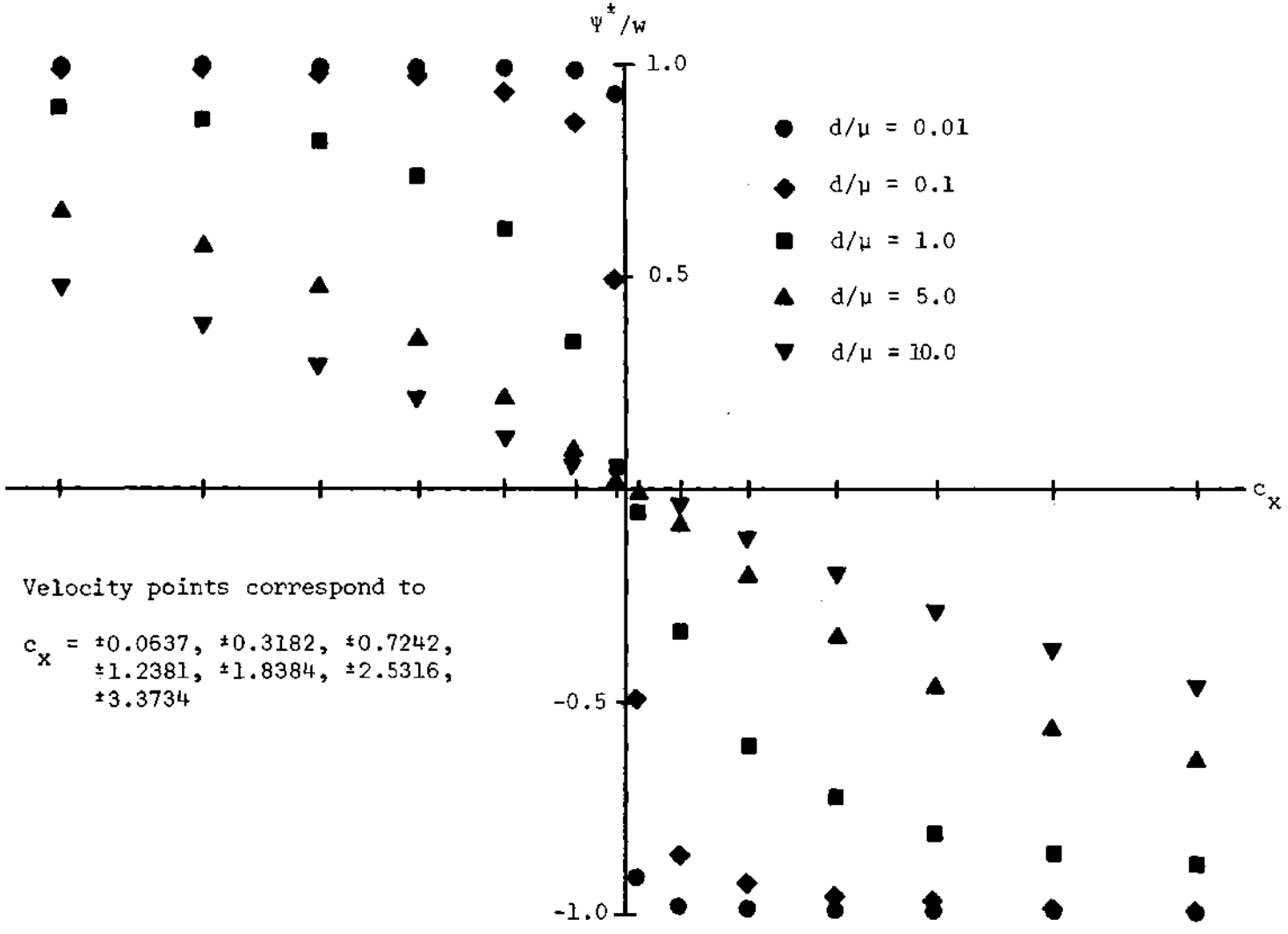

Figure 8. The Point-Function Description of the Perturbed Distribution Functions, Ψ^{+} and Ψ^{-}, at the Centerline Between the Plates as the Inverse Knudsen Number Varies.

N = 7. These figures indicate how the distribution function develops as the gas proceeds from a very rarefied to a near continuum condition.

It is interesting to compare the discrete ordinate solution for the perturbed distribution function in near free molecular flow to the solution obtained by using the iteration method with the free molecular collisionless solution as the zeroth iteration. The first iteration solution, given by Equation (4.19) of Willis [4], is

$$\Psi^{\pm} = \bar{+} \, e^{-\frac{d}{\mu}(\frac{1}{2} \pm \xi)/c_x} \tag{50}$$

Table 10 compares these values for $\Psi^{\pm}$ at the appropriate discrete velocity ordinates for c_x with the values obtained using the discrete ordinate method with modified quadrature for N = 7. The inverse Knudsen numbers considered are d/μ = 0.01, 0.1, and 1.0; and ξ is evaluated at the centerline between the plates so that ξ = 0. Although the macroscopic properties differ slightly from those obtained by Willis for the lowest value of Knudsen number (see Tables 5, 7, and 9), it can be seen from Table 10 that the agreement with the perturbed distribution function itself is excellent. In fact, the average percentage difference for the seven points is only 0.017. This indicates that there is little error incurred by replacing the integro-differential equation by the system of linear ordinary differential equations. Thus, any inaccuracies in the flow properties in the extremely rarefied cases ($d/\mu < 0.01$) must be due almost entirely to replacing the velocity moment integrations by the quadrature in Equations (45) and (46).

Since the accuracy of the discrete ordinate method increases with

Table 10. The Absolute Values of the Perturbed Distribution Function at the Center Line

Ψ_i/w	$d/\mu = 0.01$		$d/\mu = 0.1$		$d/\mu = 1.0$	
	A*	B**	A	B	A	B
Ψ_1/w	.924527	.925319	.456244	.490533	.000391	.057010
Ψ_2/w	.984409	.984574	.854587	.864859	.207760	.343504
Ψ_3/w	.993119	.993193	.933286	.938071	.501359	.603174
Ψ_4/w	.995970	.996012	.960420	.963272	.667745	.739345
Ψ_5/w	.997284	.997313	.973170	.975107	.761877	.814447
Ψ_6/w	.998027	.998048	.980443	.981857	.820774	.860877
Ψ_7/w	.998519	.998535	.985288	.986353	.862244	.893341

Average difference is 0.017 per cent for $d/\mu = 0.01$.

*A corresponds to results obtained using the iteration method with the zeroth iteration being the free molecular solution.

**B corresponds to the solution of the perturbed distribution function using the modified quadrature in the discrete ordinate method for N = 7.

increasing d/μ while that of the first iteration on the free molecular solution decreases, such a comparison as Table 10 may be useful in determining just how far a single iteration may be accurately carried out.

Finally, in order to demonstrate that the discrete ordinate method can yield accurate solutions well toward the continuum flow regime, the slip velocity, shear stress ratio, and velocity slope at the centerline are tabulated for N = 3 and values of d/μ from 20 to 50 in Table 11. Since the convergence of the method is quite rapid in the slip flow regime, values of N as low as two or three give quite good results for large values of d/μ.

Table 11. Results for the Flow Quantities for Large d/μ Using the Discrete Ordinate Method with Modified Quadrature, N = 3

d/μ	$q_z(\xi=1/2)/(w/2)$	$P_{xz}/P_{xz_{f.m.}}$	$1/2(dq_z/d\xi)_{\xi=0}$
20.0	.9348	.08044	.9079
30.0	.9558	.05533	.9365
40.0	.9664	.04217	.9516
50.0	.9728	.03406	.9609
∞	1.0000	0	1.0000

CHAPTER V

FULLY DEVELOPED CHANNEL FLOW

Definition of the Problem

The problem of fully developed flow between two infinite parallel plates offers another convenient test of the method of discrete ordinates. The geometry and coordinate system of this problem are shown in Figure 9. Experimentally, it has been observed that there is a minimum in the volume flow rate of the gas in the transition regime when plotted versus inverse Knudsen number. This has been indicated in the experimental results of Knudsen [29], Gaede [30], Rasmussen [31], and Dong [32]. However, there was no rigorous proof of the minimum flow rate at that time. In 1960 Takao [33] solved the Boltzmann equation with the BGK model and obtained a minimum in the volume flow rate for this problem; however, his solution was based on some unjustified physical and mathematical assumptions. Ziering [34] in 1960 solved this same problem by using the integral and half-range moment methods; unfortunately, his solution did not exhibit the desired minimum because he omitted a term in the Boltzmann equation.

Cercignani and Daneri [7] numerically solved the linearized Boltzmann equation with the BGK model in 1962 and obtained a minimum in the volume flow rate at an inverse Knudsen number very close to one. Stoy [5] and Huang and Stoy [6] applied the half-range moment method to this problem, obtained the desired minimum, and made a detailed study

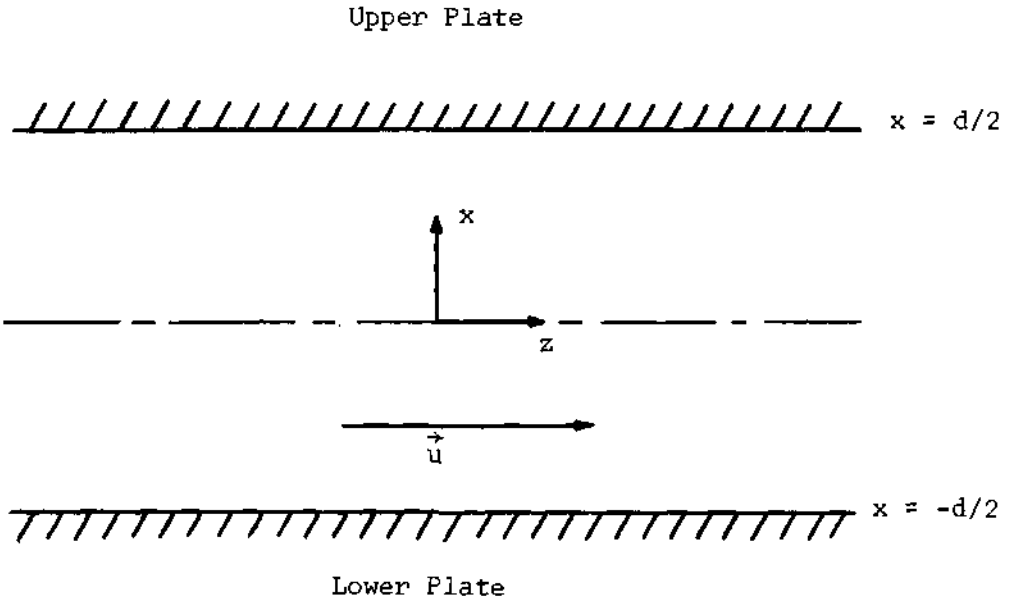

Figure 9. Geometry and Coordinate System for the Problem of Fully Developed Channel Flow.

of three different molecular models for the collision term in the Boltzmann equation--the BGK, hard sphere, and Maxwellian models.

In this chapter the discrete ordinate method is applied to this problem of fully developed flow between two infinitely long parallel plates with a constant pressure gradient in the z-direction, and the results are compared with the numerical solution of Cercignani and Daneri and with the analytical solution of Huang and Stoy using the half-range moment method.

Solution of the Governing Equation for Fully Developed Flow Between Two Parallel Plates

General Solution

It is assumed: (1) the flow is incompressible and isothermal, (2) the mass velocity profile is constant in the z-direction, and (3) the pressure gradient is constant. Thus, the linearized Boltzmann equation may be applied to the problem. Under the perturbation assumption that

$$f^{\pm} = f_o[1 + \Phi^{\pm}] \tag{51}$$

where

$$f_o = n_o \beta_o^3 \pi^{-3/2} e^{-c^2}$$

and

$$n_o = P_o/kT_o = P_i(1 + \bar{\kappa}z)/kT_o$$

the linearized Boltzmann equation becomes (see Huang and Stoy [6])

$$\bar{\kappa}\, c_z + c_x \frac{\partial \Phi^{\pm}}{\partial x} + \frac{\Phi^{\pm}}{\mu} = \frac{2}{\mu\pi^{3/2}} c_z \iiint_{-\infty}^{\infty} c_z \Phi e^{-c^2} d^3c \tag{52}$$

The $\bar{\kappa}$ is a constant which is proportional to the pressure gradient (assumed to be constant) and P_i is a reference pressure upstream. Assuming completely diffuse reflection from the surfaces, the boundary conditions are

$$f^{\pm}(x = \mp d/2, c_x) = f_o(z,\vec{c})\left\{\frac{1 \pm \text{sign } c_x}{2}\right\} \tag{53}$$

where

$$\text{sign } c_x = \begin{cases} +1 \ , & c_x > 0 \\ \\ -1 \ , & c_x < 0 \end{cases}$$

Again the relation $\Phi^{\pm}(x,\vec{c}) = c_z \Psi^{\pm}(x,c_x)$ satisfies the equation exactly so that the governing form is

$$\bar{\eta} + \frac{\mu}{d} c_x \frac{\partial \Psi^{\pm}}{\partial \xi} = -\Psi^{\pm} + \frac{1}{\sqrt{\pi}} \left[\int_o^{\infty} e^{-c_x^2} \Psi^{+} dc_x + \int_{-\infty}^{o} e^{-c_x^2} \Psi^{-} dc_x \right] \tag{54}$$

where $\xi = x/d$ and $\bar{\eta} = \bar{\kappa}\mu$. Note that Equation (54) is the same as that governing the Couette flow problem with the exception of the constant term $\bar{\eta}$. Thus, some of the work done in solving for the Couette flow case may be utilized here. First, the integral is replaced by a quadrature to yield

$$\bar{\eta} \pm \frac{\mu}{d} \alpha_\kappa \frac{d\Psi_\kappa^{\pm}}{d\xi} = - \Psi_\kappa^{\pm} + \frac{1}{\sqrt{\pi}} \sum_{i=1}^{N} H_i(\Psi_i^{+} + \Psi_i^{-}) \qquad (55)$$

This represents a system of 2N simultaneous, first-order, nonhomogeneous, linear, ordinary differential equations in the 2N unknowns $\Psi_\kappa^{\pm}$ for $\kappa = 1,2,\ldots,N$. Since the nonhomogeneous term is a constant and since the characteristic equation gives a two-fold degeneracy $p^2 = 0$, the complete solution exhibits a quadratic form in addition to the N - 1 pairs of exponential solutions. The details for solving this system are carried out in Appendix B. The complete solution may be written in the form

$$\frac{\Psi_\kappa^{+}}{\bar{\eta}} = \frac{1}{\sqrt{\pi}} \sum_{j=1}^{N-1} \left[\frac{\tilde{C}_j}{1 + \sqrt{\eta_j}\,\alpha_\kappa} e^{p_j \xi} + \frac{\tilde{D}_j}{1 - \sqrt{\eta_j}\,\alpha_\kappa} e^{-p_j \xi} \right] + \left(\frac{d}{\mu}\right)^2 \xi^2 \qquad (56)$$

$$+ \left(\tilde{S} - 2\alpha_\kappa \frac{d}{\mu}\right)\xi + \left(-1 + 2\alpha_\kappa^2 - \frac{\mu}{d}\alpha_\kappa \tilde{S} + \tilde{T}\right)$$

and

$$\frac{\Psi_\kappa^{-}}{\eta} = \frac{1}{\sqrt{\pi}} \sum_{j=1}^{N-1} \left[\frac{\tilde{C}_j}{1 - \sqrt{\eta_j}\,\alpha_\kappa} e^{p_j \xi} + \frac{\tilde{D}_j}{1 + \sqrt{\eta_j}\,\alpha_\kappa} e^{-p_j \xi} \right] + \left(\frac{d}{\mu}\right)^2 \xi^2 \qquad (57)$$

$$+ \left(\tilde{S} + 2\alpha_\kappa \frac{d}{\mu}\right)\xi + \left(-1 + 2\alpha_\kappa^2 + \frac{\mu}{d}\alpha_\kappa \tilde{S} + \tilde{T}\right)$$

The boundary conditions may be linearized to the relations

$$\psi_\kappa^{\pm}(\xi = \mp 1/2) = 0 \quad , \qquad \kappa = 1,2,\ldots,N$$

and are applied to Equations (56) and (57) in order to determine the constants $\tilde{C}_j$, $\tilde{D}_j$, $\tilde{S}$, and $\tilde{T}$. Due to the condition of symmetry of the problem, it may be shown from the resulting relations that $\tilde{C}_j = \tilde{D}_j$ and $\tilde{S} = 0$ so that the solution to Equation (55) may be written as

$$\frac{\psi_\kappa^{+}}{\bar{\eta}} = \frac{1}{\sqrt{\pi}} \sum_{j=1}^{N-1} \tilde{C}_j \left[\frac{e^{p_j \xi}}{1 + \sqrt{\eta_j}\,\alpha_\kappa} + \frac{e^{-p_j \xi}}{1 - \sqrt{\eta_j}\,\alpha_\kappa} \right] \tag{58}$$

$$+ \left(\frac{d}{\mu}\right)^2 \xi^2 - 2\alpha_\kappa \frac{d}{\mu}\,\xi + (-1 + 2\alpha_\kappa^2 + \tilde{T})$$

and

$$\frac{\psi_\kappa^{-}}{\bar{\eta}} = \frac{1}{\sqrt{\pi}} \sum_{j=1}^{N-1} \tilde{C}_j \left[\frac{e^{p_j \xi}}{1 - \sqrt{\eta_j}\,\alpha_\kappa} + \frac{e^{-p_j \xi}}{1 + \sqrt{\eta_j}\,\alpha_\kappa} \right] \tag{59}$$

$$+ \left(\frac{d}{\mu}\right)^2 \xi^2 + 2\alpha_\kappa \frac{d}{\mu}\,\xi + (-1 + 2\alpha_\kappa^2 + \tilde{T})$$

for $\kappa = 1,2,\ldots,N$. The constants $\tilde{C}_j$ and $\tilde{T}$ are to be determined from the equations

$$\frac{1}{\sqrt{\pi}} \sum_{j=1}^{N-1} \tilde{C}_j \left[\frac{e^{-p_j/2}}{1 + \sqrt{\eta_j}\,\alpha_\kappa} + \frac{e^{p_j/2}}{1 - \sqrt{\eta_j}\,\alpha_\kappa} \right] + \tilde{T} = \tag{60}$$

$$1 - \frac{1}{4}\left(\frac{d}{\mu}\right)^2 - \alpha_\kappa \frac{d}{\mu} - 2\alpha_\kappa^2$$

which result when the boundary conditions are applied. The p_j and η_j are again determined from the characteristic equation

$$\sum_{i=1}^{N} H_i \frac{1}{1 - \eta\alpha_i^2} = \frac{\sqrt{\pi}}{2} \tag{39}$$

and the relation $\eta = \left(\frac{\mu}{d} p\right)^2$.

Computation of the Volume Flow Rate

Applying the quadrature technique to the velocity moment integration gives the form

$$\frac{q_z(\xi)}{\bar{\eta}} = \frac{2}{\pi} \sum_{i=1}^{N} \sum_{j=1}^{N-1} H_i \tilde{C}_j \frac{\cosh(p_j \xi)}{1 - \eta_j \alpha_i^2} + \frac{1}{2}\left[\left(\frac{d}{\mu}\right)^2 \xi^2 + \tilde{T}\right] \tag{61}$$

The volume flow rate Q is obtained by integrating the velocity profile over the height of the channel and then dividing by this height and unit width to convert the quantity to volume flow rate per unit area. In order to compare directly with Cercignani's results the volume flow rate is then nondimensionalized by $\bar{\kappa}/2$. Thus, the expression for the nondimensional volume flow rate is

$$\bar{Q} = \frac{Q}{(\bar{\kappa}d/2)} = 2\,\frac{\mu}{d}\,\frac{Q}{\bar{\eta}}$$

or

$$\bar{Q} = \frac{8}{\pi} \sum_{i=1}^{N} \sum_{j=1}^{N-1} H_i \tilde{C}_j \frac{\sinh(p_j/2)}{p_j(1 - \eta_j \alpha_i^2)} + \frac{1}{12}\left(\frac{d}{\mu}\right)^2 + \tilde{T} \qquad (62)$$

It is this relation which is compared to the results of Cercignani and of Huang and Stoy in the following discussions. Computational procedures for this problem are very similar to those for the Couette problem of Chapter IV. Both the Gauss-Hermite and the modified quadratures were used and inverse Knudsen numbers ranged from 0.01 to 20.0. Values of N used were N = 4 and 8 for the Gauss-Hermite case and N = 2 through 7 for the modified quadrature. The perturbed distribution function, velocity profile, and volume flow rate were all computed; however, only the results for the velocity profile and the volume flow rate are presented here.

Results

The results obtained by applying the discrete ordinate method to this problem are compared with the numerical solution by Cercignani and Daneri and with the solution by the half-range moment method of Huang and Stoy. Figure 10 gives a comparison of the discrete ordinate results using the Gauss-Hermite (N = 4 and N = 8) and modified quadratures (N = 4 and N = 7). Note that there is no minimum in the volume flow rate even for the high order approximation N = 8 using the Gauss-Hermite

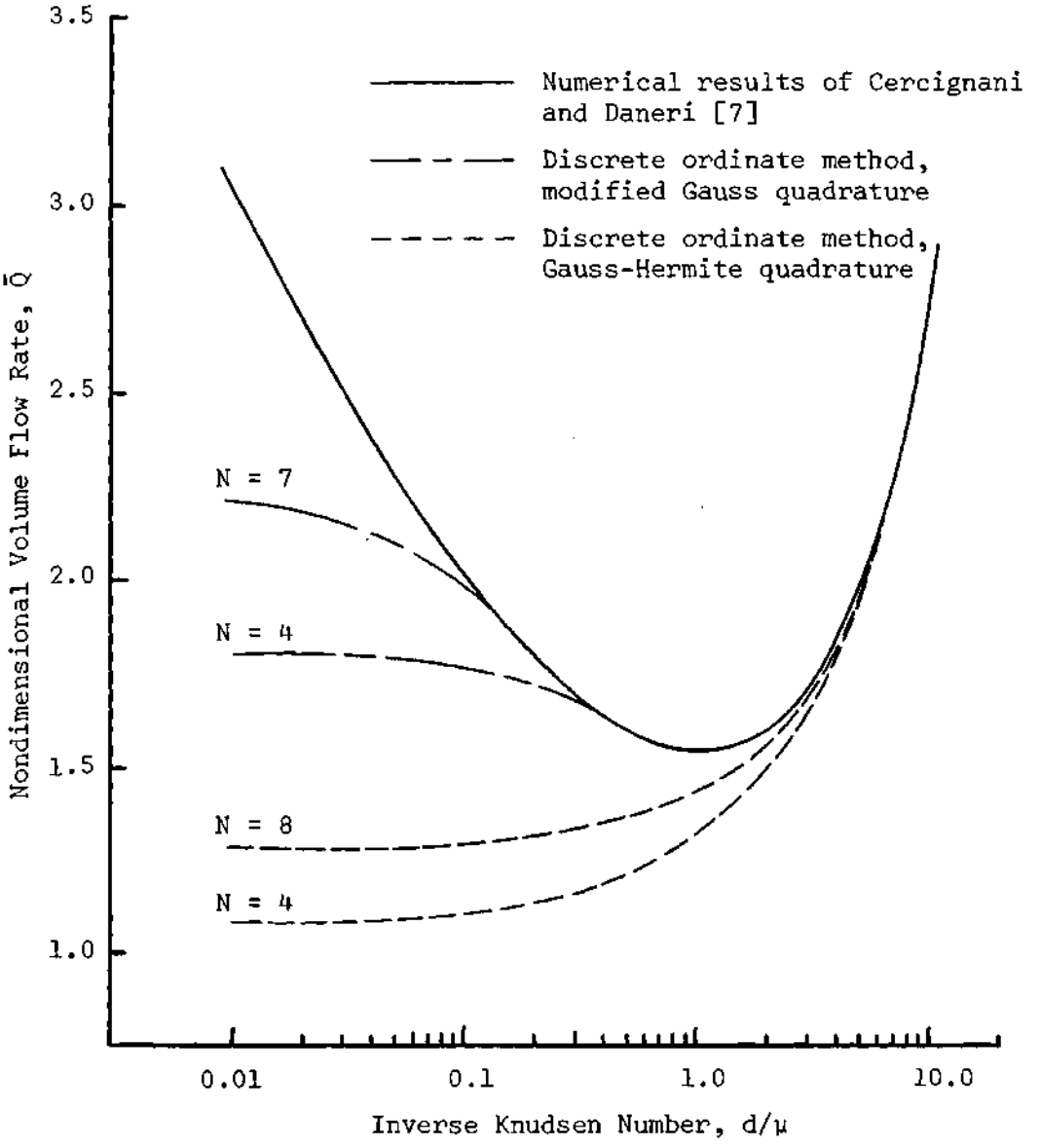

Figure 10. Solution for the Volume Flow Rate Using the Discrete Ordinate Method Compared with the Numerical Results of Cercignani and Daneri.

quadrature. However, the modified quadrature yields a well-defined minimum for N = 4 and the results for N = 7 extend accurately well into the near free molecular flow regime. It is important to note that the trend of the volume flow rate toward infinity as d/μ approaches zero is not predicted by the discrete ordinate method or by the moment method as will be seen in the next figure. Physically, this behavior of the volume flow rate toward infinity is incorrect; it should actually approach some limiting value as experiments indicate. Mathematically, however, this behavior does satisfy Equation (52) as is evidenced both by the numerical results and by an earlier iteration argument of Cercignani [35]. This is due to the fact that the important assumption that the mass velocity profile is constant in the z-direction becomes questionable at the low densities. It is felt that if the two dimensional problems were considered (i.e. include the z-dependence in the Ψ function), a finite limit for $\bar{Q}$ would be obtained as the inverse Knudsen number approaches zero. This problem is being investigated (see Huang and Stoy [6]). Despite this physical evidence, it is seen mathematically that it is necessary to go to higher values of N in order to obtain accurate solutions to Equation (52) in extremely rarefied flows (corresponding to $d/\mu < 0.01$).

Figure 11 gives the results of the volume flow rate for the modified quadrature for N = 2 through 7. The second and third half-range moment approximations yield results which fall exactly on the curves reported for the modified quadrature with N = 2 and 3. The results for the moment method are taken from Stoy [5]. Reference to Stoy's thesis or to the paper by Huang and Stoy [6] indicates that a considerable

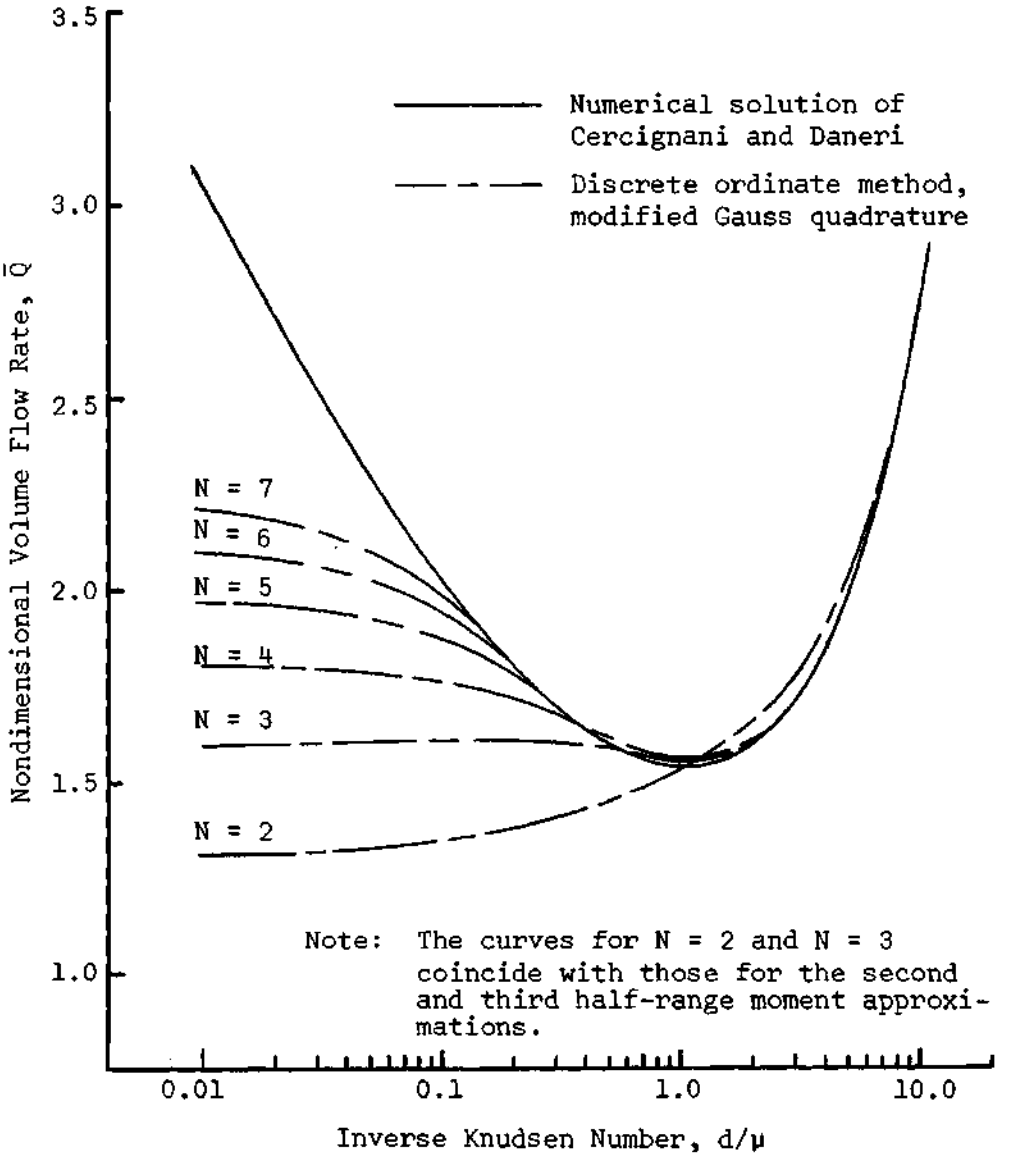

Figure 11. The Volume Flow Rate Using the Discrete Ordinate Method with Modified Quadrature Compared with the Numerical Results of Cercignani and Daneri and with the Analytic Results of Huang and Stoy.

amount of work is involved in obtaining the third moment approximation, and to try to obtain higher approximations requires considerably more effort since the method does not appear to lend itself to a general solution for an arbitrary order of approximation. These particular curves in Figure 11 point out the time saving advantages of the discrete ordinate method.

It may also be seen in this figure that for $d/\mu > 4.0$ the results for $N \geq 2$ with the modified quadrature and those for the second and third half-range moment approximations all give good agreement with the numerical solution of Cercignani. This is indicative of the rapid convergence of the quadrature and moment methods in the slip flow regime. Some of the results of the calculations of volume flow rate using the modified quadrature method are recorded in Table 12 along with the values reported by Cercignani and Daneri.

It is interesting to note the development of the velocity profiles as the Knudsen number varies. Figure 12 illustrates several of these, indicating the changes as the gas proceeds from a near free molecular state to a near continuum one. For small d/μ the shape of the profile is nearly flat. As the mean free path decreases, this shape develops toward the parabolic form typical of continuum flow. The slip velocity at the wall decreases since more intermolecular collisions are taking place close to the surface.

Finally, it can be concluded that according to the discrete ordinate method general solutions of Equation (55) can readily be found. It is expected that the numerical results can be obtained to any desired degree of accuracy by increasing the number of discrete ordinates.

Table 12. Results for the Channel Flow Solution by Discrete Ordinate Method Using Modified Quadrature Compared to the Numerical Results of Cercignani and Daneri [7]

d/μ	Reference [7]	Modified Quadrature N = 4	Modified Quadrature N = 7
0.01	3.0499	1.8065	2.2114
0.02	2.7114	1.8027	2.1819
0.03	2.5242	1.7988	2.1533
0.04	2.3973	1.7947	2.1259
0.05	2.3026	1.7906	2.0994
0.06	2.2228	1.7864	2.0741
0.07	2.1668	1.7821	2.0497
0.08	2.1154	1.7778	2.0264
0.09	2.0716	1.7734	2.0004
0.1	2.0331	1.7690	1.9829
0.2	1.8087	1.7246	1.8167
0.3	1.7030	1.6834	1.7131
0.4	1.6415	1.6478	1.6474
0.5	1.6025	1.6187	1.6050
0.6	1.5769	1.5956	1.5772
0.7	1.5599	1.5780	1.5592
0.8	1.5491	1.5651	1.5478
0.9	1.5471	1.5562	1.5412
1.0	1.5396	1.5506	1.5381
2.0	1.5963	1.5951	1.5950
3.0	1.7117	1.7100	1.7106
4.0	1.8468	1.8460	1.8459
5.0	1.9928	1.9912	1.9908
6.0	2.1421	2.1416	2.1411
7.0	2.2957	2.2955	2.2945
8.0	2.4516	2.4517	2.4512
9.0	2.6091	2.6097	2.6093
10.0	2.7669	2.7691	2.7687

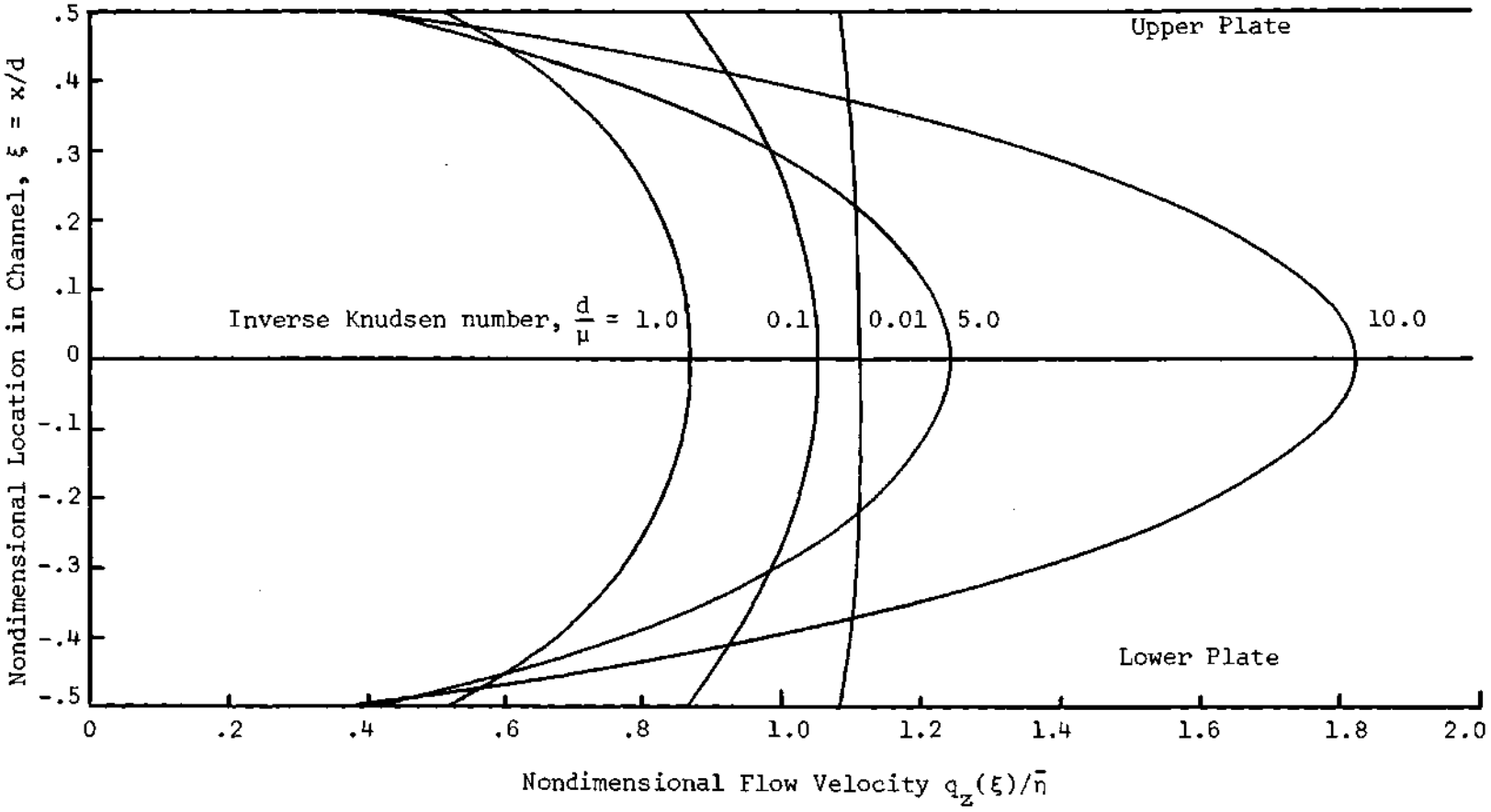

Figure 12. Variation of the Velocity Profile Across the Channel as the Inverse Knudsen Number Changes.

CHAPTER VI

TRANSIENT DEVELOPMENT OF COUETTE FLOW BETWEEN PARALLEL PLATES

Background of the Problem

The problem of describing the transient development of the flow between two parallel plates which are accelerated in opposite directions from rest to some constant velocity has been solved only for the case of continuum flow. This may easily be done by assuming an impulsive acceleration and then finding a corresponding time dependent solution to the Navier-Stokes equations. For example, this is done in Schlichting [36]. This problem has not previously been approached from the kinetic theory viewpoint, although it offers an interesting and convenient geometry on which to test any new techniques for solving the time dependent Boltzmann equation.

A study of this problem by the method of discrete ordinates not only serves as an application of the method to a time dependent problem, but it also contributes to a thorough understanding of the physical phenomena occurring during the time from which the fluid is initially disturbed until it reaches a steady state condition. Examining this transient behavior from the kinetic theory approach gives a clear picture of how the molecules are initially disturbed, propagate their disturbances to other particles in the flow field, and finally, through the collisional process, come to a statistically steady distribution.

The Unsteady Linearized Equation

Solution for Very Small Time

If the time after the initial disturbance of the boundaries is very small compared to the collision time of the gas molecules, then the problem may be treated as a free molecular flow case. This is due to the fact that there has been insufficient time for a significant number of collisions to occur, and the transport phenomena are a diffusive rather than a collisional process.

The Boltzmann equation for this case is

$$\frac{\partial f^{\pm}}{\partial t} + v_x \frac{\partial f^{\pm}}{\partial x} = 0 \tag{63}$$

where the notation $f^{\pm}$ signifies the two-stream character of the distribution function. For the case of impulsively accelerating the plates with velocities $\pm w/2$, this problem is readily solved by the method of Laplace transforms. However, since the discrete ordinate method is to be applied in this research to the linearized form of the Boltzmann equation, attention will be turned to the solution of the equation

$$\frac{\partial \Psi^{\pm}}{\partial \tau_1} + c_x \frac{\partial \Psi^{\pm}}{\partial x} = 0 \tag{64}$$

with the linearized boundary conditions $\Psi^{\pm}(x = \mp d/2, \tau_1) = \mp w$ and initial conditions $\Psi^{\pm}(x \neq \mp d/2, \tau_1 = 0) = 0$. Here, $\Psi^{\pm}$ is defined in Equation (19) and $\tau_1 = t/\beta$ which has the dimension of distance.

Equation (64) is solved in detail in Appendix C. For the case of impulsive acceleration the resulting solution is

$$\psi^{+}(x,\tau_1) = \begin{cases} 0 & \text{for } x > \tau_1 c_x - d/2 \ , \quad c_x > 0 \\ -w & \text{for } x < \tau_1 c_x - d/2 \ , \quad c_x > 0 \end{cases} \tag{65}$$

$$\psi^{-}(x,\tau_1) = \begin{cases} 0 & \text{for } x < d/2 + \tau_1 c_x \ , \quad c_x < 0 \\ +w & \text{for } x > d/2 + \tau_1 c_x \ , \quad c_x < 0 \end{cases}$$

Note that this solution represents a step-like propagation of the perturbed distribution function with the nondimensional velocity c_x and the magnitude w, so that this is a discontinuous function. However, the macroscopic properties are all continuous since they are formed by integrations over velocity space. For example, the flow velocity is given by

$$q_z(x,\tau_1) = \frac{1}{2\sqrt{\pi}} \left[\int_0^{\infty} e^{-c_x^2} \psi^{+}(x,\tau_1) dc_x + \int_{-\infty}^{0} e^{-c_x^2} \psi^{-}(x,\tau_1) dc_x \right] \tag{66}$$

so that, from Appendix C,

$$\frac{q_z(x,\tau_1)}{(w/2)} = \frac{1}{2} \left[\operatorname{erfc} \left(\frac{d/2 - x}{\tau_1} \right) - \operatorname{erfc} \left(\frac{d/2 + x}{\tau_1} \right) \right] \tag{67}$$

where $\tau_1 = t/\beta$. These results are illustrated in Figure 13. It is seen that the velocity at the top plate remains at the initial value of $q_z/(w/2) = 1/2$ until the stream of molecules from the bottom plate, which has a net macroscopic velocity in the opposite direction, has had time to diffuse across the channel and affect the flow velocity at the upper wall. If the flow is in a truly free molecular state, this process will continue until the flow velocities of the opposing streams have had time to exactly cancel each other leaving a net velocity of zero. If, however, the gas is of sufficient density for collisions to occur between the opposing streams, the solutions presented in Equations (65) and (67) are valid only for a length of time somewhat less than the collision time of the gas molecules. If Equation (64) is multiplied by μ, the mean free path, then it may be written as

$$\frac{\partial \Psi^{\pm}}{\partial \bar{\tau}} + c_x \frac{\partial \Psi^{\pm}}{\partial \bar{x}} = 0$$

where $\bar{x} = x/\mu$ is the ratio of actual length to mean free path and $\bar{\tau} = t/\beta\mu$ is the ratio of true time to the collision time. Hence, for finite values of μ, Equations (65) and (66) may be applied for $\bar{\tau} < 1$ or $\bar{x} < 1$.

Solution by Discrete Ordinates

In Chapter II the discrete ordinate method was applied to the linearized, time dependent Boltzmann equation with the resulting form being

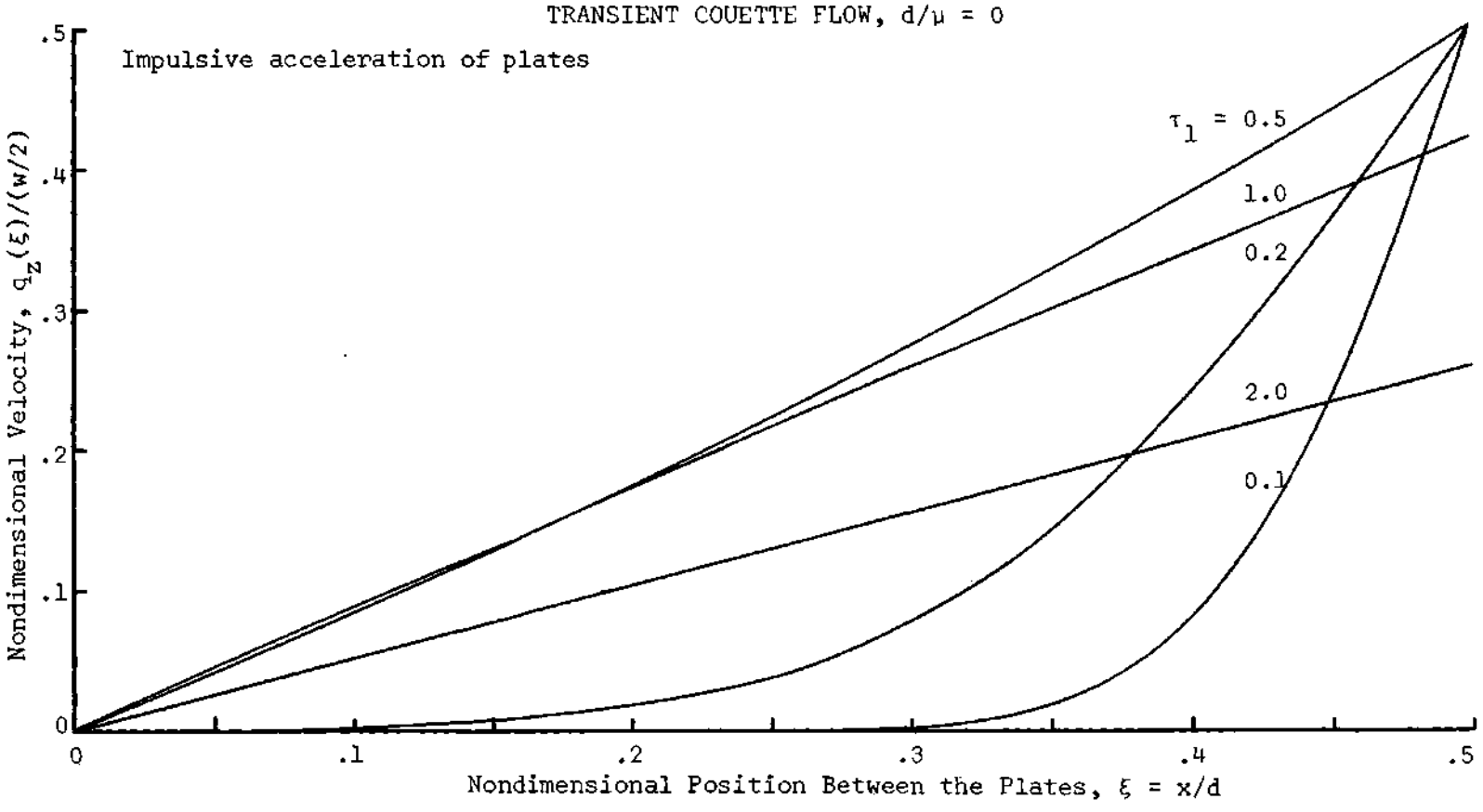

Figure 13. Analytic Solution for the Time Dependent Velocity Profile Development for Free Molecular Flow of the Transient Couette Problem with Impulsive Acceleration of the Plates.

$$\beta \frac{\partial \Psi_\kappa^{\pm}}{\partial t} \pm \alpha_\kappa \frac{\partial \Psi_\kappa^{\pm}}{\partial x} = \frac{n\beta}{\sigma} \left[-\Psi_\kappa^{\pm} + \frac{1}{\sqrt{\pi}} \sum_{i=1}^{N} H_i (\Psi_i^{+} + \Psi_i^{-}) \right] \tag{17}$$

Letting $\mu = \sigma/n\beta$ and $\xi = x/d$ as before, this equation may be written as

$$\frac{\partial \Psi_\kappa^{\pm}}{\partial \tau} \pm \alpha_\kappa \frac{\partial \Psi_\kappa^{\pm}}{\partial \xi} = \frac{d}{\mu} \left[-\Psi_\kappa^{\pm} + \frac{1}{\sqrt{\pi}} \sum_{i=1}^{N} H_i (\Psi_i^{+} + \Psi_i^{-}) \right] \tag{68}$$

where $\tau = t/\beta d$ is the ratio of actual time to the average time required for a molecule to traverse the distance between the plates. The boundary conditions for accelerating the plates impulsively are

$$\Psi_\kappa^{\pm}(\xi = \bar{+}1/2, \tau) = \bar{+}w \quad ; \qquad \kappa = 1,2,\ldots,N \tag{69}$$

while the initial conditions describing the requirement that the gas is at rest in Maxwellian equilibrium before the motion starts are

$$\Psi_\kappa^{\pm}(\xi \neq \bar{+}1/2, \tau = 0) = 0 \; ; \quad \kappa = 1,2,\ldots,N \tag{70}$$

From the experience gained in the solution of steady Couette flow it is known that in order to achieve accurate results, N (the number of discrete points) must be two or larger. This means that the problem is now represented by a linear system of homogeneous, first order, partial differential equations which are coupled by the summation term in each relation. Since it is quite difficult to obtain an analytic solution for such a problem, this system of differential equations was transformed

into a set of finite difference equations. A von Neumann stability analysis [37] indicated that it was possible to use an explicit, forward difference scheme in time and an implicit, central difference scheme in space. This is demonstrated in Appendix D. Thus, the difference forms are

$$\frac{\partial \psi_\kappa^{\pm}}{\partial \tau} = \frac{\psi_\kappa^{\hat{n}+1}(\hat{i})^{\pm} - \psi_\kappa^{\hat{n}}(\hat{i})^{\pm}}{\delta\tau} \tag{71}$$

$$\frac{\partial \psi_\kappa^{\pm}}{\partial \xi} = \frac{\psi_\kappa^{\hat{n}+1}(\hat{i}+1)^{\pm} - \psi_\kappa^{\hat{n}+1}(\hat{i}-1)^{\pm}}{2h} \tag{72}$$

where $\delta\tau$ and h are the time and space finite difference steps, and $\psi_\kappa^{\hat{n}}(\hat{i})^{\pm}$ represents the value of the function $\psi_\kappa(\xi,\tau)^{\pm}$ at time step $\hat{n}$ and space step $\hat{i}$. Thus, the system of difference equations becomes

$$\frac{\psi_\kappa^{\hat{n}+1}(\hat{i})^{\pm} - \psi_\kappa^{\hat{n}}(\hat{i})^{\pm}}{\delta\tau} \pm \alpha_\kappa \frac{\psi_\kappa^{\hat{n}+1}(\hat{i}+1)^{\pm} - \psi_\kappa^{\hat{n}+1}(\hat{i}-1)^{\pm}}{2h} \tag{73}$$

$$= \frac{d}{\mu}\{-\psi_\kappa^{\hat{n}}(\hat{i})^{\pm} + \frac{1}{\sqrt{\pi}} \sum_{i=1}^{N} H_i[\psi_i^{\hat{n}}(\hat{i})^{+} + \psi_i^{\hat{n}}(\hat{i})^{-}]\} \quad \text{for } \kappa = 1,2,\ldots,N.$$

Results

The system of Equations (73) was solved on the Burroughs B-5500 digital computer for various values of d/μ with N = 4 and N = 7 using the modified quadrature. Figures 14 through 17 report typical results

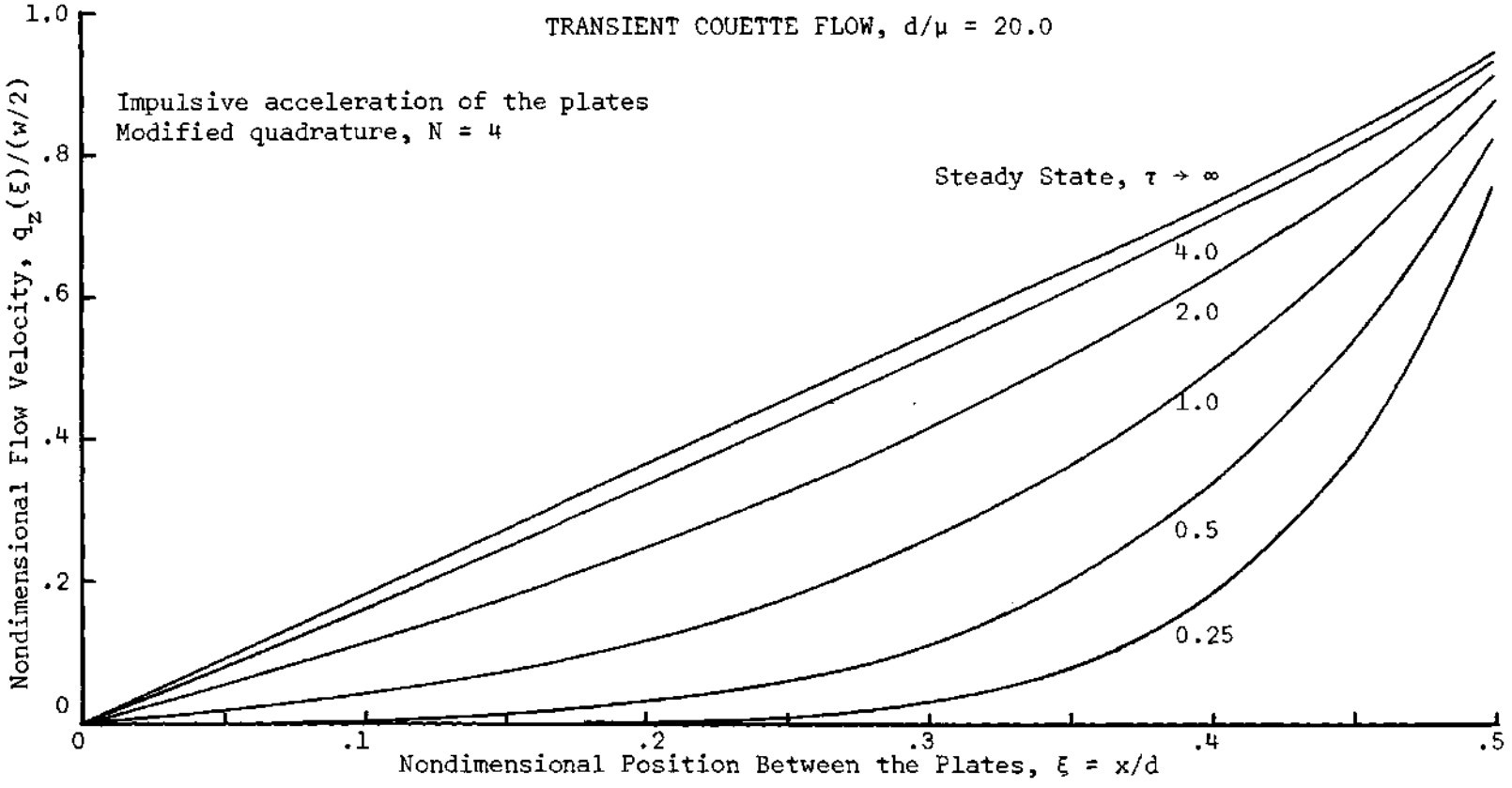

Figure 14. Transient Development of the Velocity Profile in Couette Flow for Impulsive Acceleration of the Plates, d/μ = 20.0 and N = 4.

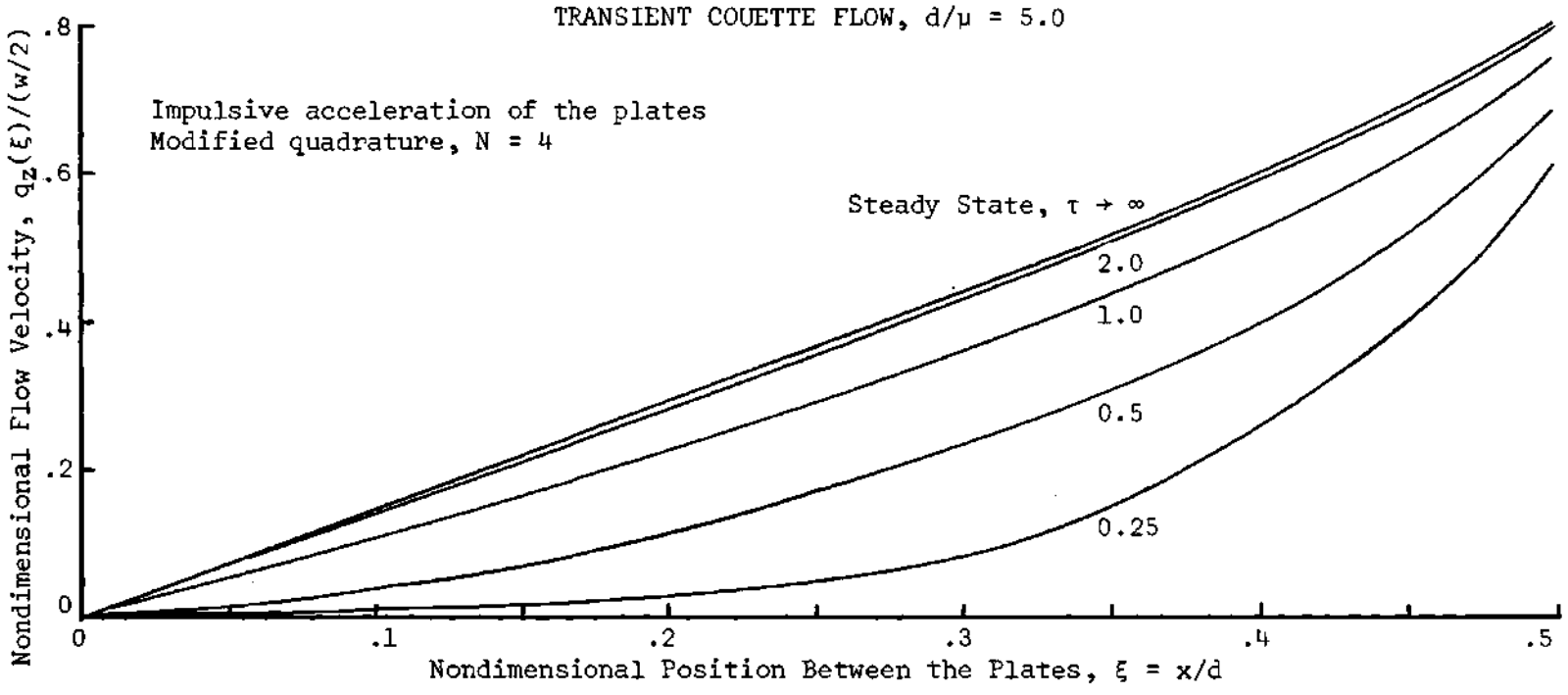

Figure 15. Transient Development of the Velocity Profile in Couette Flow for Impulsive Acceleration of the Plates, d/μ = 5.0 and N = 4.

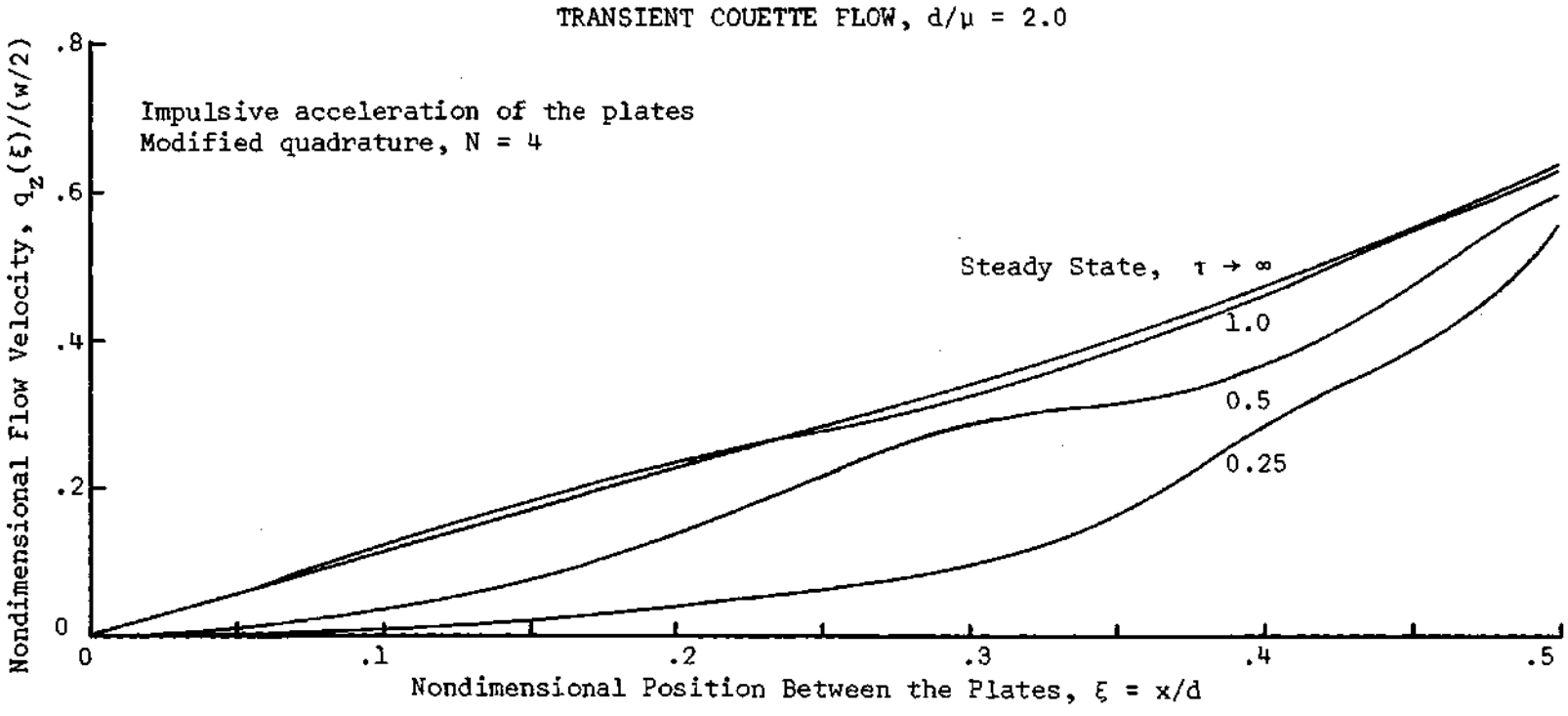

Figure 16. Transient Development of the Velocity Profile in Couette Flow for Impulsive Acceleration of the Plates, d/μ = 2.0 and N = 4.

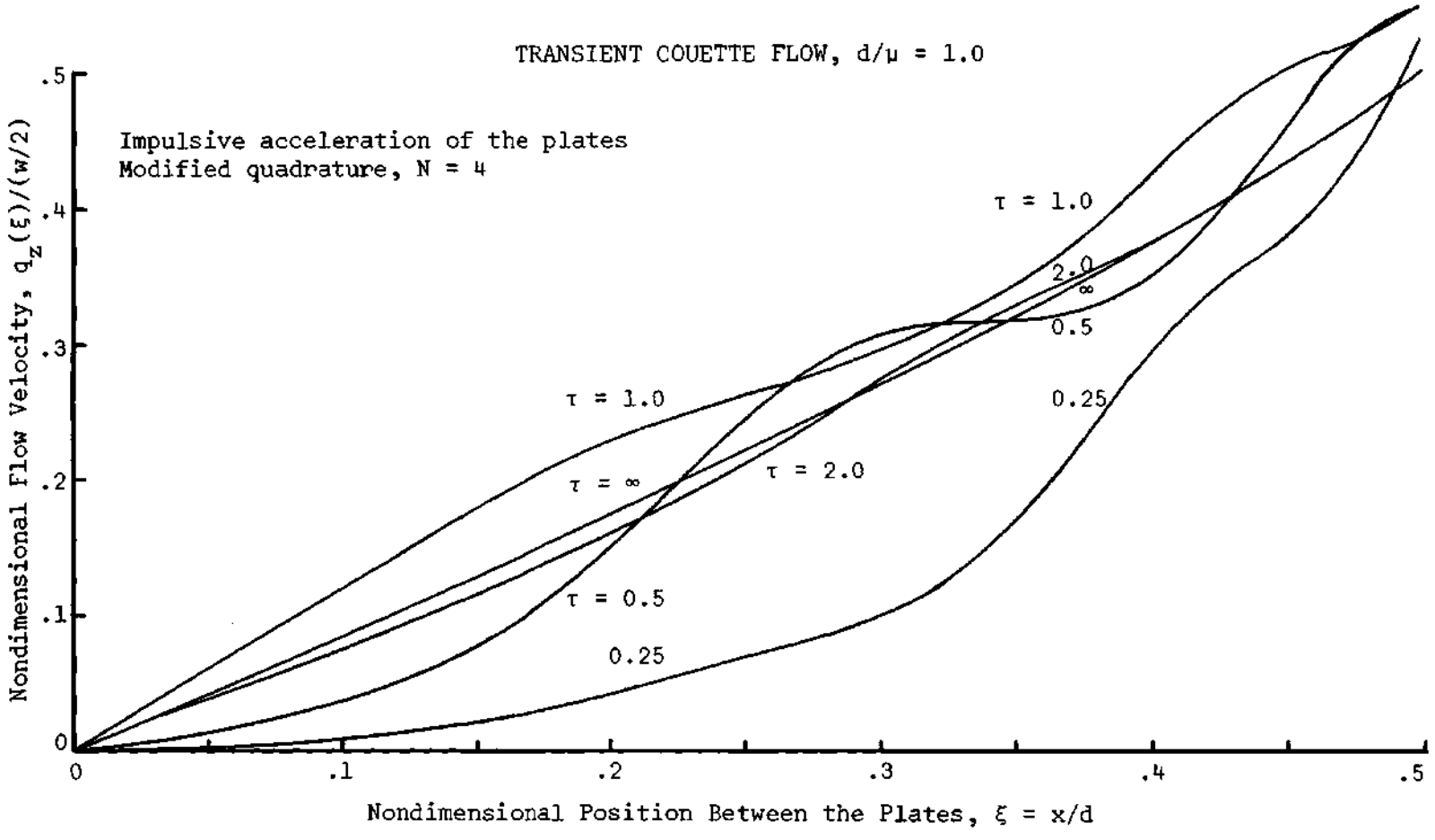

Figure 17. Transient Development of the Velocity Profile in Couette Flow for Impulsive Acceleration of the Plates, d/μ = 1.0 and N = 4.

of these calculations for N = 4. The graphs for the cases $d/\mu = 5.0$ and 20.0 exhibit characteristics which might be expected from physical intuition; that is, the velocity of the gas starts out at its initial condition and increases with time, asymptotically approaching the steady state solution. These results were obtained using forty space steps across the channel and a time increment of $\delta\tau = 0.005$. Convergence of the solution to a unique set of values was checked by running cases with 100 space steps and $\delta\tau = 0.002$.

It will be noted that for this case of impulsively accelerating the plates, the curves for $d/\mu = 1.0$ and 2.0 take on an irregular shape. This is due to the appearance of numerical errors for $d/\mu \leq 2.0$, and Figure 18 demonstrates the difficulties encountered. In this figure the solutions for $d/\mu = 2.0$ at time $\tau = 0.5$ are compared using two different grid sizes. Note that the different solutions do not converge to the same values. The reason for this is that with the impulsive acceleration, the distribution function is propagated as a step function in the free molecular limit as shown by Equation (65). When the discrete ordinate method is applied, $\Psi_K^{\pm} = \bar{+}w$ is propagated as N step functions, each moving with a different value of c_x corresponding to the N discrete velocity ordinates. This step function character of the solution is quite difficult to handle with the finite difference method since there is an infinite derivative at the point of discontinuity forming the step. When the infinite derivative occurs, it is necessary to go to extremely small step sizes to approximate this behavior; and this can lead to excess time and storage problems on a computer. Also, there is the possibility that the smaller step sizes, although approximating the

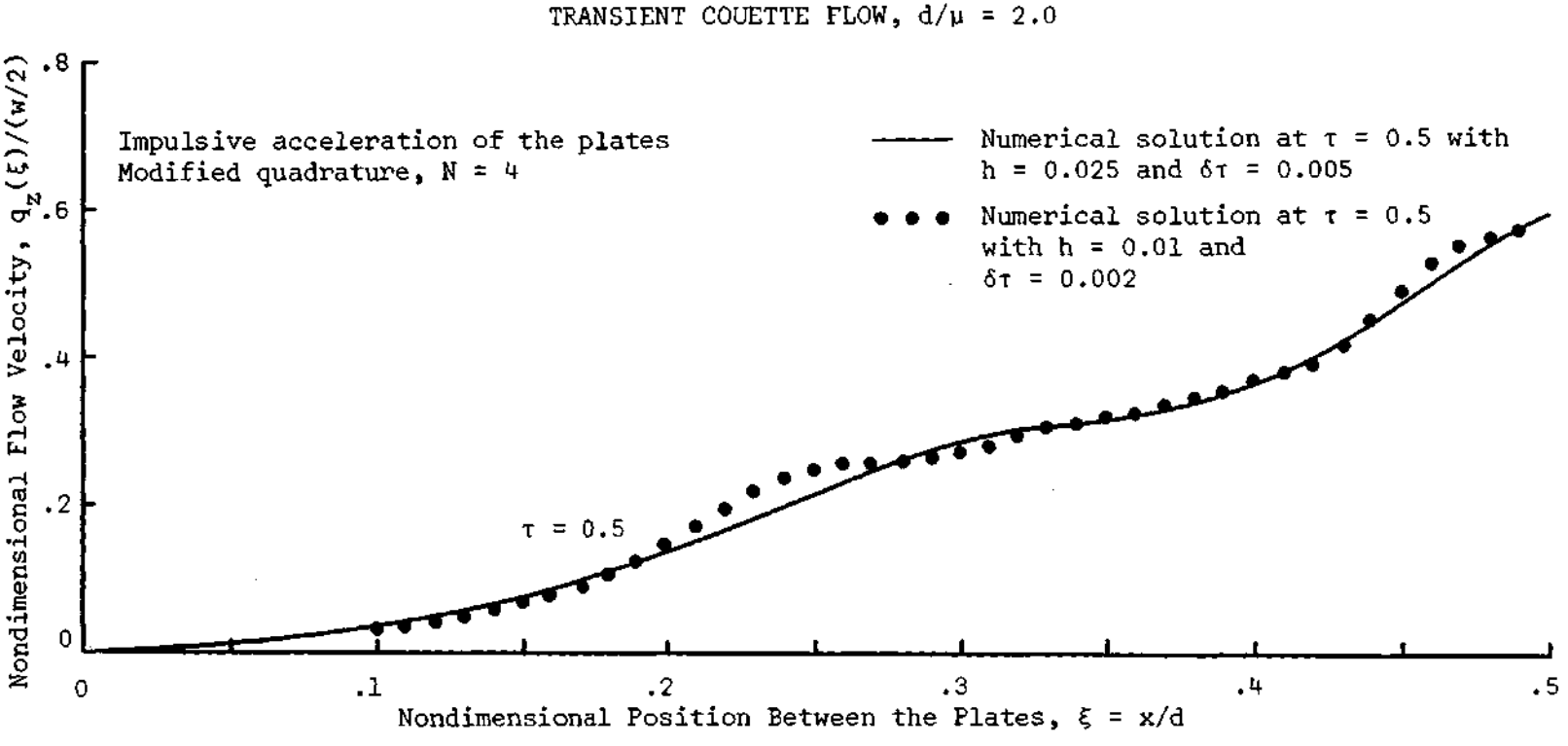

Figure 18. Comparison of the Velocity Profile Development in Couette Flow Using Two Different Step Sizes in the Numerical Solution, d/μ = 2.0 and N = 4.

derivative at the step adequately, may not allow the rapid changes in this derivative which are necessary to carry the slope from its infinite value at the step discontinuity to the zero value immediately on either side of this point. This perhaps could be overcome by some procedure to manually correct the slope on either side of the discontinuity.

Thus, these numerical difficulties coupled with the computer time and storage problems appear when the gas approaches a free molecular state. This condition not only applies when the inverse Knudsen number is small ($d/\mu \leq 2$), but it is also present for flows with larger values of d/μ if the ratios of distance to mean free path or of time to collision time are much less than unity. As a result of these difficulties when the finite difference method was applied to the problem with an impulsive acceleration, the numerical results cannot be expected to be quantitatively accurate for extremely short times after the initial disturbance or for distances from the surface much shorter than a mean free path.

In spite of these limitations, the results obtained in Figures 14 through 17 may be quite useful in some circumstances. An example of this is a situation in which it is desired to find flow characteristics at distances greater than a mean free path or so away from a surface. In such cases the numerical shortcomings near the wall have little effect on the solution several mean free paths away. Evidence of this fact is given by the success of the full range moment methods when applied to slip flow and near continuum flow problems, i.e. see Gross and Jackson [12]. These results show that the microscopic effects of the boundaries in Couette flow are confined to within several mean free

paths of the surface and have little influence on the majority of the gas if d/μ is five or larger.

The entire problem discussed above may be avoided, however, by allowing the surfaces to accelerate continuously from rest up to some fixed velocity with a proper acceleration function. This avoids the large initial step of the impulsive acceleration and allows the solution by finite differences to be applicable to much lower values of inverse Knudsen number. In addition, this situation is much more realistic than that of an impulsive acceleration.

Following this principle, several calculations were made for the case where the plates are accelerated from rest up to the velocities $\pm w/2$ by using a constant acceleration so that the plate velocity is given by

$$q_z(\xi = \pm 1/2, \tau) = \begin{cases} \pm w\tau/2 & \text{for } 0 < \tau \leq 1 \\ \pm w/2 & \text{for } \tau > 1 \end{cases} \tag{74}$$

The free molecular case corresponding to these conditions may be solved analytically for $0 < \tau \leq 1$ as indicated in Appendix C. The solution for the flow velocity for free molecular flow is

$$\frac{q_z(\xi)}{w/2} = \frac{1}{\sqrt{\pi}} \left\{ \frac{\sqrt{\pi}}{2} \tau \left[\operatorname{erfc}\left(\frac{1/2 - \xi}{\tau}\right) - \operatorname{erfc}\left(\frac{1/2 + \xi}{\tau}\right) \right] \right. \tag{75}$$

$$\left. - \left(\frac{\xi + 1/2}{2}\right) \operatorname{Ei}\left[-\left(\frac{\xi + 1/2}{\tau}\right)^2\right] + \left(\frac{1/2 - \xi}{2}\right) \operatorname{Ei}\left[-\left(\frac{1/2 - \xi}{\tau}\right)^2\right] \right\}$$

This solution for $0 \leq \tau \leq 1$ may be used as a check on the computations for small τ in order to determine if the numerical scheme is adequate in the near free molecular flow region.

The numerical calculations with the new conditions described by Equation (74) were performed for values of d/μ ranging from 20.0 down to 0.1, and the results are reported in Figures 19 through 22. The curves for $d/\mu = 2.0$ and 20.0 behave as expected in that the velocity starts from zero and increases, asymptotically approaching the steady state condition. The time required for convergence is essentially $\tau \leq 5.0$.

Figures 21 and 22 show a more radical behavior for the velocity development. This is not due to numerical difficulties in this case, however, as was verified by examining solutions using different grid sizes. There is an interesting physical reason for this behavior which may be explained from the molecular viewpoint. As the surface begins to accelerate, the flow velocity adjacent to it is governed almost entirely by the molecules which are emitted from that surface. Thus, since there are at first few gas-gas collisions, there is essentially a "half-slip" between the flow immediately next to the wall and the motion of the wall itself when the time is much less than the mean collision time of the gas. That is, the velocity of the gas at $\xi = \pm 1/2$ is essentially

$$\frac{q_z(\xi = \pm 1/2,\ \tau << 1)}{w/2} = \pm 1/2$$

This situation will continue until either (i) there are collisions with

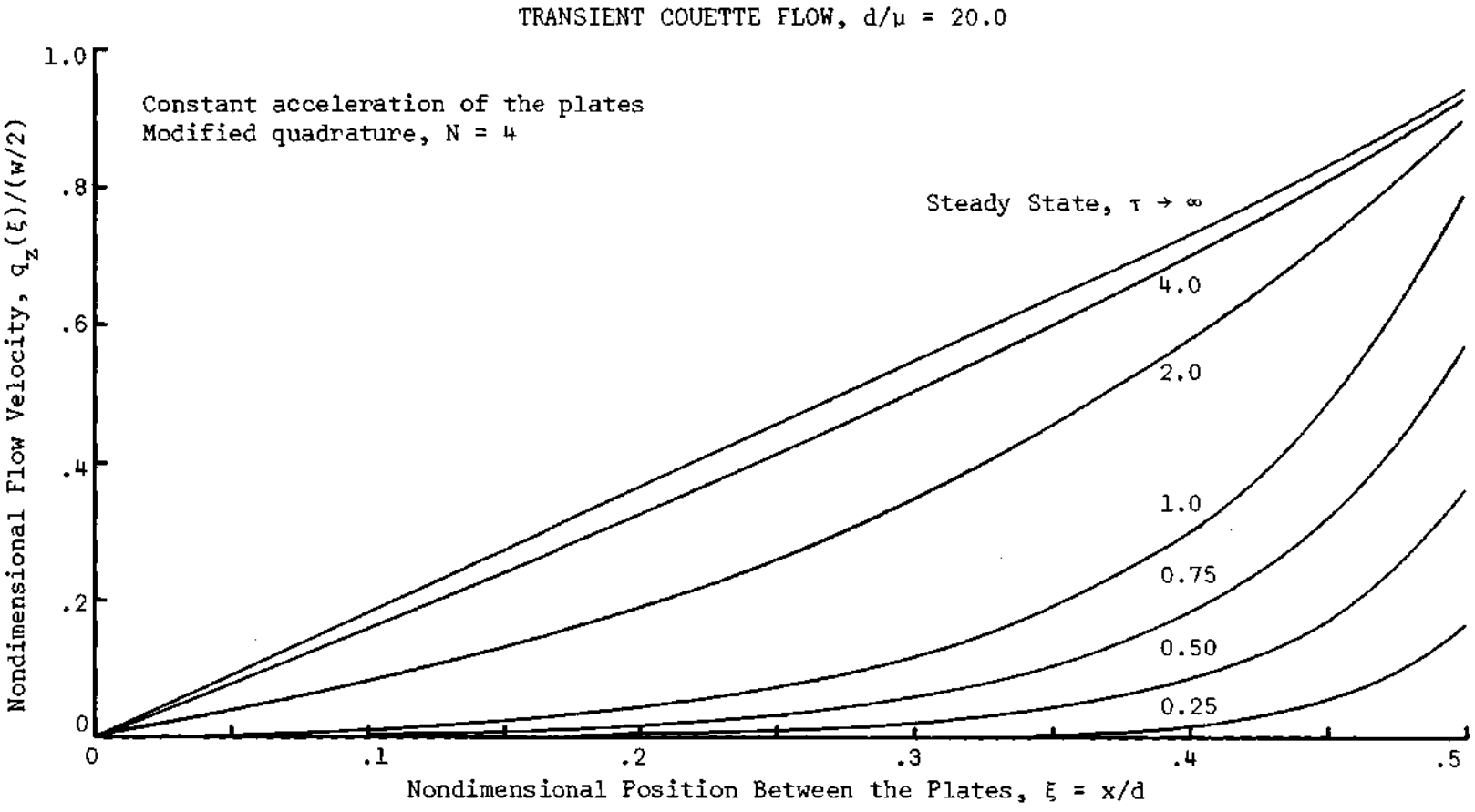

Figure 19. Transient Development of the Velocity Profile in Couette Flow for Constant Acceleration of the Plates, $d/\mu = 20.0$ and $N = 4$.

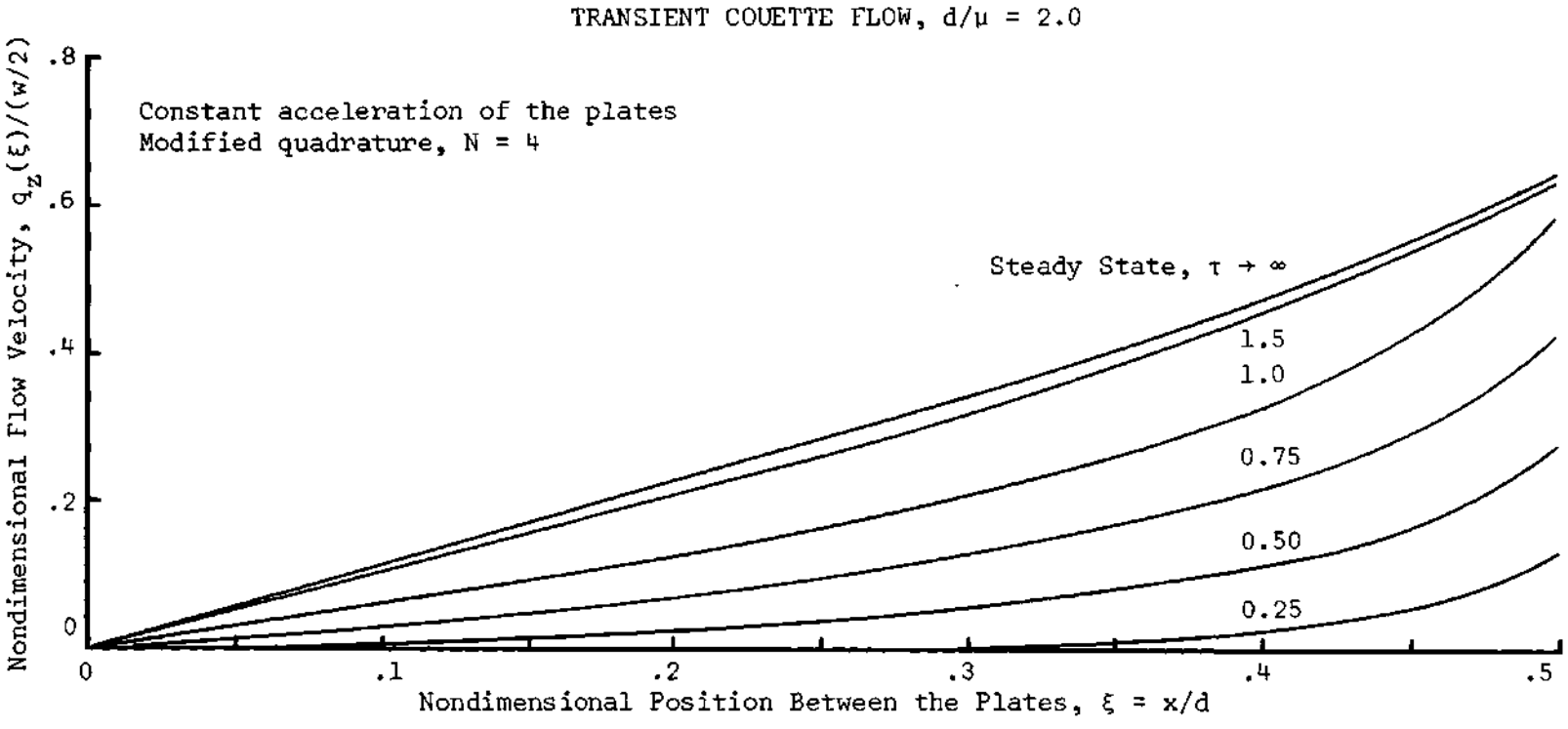

Figure 20. Transient Development of the Velocity Profile in Couette Flow for Constant Acceleration of the Plates, d/μ = 2.0 and N = 4.

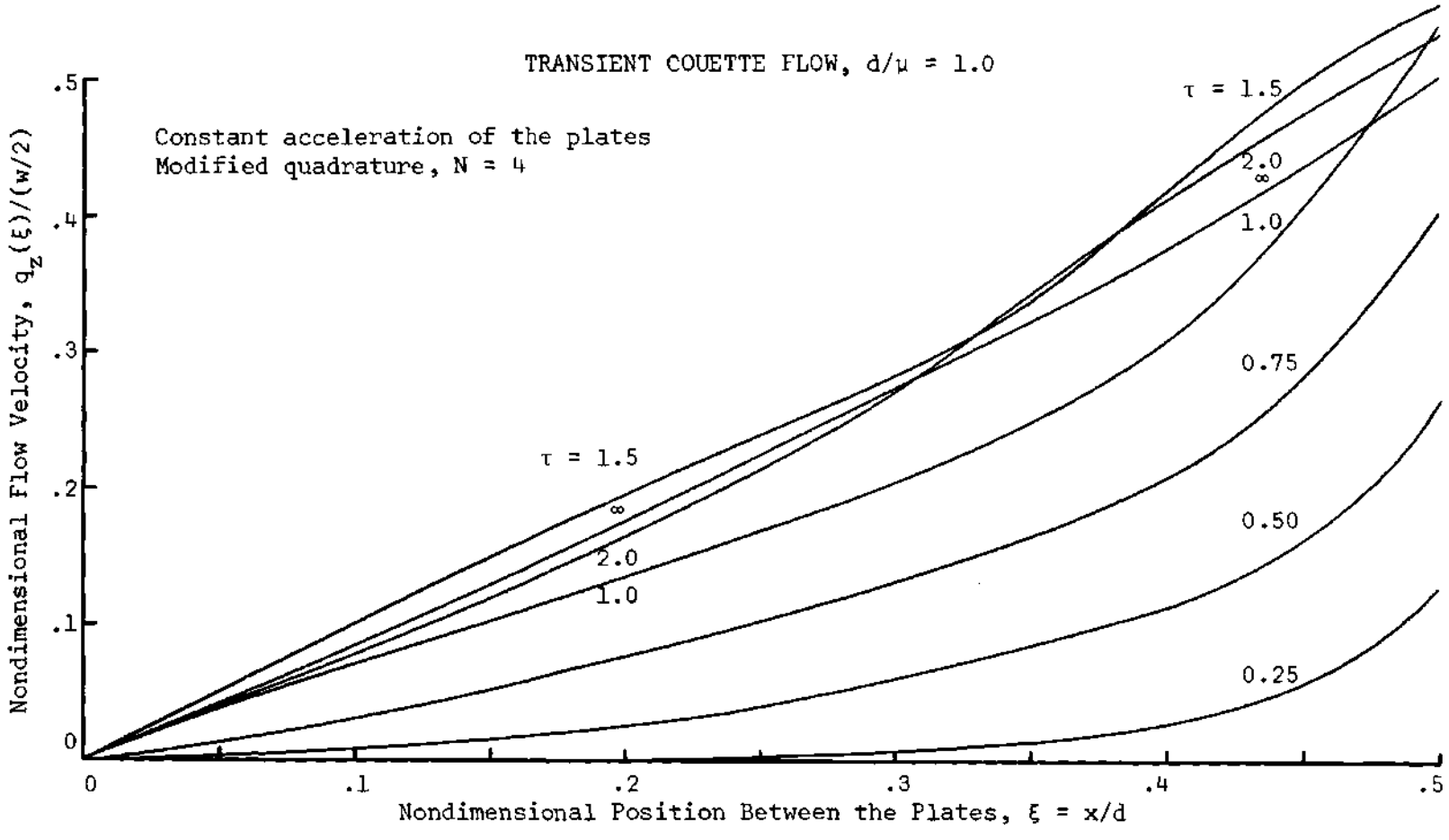

Figure 21. Transient Development of the Velocity Profile in Couette Flow for Constant Acceleration of the Plates, d/μ = 1.0 and N = 4.

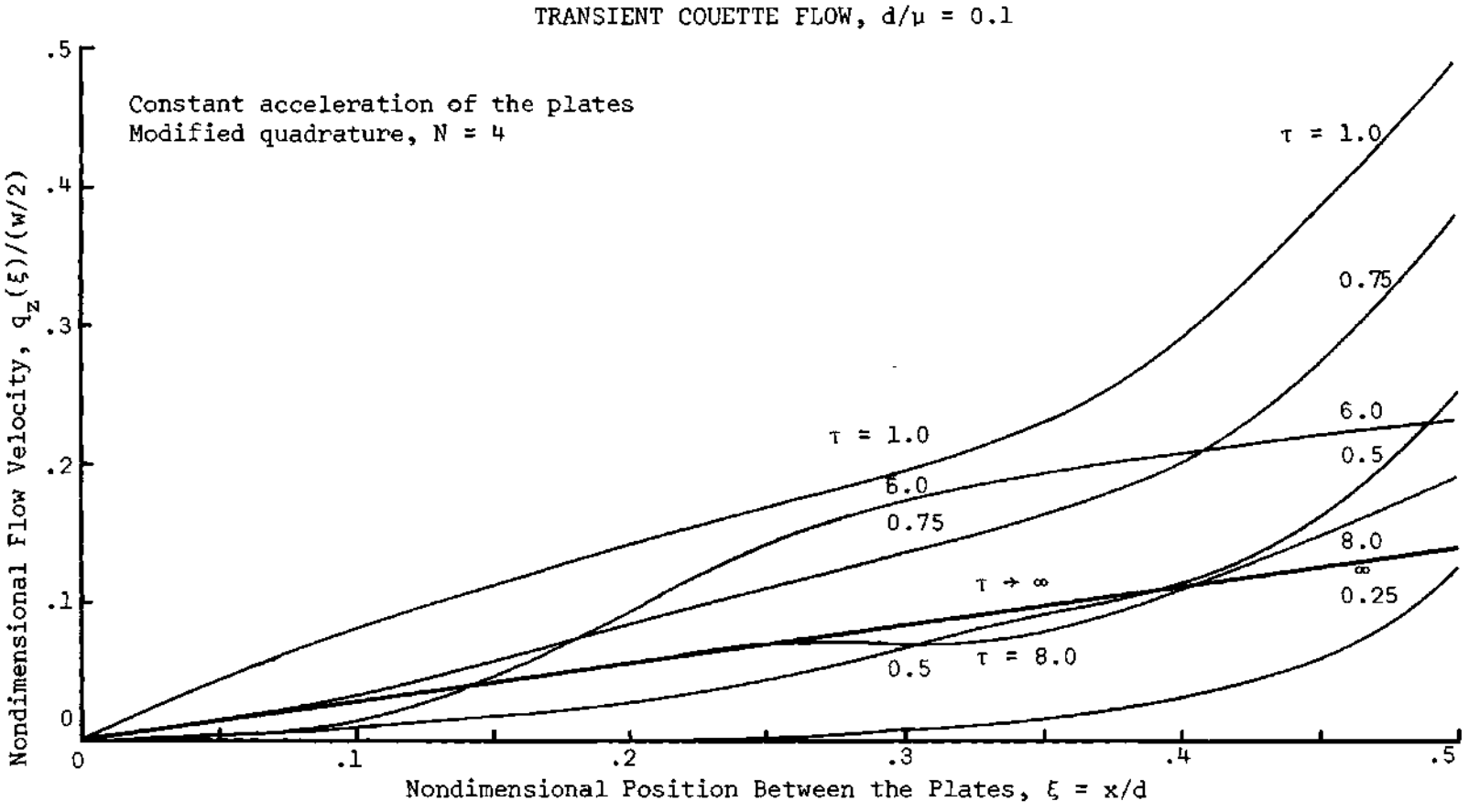

Figure 22. Transient Development of the Velocity Profile in Couette Flow for Constant Acceleration of the Plates, d/μ = 0.1 and N = 4.

the other gas molecules away from the surface, or (ii) the stream of molecules leaving the opposite wall arrives to statistically counter this effect. This is best illustrated by the velocity development for the strictly free molecular case in which no gas-gas collisions occur as was discussed in a previous section (see Figure 13). The cases for $d/\mu \leq 1.0$ are analogous to this in that it takes an appreciable amount of time for (i) and (ii) above to occur. Thus, the flow velocity at the surface starts from rest, increases at one-half the rate of increase of the surface speed, "overshoots" its steady state value, and then finally settles down to the asymptotic solution as the effects of gas-gas collisions and of molecules arriving from the opposite wall are experienced.

A check of different grid sizes gave assurance that the convergence of the numerical solution was good down to an inverse Knudsen number of 0.1. Computer time required to essentially reach the steady state solution varied from several minutes for high values of d/μ up to approximately 30 minutes for $d/\mu = 0.1$ for the case $N = 4$. Grid sizes for the reported solutions are 40 steps across the channel ($h = 0.025$) and $\delta\tau = 0.005$. To check convergence of the solutions the values $h = 0.01$ and $\delta\tau = 0.002$ were used.

Several cases were run with $N = 7$ using both the impulsive acceleration and the constant acceleration conditions. The results were similar to those for $N = 4$ and some of these calculations are reported in Figures 23 and 24. Again, accuracy of the solutions illustrated in these figures was checked by using a finer grid size, and the solutions always converged to the steady state results.

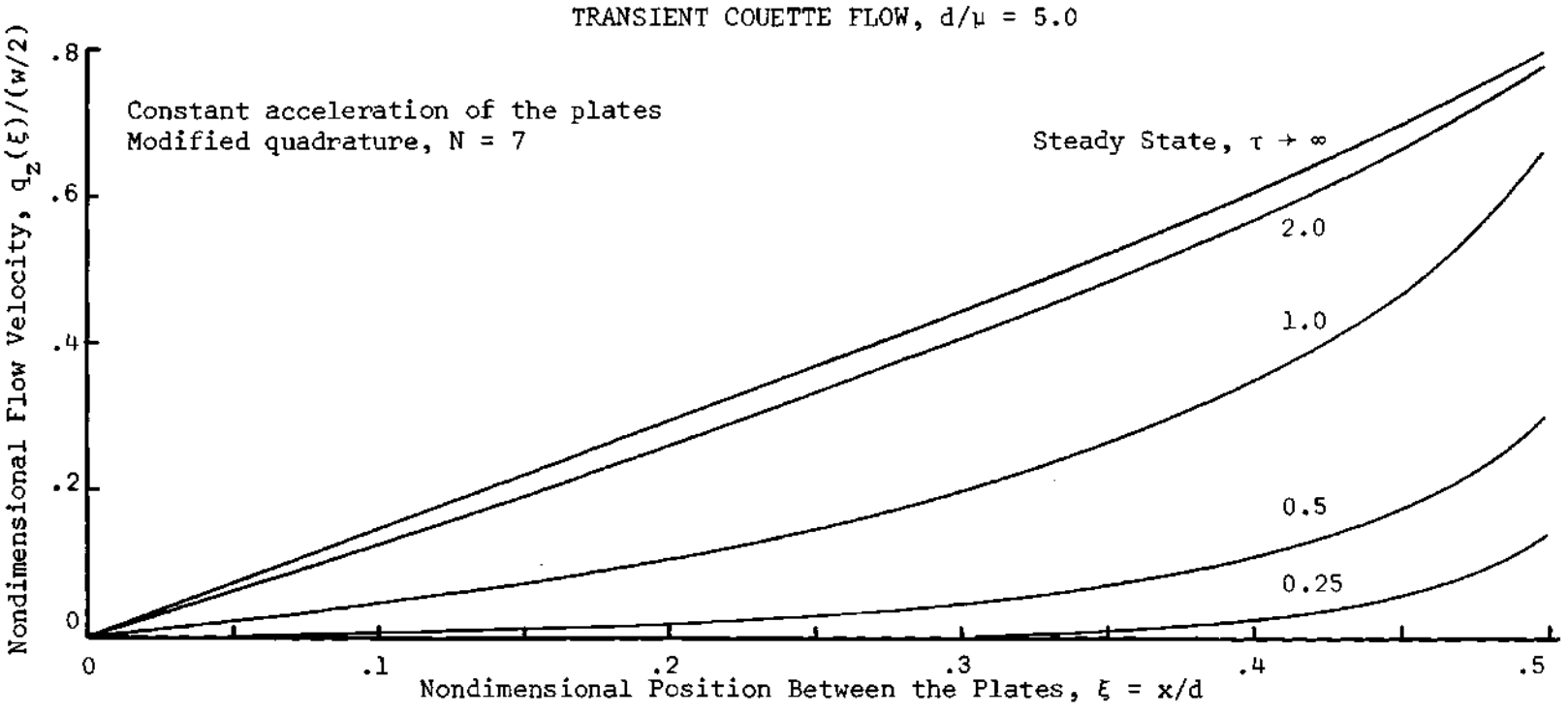

Figure 23. Transient Development of the Velocity Profile in Couette Flow for Constant Acceleration of the Plates, d/μ = 5.0 and N = 7.

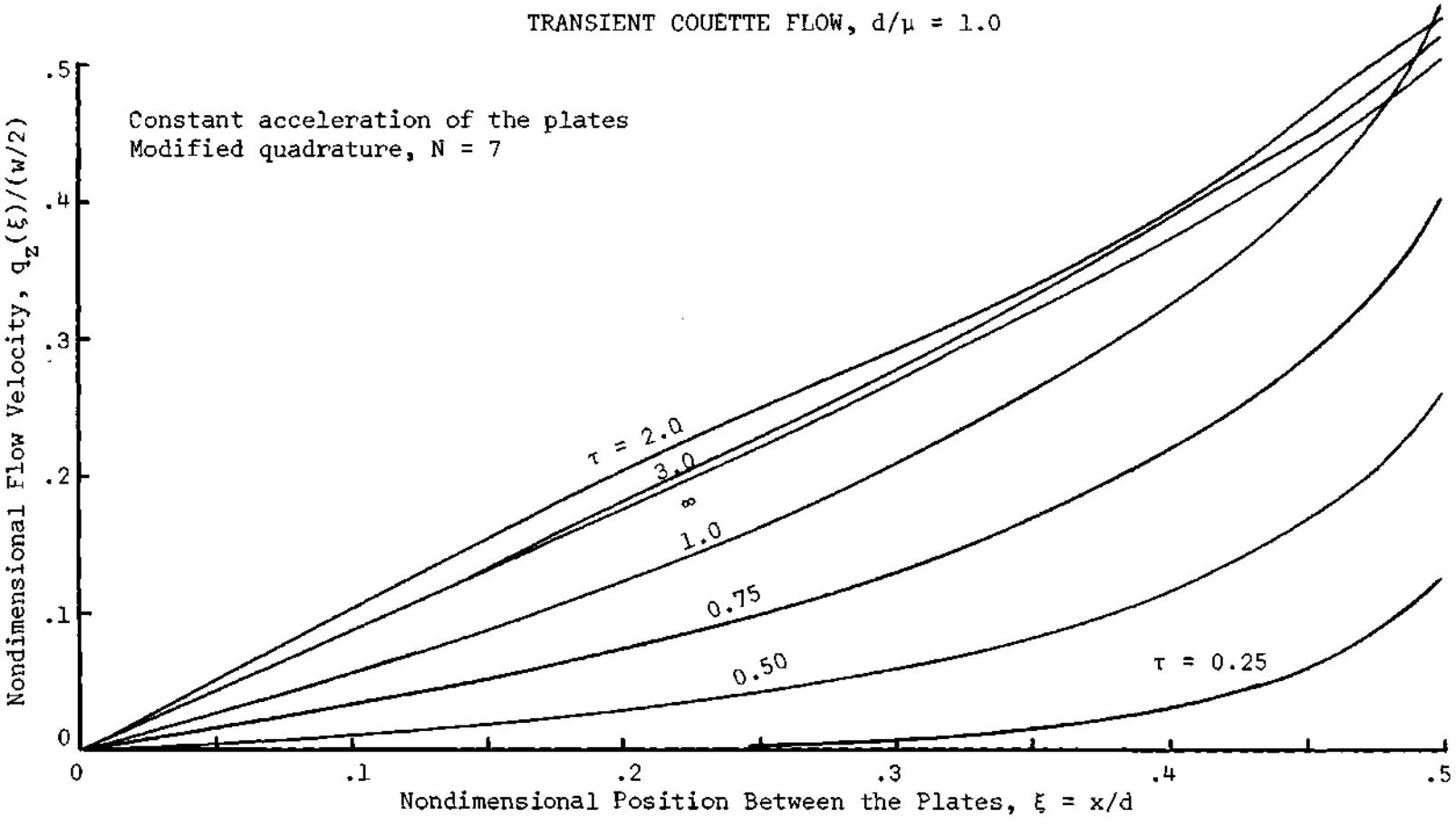

Figure 24. Transient Development of the Velocity Profile in Couette Flow for Constant Acceleration of the Plates, $d/\mu = 1.0$ and $N = 7$.

Since there has been no other work on the time dependent development of Couette flow from the kinetic theory viewpoint, there are no results with which the present theory may be compared during much of the transient period. However, the results for extremely long times and for extremely short times may be checked with the analytic steady state and free molecular time dependent solutions, respectively. As indicated in each of the previous figures discussed, the numerical results always converged to the steady state solution so that this serves as one check on the calculations. For very short times the numerical solution is compared with the analytic free molecular solutions of Appendix C in Figures 25 and 26. The case for impulsive acceleration with $N = 4$ and $d/\mu = 5.0$ is examined at $\tau = 0.1$ in Figure 25. This corresponds to a ratio of true time to collision time of one half. Note that, in view of the previous remarks on the accuracy of the impulsive acceleration solutions for extremely short times, the comparison is quite good. The case for constant acceleration using $N = 7$ and $d/\mu = 1.0$ at $\tau = 0.5$ is presented in Figure 26. This corresponds to a true time to collision time ratio of 0.5. Again the comparison is very satisfactory.

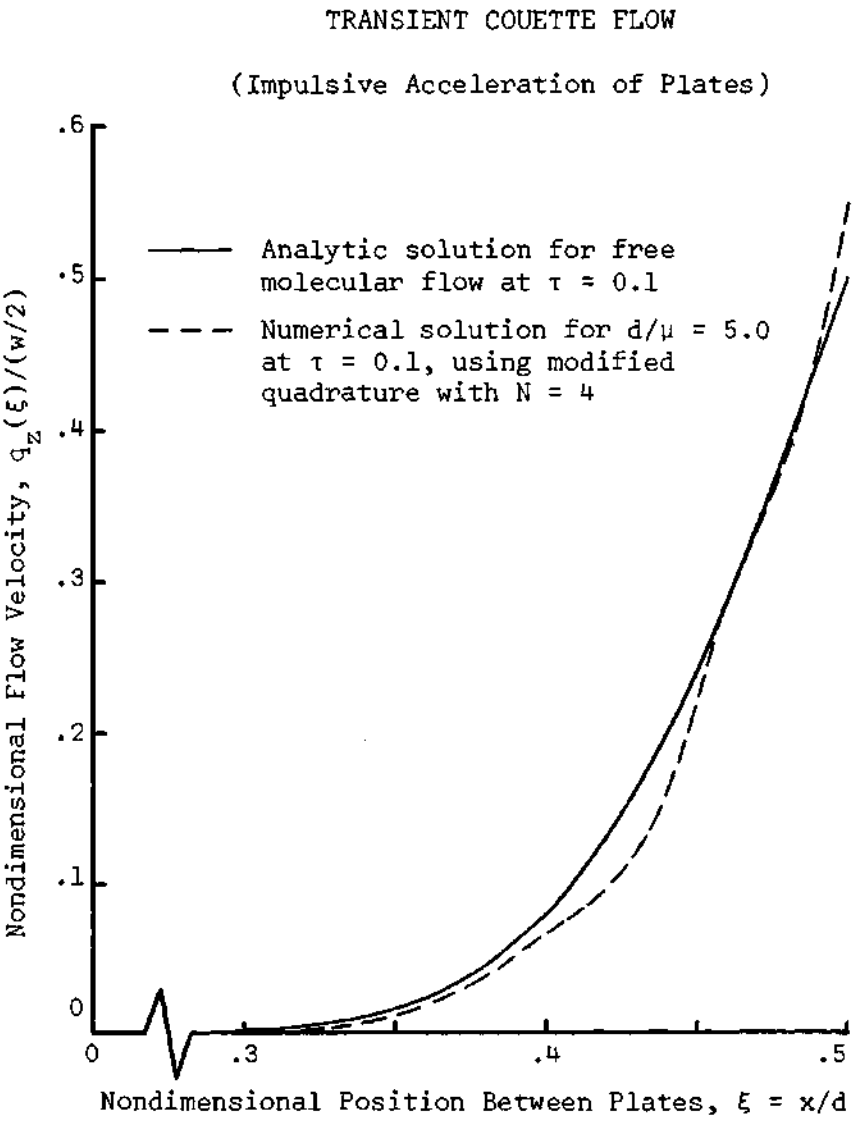

Figure 25. Comparison of Numerical Results for Small Time with the Analytic Free Molecular Solution for the Transient Development of the Velocity Profile in Couette Flow with Impulsive Acceleration of the Plates.

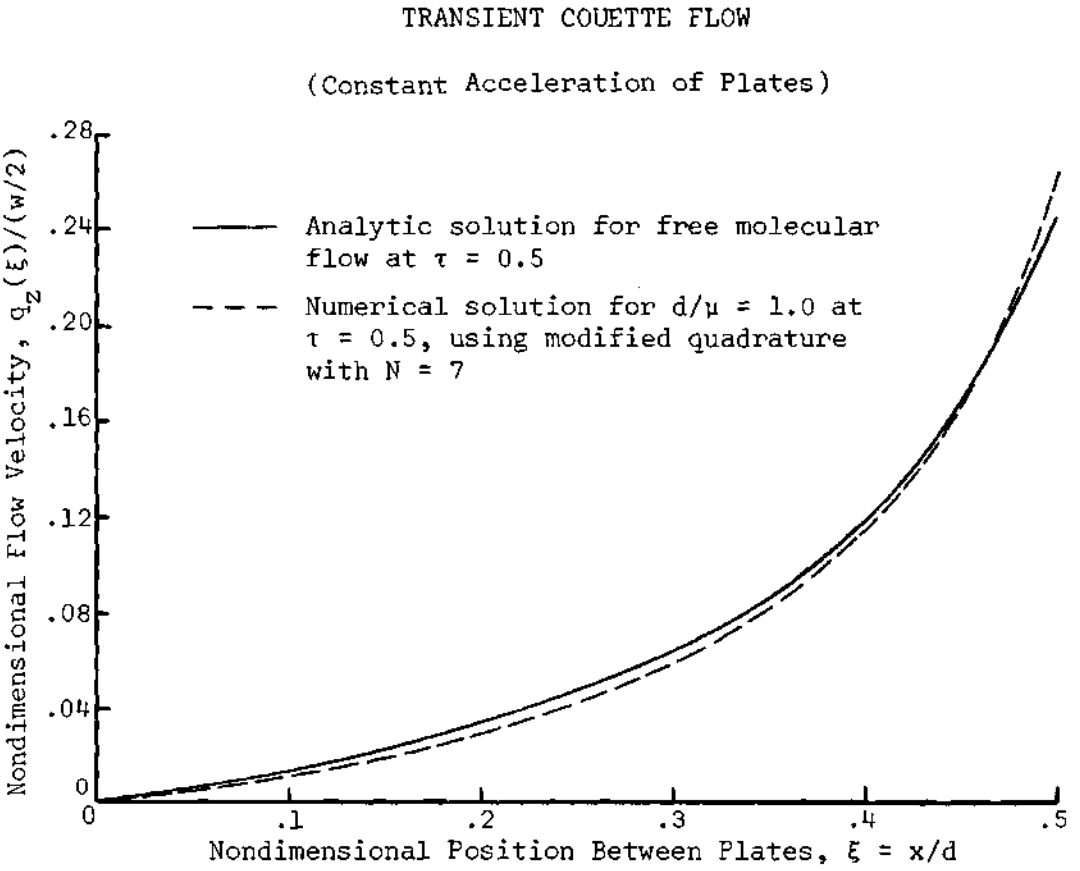

Figure 26. Comparison of Numerical Results for Small Time with the Analytic Free Molecular Solution for the Transient Development of the Velocity Profile in Couette Flow with Constant Acceleration of the Plates.

CHAPTER VII

RAYLEIGH'S PROBLEM--THE ACCELERATION OF AN INFINITE PLATE IN ITS OWN PLANE

Previous Work on the Problem

When an infinite plate is accelerated in its own plane, the disturbance is first felt in the gas adjacent to the surface and then is propagated into the main portion of the stream until finally, as time approaches infinity, the entire gas has experienced this disturbance. The geometry and coordinate system for this problem were shown in Figure 1. Although this is usually referred to as Rayleigh's problem, Schlichting [36] indicates that it was first solved by Stokes [38] for the case of continuum flow under the condition of an impulsive acceleration. Several authors have approached this problem for rarefied gases from the kinetic theory viewpoint. Yang and Lees [2] presented a solution in 1956 based on Grad's 13 moment equations. This method proved unsatisfactory, however, in that the free molecular limit--which corresponds to the small time conditions regardless of Knudsen number--yields a velocity which is 26 per cent too small and a shear stress which is 10 per cent too large. In 1960 Yang and Lees [3] applied the collisionless Boltzmann equation to this problem for the free molecular limit. In this paper they considered several cases of wall heat transfer conditions and obtained velocity and temperature distributions for these cases.

Gross and Jackson [39] presented a solution based on the second approximation of the half-range moment method in 1958 and considered only the limiting cases of short and long time due to the mathematical difficulties. However, the accuracy of the short time case in which results are analogous to those of near free molecular flow must be questioned with regard to their quantitative accuracy. Although the limits as time approaches zero are correct, previous comparisons in this dissertation and by Huang and Giddens [19] of the half-range moment method with the discrete ordinate and iteration methods indicate that the second approximation with half-range moments does not adequately describe the flow phenomena in the plane Couette flow problem for near free molecular flow. Hence, the application to the near free molecular portion of Rayleigh flow, which corresponds to early values of time and short distances away from the surface, may lead to results which are at best qualitative in nature.

The Rayleigh problem was treated by Broadwell [16] in his paper on the discrete velocity method in 1964, and he also found asymptotic expressions for short and long time. The results agree qualitatively with those of Yang and Lees using the Grad 13 moment equations, but do not appear to give as accurate a solution as that of Gross and Jackson. It will be shown in the next section that the application of the present model of discrete ordinates to the Rayleigh problem reduces in the lowest order approximation, N = 1, to the same governing equation as Broadwell found using his eight-cell discrete velocity model.

Application of the Equations to the Rayleigh Problem

Solution for Very Small Time

The solution of the Rayleigh problem for the very short time during which the molecular collisions may be neglected is very similar to the corresponding solution of the Couette flow case, with the exception that there is an initial disturbance of only the Ψ^+ function. If the plate is impulsively accelerated with velocity w in its own plane, then only the equation

$$\frac{\partial \Psi^+}{\partial \tau_1} + c_x \frac{\partial \Psi^+}{\partial x} = 0 \tag{76}$$

need be considered for the collisionless case. Here Ψ^+ is defined in Equation (19) and $\tau_1 = t/\beta$. The boundary condition is that $\Psi^+(x=0,\tau_1) = 2w$ and the initial condition is that the remainder of the gas be undisturbed at $\tau_1 = 0$. Thus, the solution for Ψ^+ is

$$\Psi^+(x,\tau_1) = \begin{cases} 0 & \text{for } x > \tau_1 c_x \\ 2w & \text{for } x < \tau_1 c_x \end{cases} \tag{77}$$

Integrating Equation (77) to find the flow velocity yields

$$\frac{q_z(x)}{w} = \frac{1}{2} \operatorname{erfc}(x/\tau_1) \tag{78}$$

This solution is used to compare with the results for extremely short

times when the solutions for finite values of mean free path are obtained. A similar expression exists when the wall is accelerated with a constant acceleration for $0 < \bar{\tau} \leq 1$ from zero velocity to a velocity of w, namely,

$$\frac{q_z(\bar{x})}{w} = \frac{1}{\sqrt{\pi}} \left\{ \frac{\sqrt{\pi}}{2} \bar{\tau} \operatorname{erfc}(\bar{x}/\bar{\tau}) - \frac{\bar{x}}{2} \operatorname{Ei}[-(\bar{x}/\bar{\tau})^2] \right\} \tag{79}$$

where $\bar{x} = x/\mu$ and $\bar{\tau} = t/\beta\mu$ which is the ratio of true time to the collision time. Here the mean free path μ is used to normalize x and τ_1 since Equation (78) may be applied to flows with $\bar{\tau} < 1$. As indicated in Appendix C, Equation (79) is valid only for $0 < \bar{\tau} \leq 1$.

Solution by Discrete Ordinates

Solution for N = 1. When the discrete ordinate method is applied to the linearized Boltzmann Equation (17), the resulting relation is

$$\frac{\partial \psi_\kappa^\pm}{\partial \tau_1} \pm \alpha_\kappa \frac{\partial \psi_\kappa^\pm}{\partial x} = \frac{1}{\mu}\left[-\psi_\kappa^\pm + \frac{1}{\sqrt{\pi}} \sum_{i=1}^{N} H_i(\psi_i^+ + \psi_i^-)\right] \tag{80}$$

for $\kappa = 1,2,\ldots,N$. For the case N = 1 this set of equations reduces to the pair

$$\frac{\partial \psi_1^+}{\partial \tau_1} + \alpha_1 \frac{\partial \psi_1^+}{\partial x} = \frac{1}{\mu}\left[-\psi_1^+ + \frac{H_1}{\sqrt{\pi}}(\psi_1^+ + \psi_1^-)\right] \tag{81}$$

$$\frac{\partial \psi_1^-}{\partial \tau_1} - \alpha_1 \frac{\partial \psi_1^-}{\partial x} = \frac{1}{\mu}\left[-\psi_1^- + \frac{H_1}{\sqrt{\pi}}(\psi_1^+ + \psi_1^-)\right] \tag{82}$$

Solving for Ψ_1^- from the first equation gives

$$\Psi_1^- = \frac{\sqrt{\pi}}{H_1}\left[\mu\left(\frac{\partial \Psi_1^+}{\partial \tau_1} + \alpha_1 \frac{\partial \Psi_1^+}{\partial x}\right) + \Psi_1^+\right] - \Psi_1^+ \tag{83}$$

Substituting this expression into (82) and using the relation $H_1 = \sqrt{\pi}/2$ results in the equation

$$\frac{1}{q^2}\frac{\partial^2 \Psi_1^+}{\partial t^2} - \frac{\partial^2 \Psi_1^+}{\partial x^2} + \frac{\Theta}{q^2}\frac{\partial \Psi_1^+}{\partial t} = 0 \tag{84}$$

where $q = \alpha_1/\beta$ and $\Theta = 1/\mu\beta$. This is the telegraph equation and is the same as that obtained by Broadwell using the eight-cell discrete velocity model. The solutions to this equation have been discussed extensively in [16] and are not repeated here. Thus, it is seen that the simplest case for the present model reduces to the solution given by Broadwell.

Solution for Arbitrary N. Based on the previous discussion, it is evident that in order to obtain better results with the discrete ordinate method, it is necessary to resort to taking higher values of N. Thus, the problem of solving a linear system of N partial differential equations again arises. Although it is difficult to obtain analytic expressions for the solutions of the resulting system for N > 1, a simple transformation permits a numerical solution by finite differences. First, Equation (80) is rewritten as

$$\frac{\partial \Psi_\kappa^\pm}{\partial \bar{\tau}} \pm \alpha_\kappa \frac{\partial \Psi_\kappa^\pm}{\partial \bar{x}} = -\Psi_\kappa^\pm + \frac{1}{\sqrt{\pi}} \sum_{i=1}^{N} H_i(\Psi_i^+ + \Psi_i^-) \tag{85}$$

Using the transformation $\bar{\xi} = 1-e^{-\bar{x}}$ then gives

$$\frac{\partial \Psi_K^{\pm}}{\partial \bar{\tau}} \pm \alpha_K (1 - \bar{\xi}) \frac{\partial \Psi_K^{\pm}}{\partial \bar{\xi}} = -\Psi_K^{\pm} + \frac{1}{\sqrt{\pi}} \sum_{i=1}^{N} H_i (\Psi_i^{+} + \Psi_i^{-}) \qquad (86)$$

This transformation not only maps the infinite $\bar{x}$ distance into a unit region ($0 \leq \bar{\xi} \leq 1$) but it does so in a most efficient manner. That is, if the region $0 \leq \bar{\xi} \leq 1$ is divided into M equal steps for the purpose of performing a finite difference solution, the points in actual physical space are quite close together in the region near the plate where gradients are largest and are spaced farther apart at regions away from the surface where there is little change in the flow properties. For example, using 40 steps over the interval $0 \leq \bar{\xi} \leq 1$ results in placing 25 grid points over a distance equal to one mean free path from the wall.

Note that the solution to Equation (86) may be applied to gases with a wide range of rarefaction since the quantities are in terms of the parameters $\bar{x}$ and $\bar{\tau}$. However, since the free molecular solution is available for the cases of small $\bar{x}$ and $\bar{\tau}$, there may arise certain situations in which it is not necessary to solve a problem to such a degree. For example, if the flow is in a state such that the mean free path is on the order of 10^{-4} centimeters and it is desired to describe flow quantities 10^{-1} centimeters away from the surface, it is clear that the phenomena occurring within a mean free path of the wall have no great effect on the flow characteristics many mean free paths away due to the effects of the collisional process. This principle has been previously discussed in Chapter VI. For such cases, it is not necessary to solve

Equation (86) on the scale $\bar{x} = x/\mu$ and $\bar{\tau} = t/\beta\mu$. Rather, it is sufficient to solve to some larger nondimensional distance and time scales such as $\bar{\tau}_1 = t/\beta k_1$ and $\bar{x}_1 = x/k_1$ where k_1 is some multiple of the mean free path. Thus, the parameter $\bar{\mu}$ is defined by

$$\bar{\mu} = \frac{\mu}{k_1} \tag{87}$$

and Equation (80) may be written as

$$\frac{\partial \Psi_\kappa^\pm}{\partial \bar{\tau}_1} \pm \alpha_\kappa \frac{\partial \Psi_\kappa^\pm}{\partial \bar{x}_1} = \frac{1}{\bar{\mu}} \left[-\Psi_\kappa^\pm + \frac{1}{\sqrt{\pi}} \sum_{i=1}^{N} H_i (\Psi_i^+ + \Psi_i^-) \right] \tag{88}$$

Note that $\bar{\mu}$ is a pure number according to the definition of Equation (87).

Again the nondimensional normal coordinate $\bar{x}_1$ is transformed according to $\bar{\xi}_1 = 1 - e^{-\bar{x}_1}$, resulting in the form

$$\frac{\partial \Psi_\kappa^\pm}{\partial \bar{\tau}_1} \pm \alpha_\kappa (1 - \bar{\xi}_1) \frac{\partial \Psi_\kappa^\pm}{\partial \bar{\xi}_1} = \frac{1}{\bar{\mu}} \left[-\Psi_\kappa^\pm + \frac{1}{\sqrt{\pi}} \sum_{i=1}^{N} H_i (\Psi_i^+ + \Psi_i^-) \right] \tag{89}$$

The same finite difference forms are next applied to this equation to yield the system of difference equations

$$\frac{\Psi_\kappa^{\hat{n}+1}(\hat{i})^\pm - \Psi_\kappa^{\hat{n}}(\hat{i})^\pm}{\delta \bar{\tau}_1} \pm \alpha_\kappa (1 - \hat{i}\bar{h}_1) \frac{\Psi_\kappa^{\hat{n}+1}(\hat{i}+1)^\pm - \Psi_\kappa^{\hat{n}+1}(\hat{i}-1)^\pm}{2\bar{h}_1} =$$

$$\frac{1}{\bar{\mu}}\{-\hat{\psi}_{\kappa}^{n}(\hat{i})^{\pm} + \frac{1}{\sqrt{\pi}} \sum_{i=1}^{N} H_i[\hat{\psi}_i^{n}(\hat{i})^{+} + \hat{\psi}_i^{n}(\hat{i})^{-}]\} \tag{90}$$

If $\bar{\mu} = 1$ in the above system, the resulting set of equations corresponds to the set which would be obtained if the finite difference technique were applied to Equation (86). Note that by taking $\bar{\mu} = 20$ and $\bar{h}_1 = 0.025$, the first grid point of the difference scheme occurs at approximately one half of a mean free path from the surface, so that the scale of description in the region away from the plate will yield detailed results for distances on the order of a mean free path.

Anticipating from the Couette flow results that for small values of x/k_1 the impulsive acceleration may not be handled well using finite differences, an alternate set of boundary conditions may be formulated in which the wall is smoothly accelerated from rest such that the perturbed distribution function satisfies the conditions

$$\psi^{+}(\bar{\xi}_1 = 0, \bar{\tau}_1) = \begin{cases} 2w\bar{\tau}_1/s_1 & \text{for } 0 < \bar{\tau}_1 \leq s_1 \\ 2w & \text{for } \bar{\tau}_1 > s_1 \end{cases} \tag{91}$$

where s_1 is some arbitrary number. As will be indicated in the next section, such a smooth acceleration will allow the finite difference procedure to yield accurate solutions for small values of x/k_1. If it is desired to precisely describe conditions for very small x/k_1, the wall must be accelerated more slowly (large s_1 must be used) in order to avoid the step function type of propagation of the distribution

function and the accompanying numerical error.

Results

Equation (90) was solved numerically on the B-5500 computer for several values of k_1 and using the modified quadrature with N = 4. Figures 27, 28, and 29 represent typical results for the case of impulsively accelerating the plate. The values of k_1 reported in these figures are k_1 = 20.0, 5.0, and 1.0, respectively. It will be noted in Figure 29 that the numerical results for d/μ = 1.0 changed significantly when a different grid size was used for the finite differences. This is the same situation which occurred in the transient development of the Couette flow problem and is related to the step-like character of the distribution function for this scale of description.

In order to obtain consistent numerical results down to k_1 = 1.0, the case of accelerating the plate with a constant acceleration was examined. A value of s_1 = 1 was chosen for the parameter in Equation (91). This corresponds to giving the plate a constant acceleration over the nondimensional time interval $0 \leq \bar{\tau}_1 \leq 1$. Figures 30, 31, and 32 illustrate typical results obtained using these conditions. The cases reported in these figures correspond to N = 4 and k_1 = 10.0, 5.0, and 1.0, respectively. It was found that the numerical results using two different grid sizes agreed for all of these cases. The slight irregularity in the curve for k_1 = 1.0 at $\bar{\tau}_1$ = 2.0 is due to the method of bringing the plate up to its final velocity. This same behavior was exhibited in the Couette flow curves for the case of constant plate acceleration. According to previous discussions on the transformation

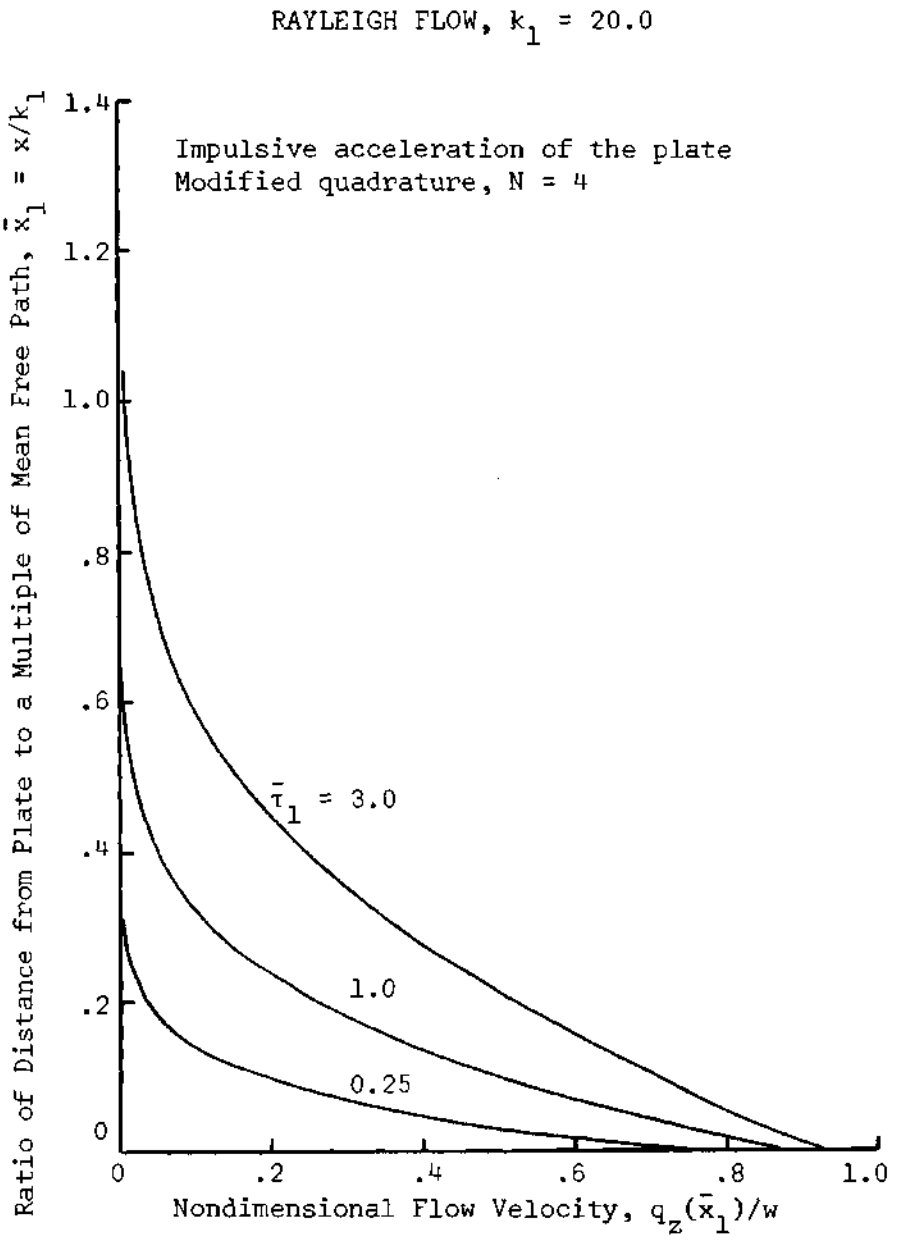

Figure 27. Transient Development of the Velocity Profile in Rayleigh Flow for Impulsive Acceleration of the Plate, k_1 = 20.0 and N = 4.

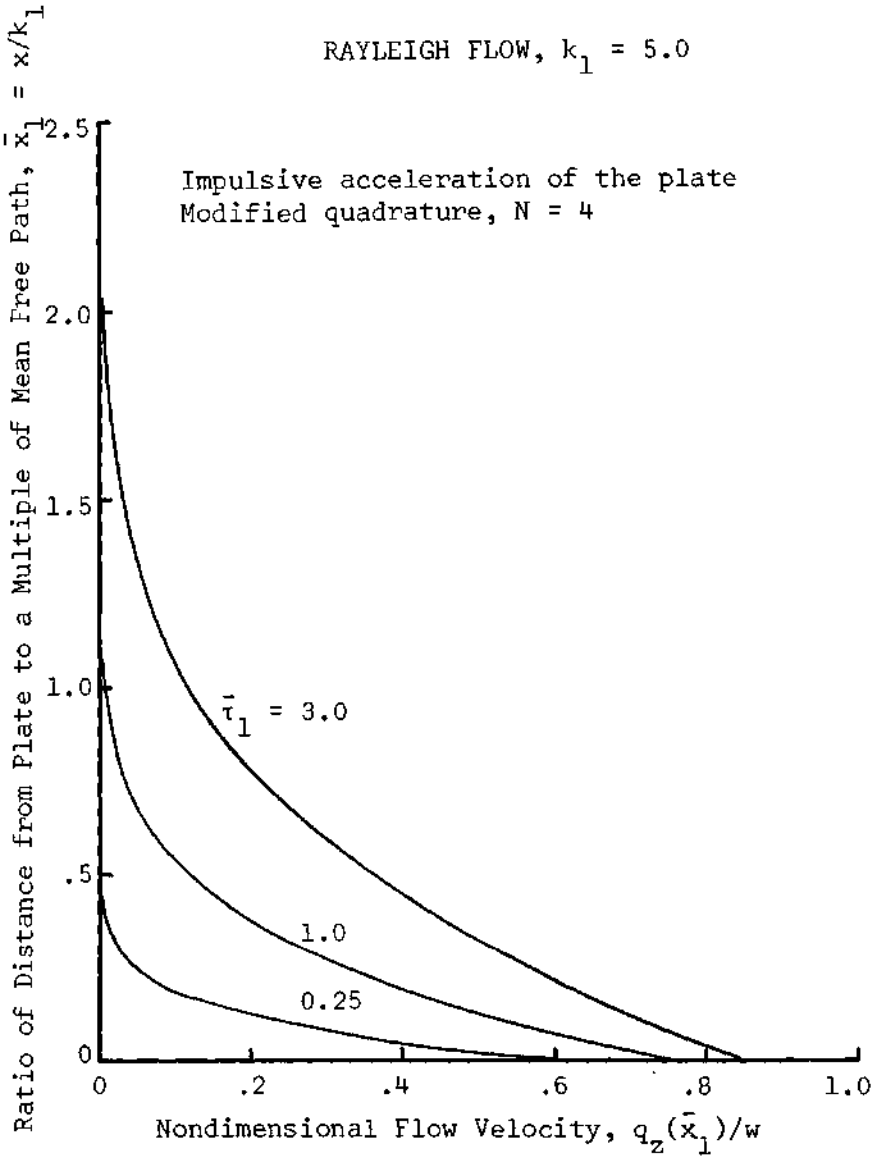

Figure 28. Transient Development of the Velocity Profile in Rayleigh Flow for Impulsive Acceleration of the Plate, k_1 = 5.0 and N = 4.

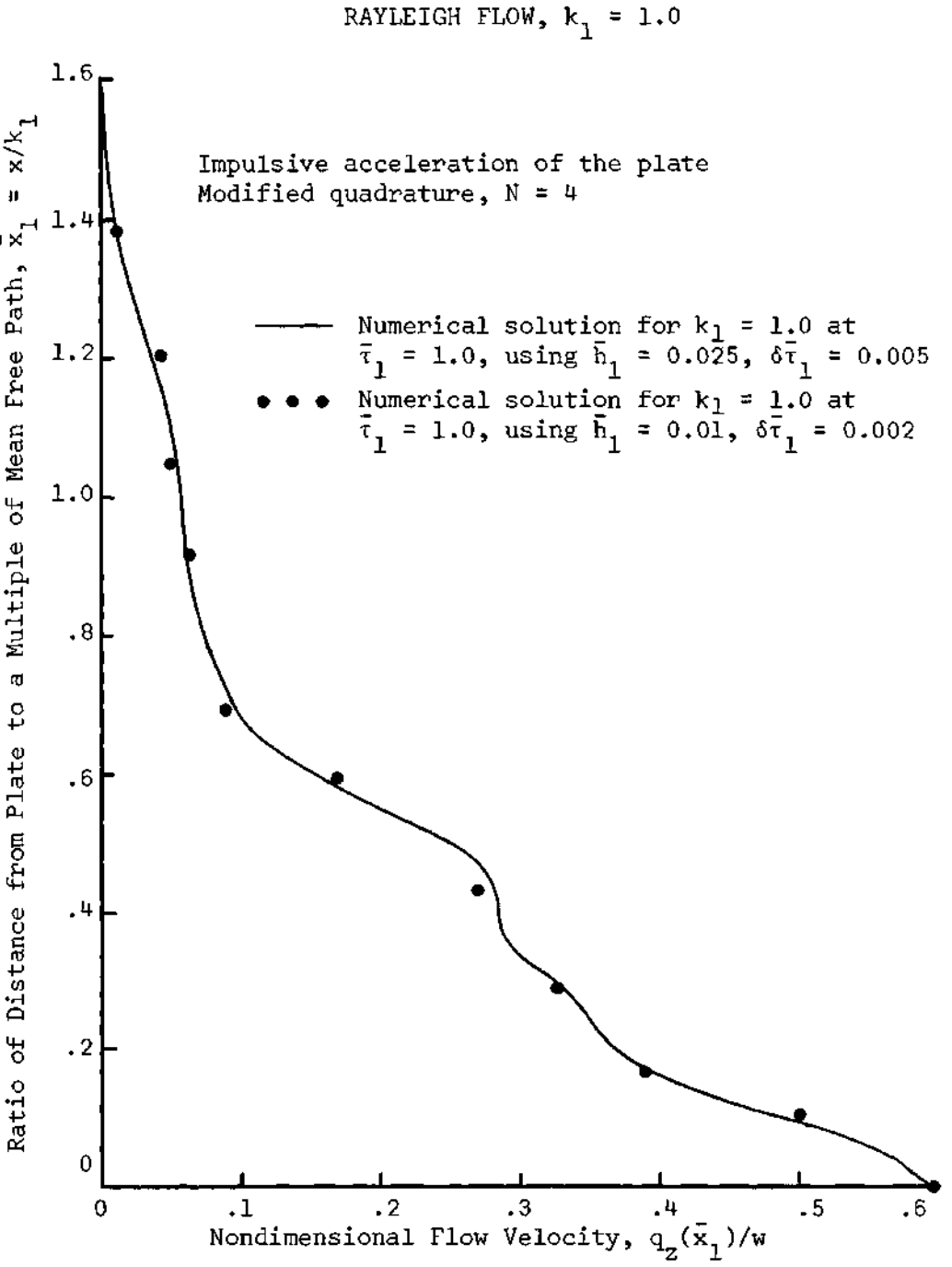

Figure 29. Comparison of the Velocity Profile Development for Rayleigh Flow Using Two Different Step Sizes in the Numerical Solution, k_1 = 1.0 and N = 4.

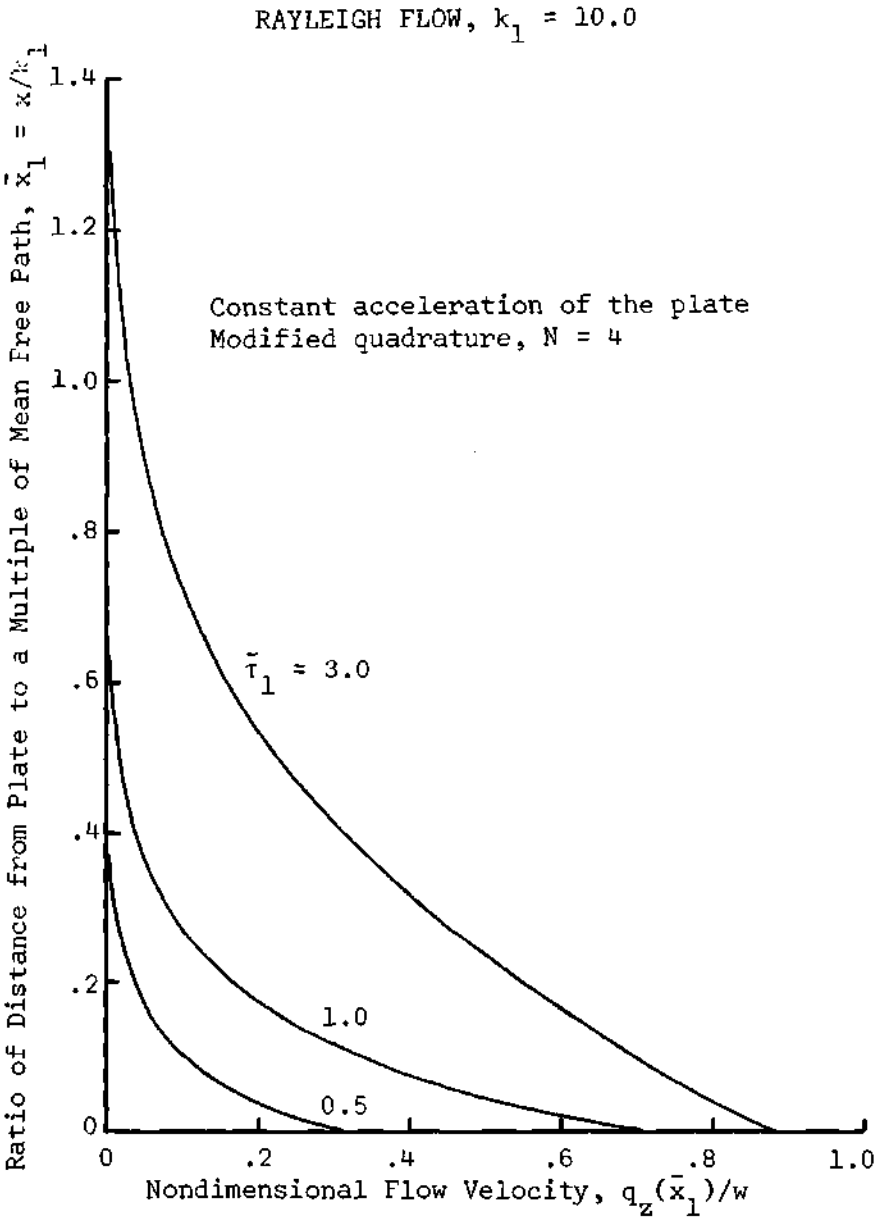

Figure 30. Transient Development of the Velocity Profile in Rayleigh Flow for a Constant Acceleration of the Plate, k_1 = 10.0 and N = 4.

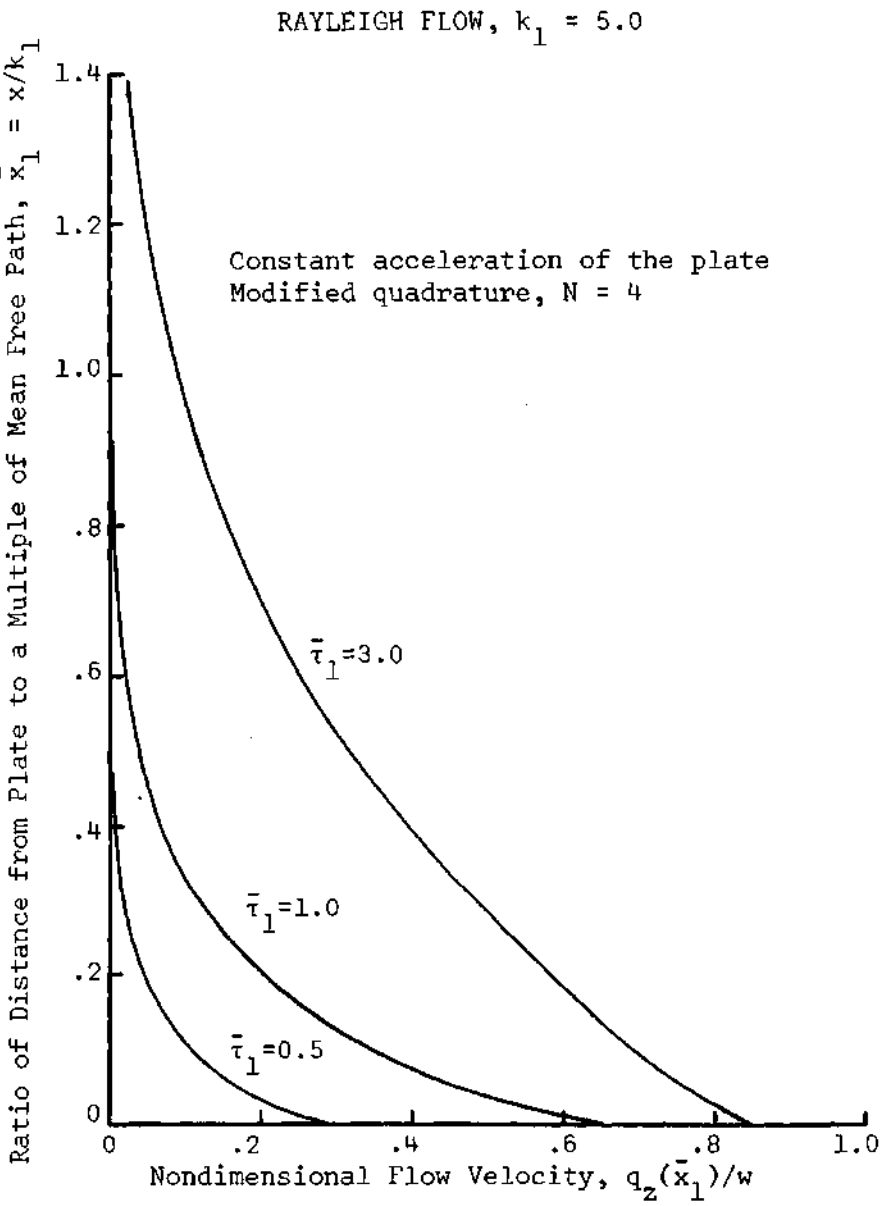

Figure 31. Transient Development of the Velocity Profile in Rayleigh Flow for a Constant Acceleration of the Plate, k_1 = 5.0 and N = 4.

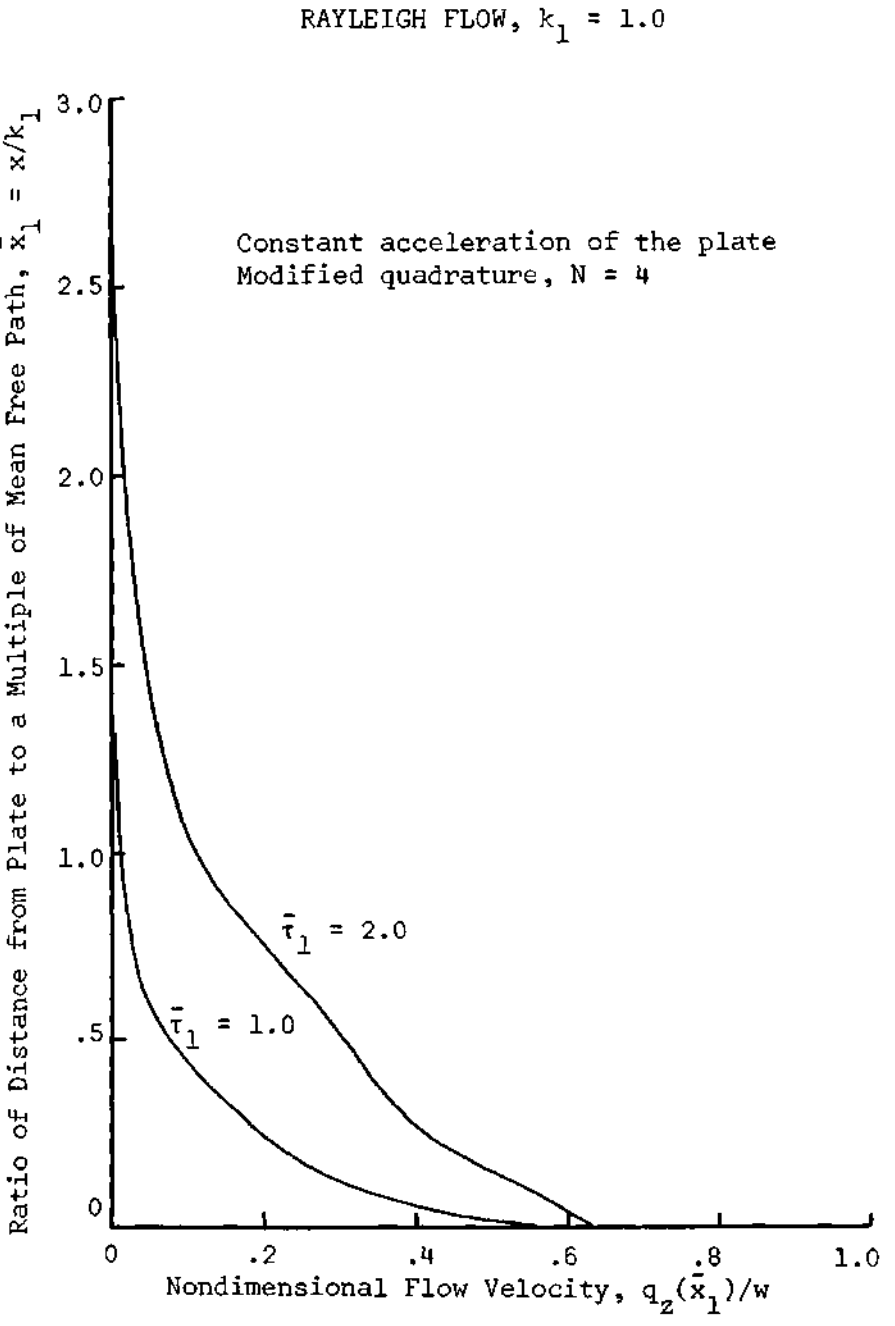

Figure 32. Transient Development of the Velocity Profile in Rayleigh Flow for a Constant Acceleration of the Plate, k_1 = 1.0 and N = 4.

from $\bar{x}_1$ to $\bar{\xi}_1$, the results for the smallest grid size ($\bar{h}_1 = 0.01$ and $\delta\bar{\tau}_1 = 0.002$) represent phenomena occurring on a scale of 1/100th of a mean free path, at least in the important region of large gradients near the plate.

The only comparison which may be made with other solutions are for the limits of short and long times. In Figure 33 the expression for free molecular flow, corresponding approximately to times much less than a collision time, is compared with the results for $k_1 = 5.0$ and $\bar{\tau}_1 = 0.1$ for the case of impulsive acceleration. This corresponds to a ratio of true time to collision time of 0.5. Note that agreement in the curves is quite satisfactory. A comparison in the limit of long time is made in Figure 34 using the numerical results for $k_1 = 5.0$ and $N = 4$ at time $\bar{\tau}_1 = 3.5$ and the long time limit relation developed by Gross and Jackson in Equation (35) of Reference [39]. Again, agreement is very good. It is important to note that for this value of $\bar{\tau}_1$ the long time solution of Gross and Jackson should be considered inaccurate for $\bar{x}_1 > 0.5$ due to their approximation which required that $\bar{x}_1/\bar{\tau}_1 \ll 1$. Thus, the numerical solution presented in this research should be superior for larger values of $\bar{x}_1/\bar{\tau}_1 = \bar{x}/\bar{\tau}$.

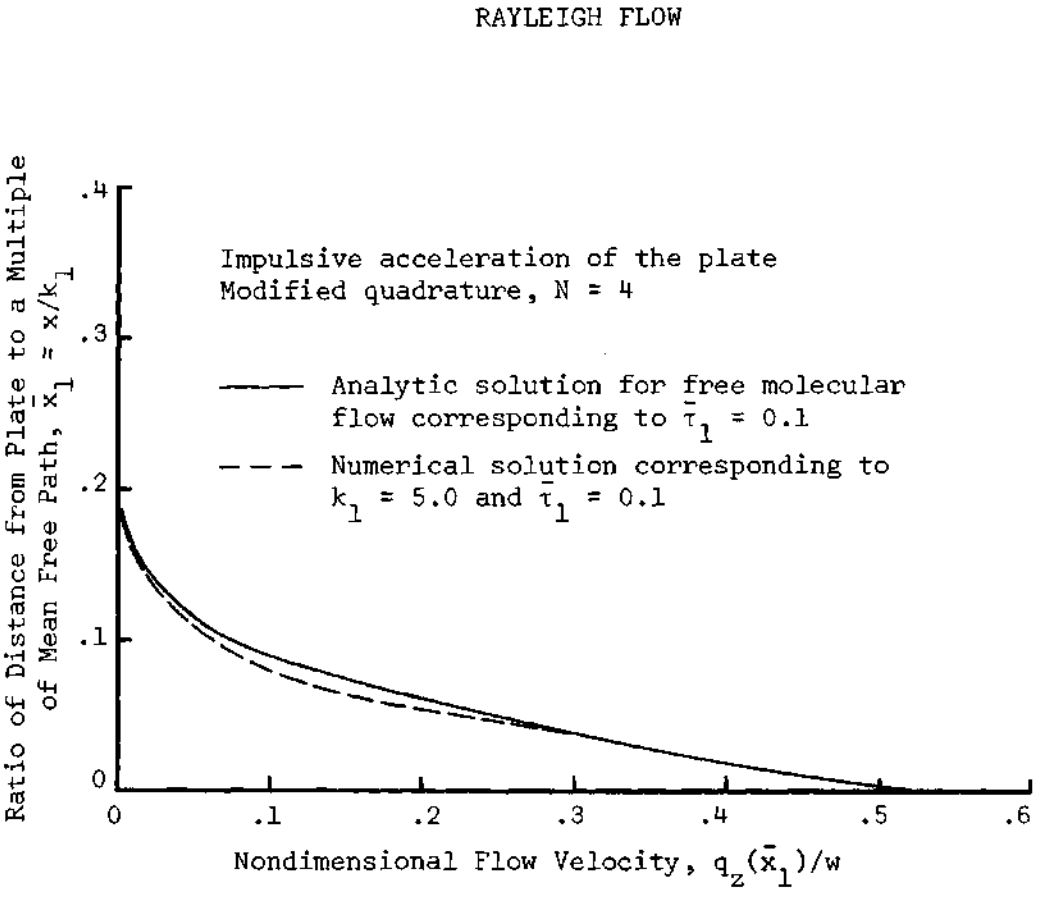

Figure 33. Comparison of the Numerical Solution at Small Time to the Analytic Free Molecular Solution for Rayleigh Flow, Impulsive Acceleration of the Plate.

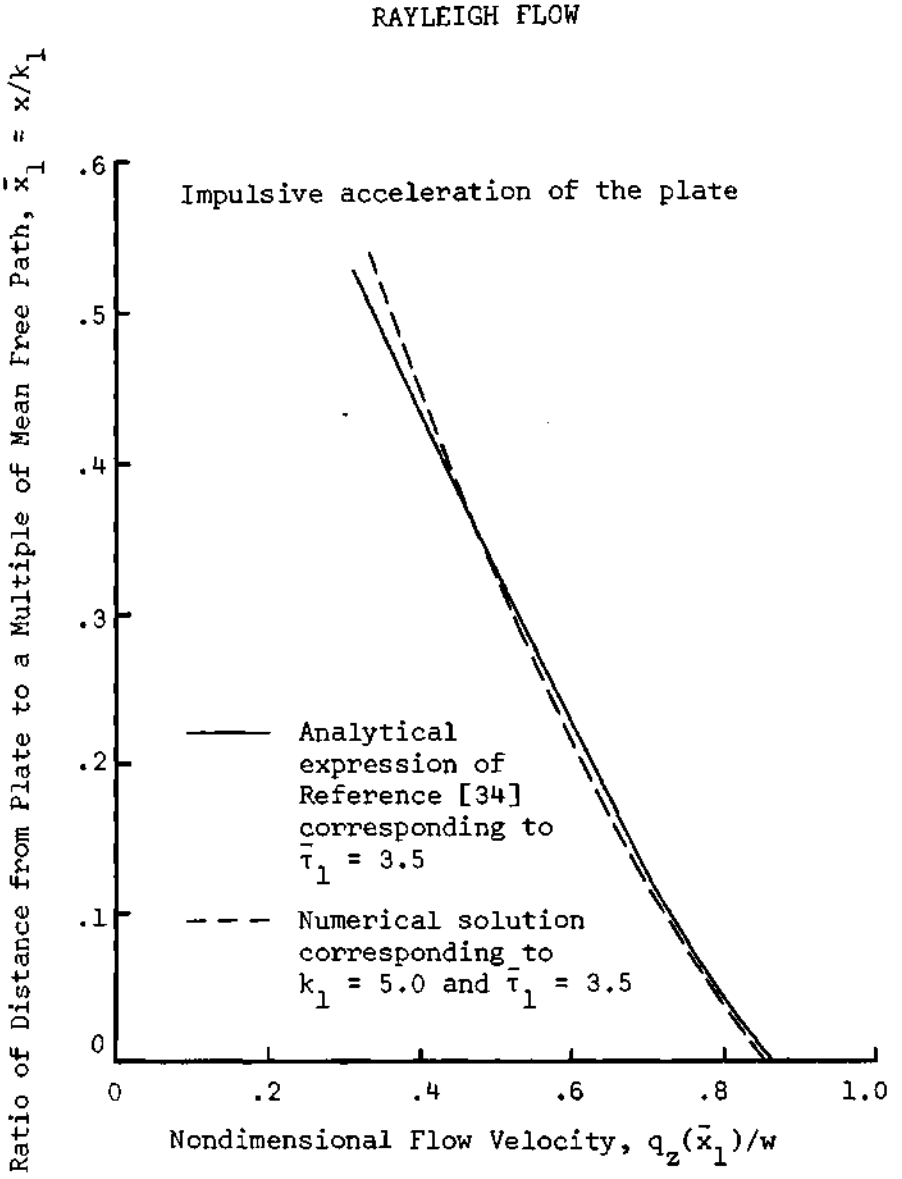

Figure 34. Comparison of the Numerical Results for Long Time with the Asymptotic Analytical Expression of Reference [39] for the Rayleigh Problem, Impulsive Acceleration of the Plate.

CHAPTER VIII

DISCUSSION AND CONCLUSIONS

The method of discrete ordinates has been applied to the linearized BGK Boltzmann equation in an effort to establish a new technique for the solution of this equation over as wide a range of Knudsen numbers as possible. Significant defects in the only other two papers dealing with the discrete ordinate method [16] and [17] were pointed out, indicating the need for a development which followed a rigorous mathematical approach with emphasis being placed upon basing the theory on a solid foundation.

A new and quite useful Gaussian quadrature was developed particularly for the type of problems encountered in kinetic theory, namely, those problems in which the distribution function possesses a streamwise character. The development of this modified quadrature is one of the primary contributions of this work since it is this device which allows the discrete ordinate method to give accurate solutions for quite large values of Knudsen number. The method was then applied to several steady and transient problems with excellent results being obtained for each case, thus establishing the accuracy and usefulness of the technique. One shortcoming is that higher order approximations (large N) are required to obtain accurate results for Knudsen numbers larger than 100.

The application of the method to time dependent problems was coupled with an application of a finite difference scheme to solve the resulting system of partial differential equations. It was found that if the boundaries are accelerated continuously, rather than impulsively, to some final velocity, then the numerical solutions are quite accurate even for ratios of distance to mean free path on the order of 0.025. Further, these solutions clearly describe the physical phenomena occurring during the time from which the gas is initially disturbed until it finally reaches a steady state condition. Of particular interest is the velocity "overshoot" at the wall which occurs in the time dependent Couette problem for values of $d/\mu < 2.0$.

The results of the investigation may be summarized in the following conclusions:

1. The discrete ordinate method has been shown to give accurate solutions over a wider range of Knudsen numbers for a given amount of computational effort than any other existing analytic method applied to the linearized BGK Boltzmann equation.

2. Much of the success of the method is due to the development of the modified quadrature. However, the Gauss-Hermite quadrature may be used with good success for values of $d/\mu > 1$.

3. The difference scheme presented for the time dependent system of partial differential equations is stable and converges to the steady state solution for the transient Couette flow problem investigated and to the appropriate asymptotic solution for the Rayleigh flow problem.

4. Shortcomings in the application of a finite difference method to an initial value problem have been pointed out, with emphasis being placed on discussing the effects of the relation of grid spacing to mean free path.

5. For physically realistic initial value problems the finite difference scheme applied in conjunction with the discrete ordinate method will give excellent results, even to a scale quite small compared to the mean free path of the gas.

6. The primary weakness in the discrete ordinate method is in the very near free molecular flow regime (Knudsen numbers greater than 100) where it is necessary to take large values of N to obtain accurate results. This weakness is not in the solution for the perturbed distribution function, but rather in applying a quadrature to form the velocity moments from this solution.

APPENDICES

APPENDIX A

SOLUTION OF THE LINEARIZED BOLTZMANN EQUATION FOR STEADY COUETTE FLOW

For the case of steady flow the linearized Boltzmann equation with Krook model takes on the form

$$\frac{\mu}{d} c_x \frac{\partial \psi^{\pm}}{\partial \xi} = -\psi^{\pm} + \frac{1}{\sqrt{\pi}} \left[\int_0^{\infty} e^{-c_x^2} \psi^{+} dc_x + \int_{-\infty}^{0} e^{-c_x^2} \psi^{-} dc_x \right] \qquad \text{(A-1)}$$

Applying the discrete ordinate method gives a system of 2N ordinary differential equations of the form

$$\pm \frac{\mu}{d} \alpha_\kappa \frac{d\psi_\kappa^{\pm}}{d\xi} = -\psi_\kappa^{\pm} + \frac{1}{\sqrt{\pi}} \sum_{i=1}^{N} H_i (\psi_i^{+} + \psi_i^{-}) \qquad \text{(A-2)}$$

for $\kappa = 1,2,\ldots,N$. Note that the summation term on the right-hand side couples these equations together so that a simultaneous solution is required. The linearized boundary conditions for the steady state Couette flow case with plates moving at velocity $\pm w/2$ are

$$\psi_\kappa^{\pm} (\xi = \mp 1/2) = \mp w \; ; \qquad \kappa = 1,2,\ldots,N \qquad \text{(A-3)}$$

In order to solve Equation (A-2) exponential solutions are assumed according to the form

$$\psi_\kappa^\pm = A_\kappa^\pm e^{p\xi} \tag{A-4}$$

Substituting this into (A-2) gives

$$\pm \frac{\mu}{d} \alpha_\kappa p A_\kappa^\pm e^{p\xi} = -A_\kappa^\pm e^{p\xi} + \frac{1}{\sqrt{\pi}} \left[\sum_{i=1}^{N} H_i (A_i^+ + A_i^-) e^{p\xi} \right] \tag{A-5}$$

Noting that the exponential terms cancel in this equation and that the summation involves only a summation of constants, it is possible to express $A_\kappa^\pm$ as

$$A_\kappa^\pm = \frac{K}{1 \pm \frac{\mu}{d} p\alpha_\kappa} \tag{A-6}$$

where $K = (1/\sqrt{\pi}) \sum_{i=1}^{N} H_i (A_i^+ + A_i^-)$ is a constant depending only on N. Now that the form of $A_\kappa^\pm$ has been established, Equation (A-6) is substituted into (A-2) to yield, after cancelling the K from each term and some slight rearrangement, the characteristic equation

$$\sum_{i=1}^{N} H_i \frac{1}{1 - \eta\alpha_i^2} = \frac{\sqrt{\pi}}{2} \tag{A-7}$$

where $\eta = (\mu p/d)^2$. Since $\sum_{i=1}^{N} H_i = \sqrt{\pi}/2$ for a Gauss-Hermite quadrature with a total of 2N points in the interval $(-\infty,\infty)$ or for the modified quadrature with N points in the interval $(0,\infty)$ or $(-\infty,0)$, Equation (A-7) possesses a degenerate solution $\eta = 0$. Thus, for arbitrary Knudsen number μ/d there results the double degeneracy condition $p^2 = 0$. This means that, in addition to the exponential solutions, there is a term

linear in ξ and a constant term. Hence, the complete solution may be written as

$$\psi_\kappa^{\pm} = \frac{1}{\sqrt{\pi}} \sum_{j=1}^{N-1} \left[C_j \frac{e^{p_j \xi}}{1 \pm \sqrt{\eta_j}\, \alpha_\kappa} + D_j \frac{e^{-p_j \xi}}{1 \mp \sqrt{\eta_j}\, \alpha_\kappa} \right] + E_\kappa^{\pm} \xi + F_\kappa^{\pm} \qquad \text{(A-8)}$$

It is now necessary to establish some relationships between the $E_\kappa^{\pm}$ and the $F_\kappa^{\pm}$. Assuming the solution

$$\psi_\kappa^{\pm} = E_\kappa^{\pm} \xi + F_\kappa^{\pm} \qquad \text{(A-9)}$$

corresponding to the degenerate characteristic values and substituting this into Equation (A-2) gives

$$\pm \frac{\mu}{d} \alpha_\kappa E_\kappa^{\pm} = -E_\kappa^{\pm} \xi - F_\kappa^{\pm} + \frac{1}{\sqrt{\pi}} \left[\sum_{i=1}^{N} H_i (E_i^{+} \xi + F_i^{+} + E_i^{-} \xi + F_i^{-}) \right] \qquad \text{(A-10)}$$

Equating the coefficients of the first powers of ξ gives

$$E_\kappa^{\pm} = \frac{1}{\sqrt{\pi}} \sum_{i=1}^{N} H_i (E_i^{+} + E_i^{-}) \qquad \text{(A-11)}$$

Since the right-hand side is a constant regardless of the value of κ and since (A-11) must hold for each κ, this implies that all the $E_\kappa^{\pm}$ quantities are equal, so that

$$E_\kappa^{\pm} = E \; ; \qquad \kappa = 1,2,\ldots,N \qquad \text{(A-12)}$$

Another relation, which is obtained by equating coefficients of the zeroth power of ξ, yields conditions on $F_\kappa^\pm$

$$F_\kappa^\pm = \mp \frac{\mu}{d} \alpha_\kappa E + \frac{1}{\sqrt{\pi}} \sum_{i=1}^{N} H_i (F_i^+ + F_i^-) \tag{A-13}$$

Again, since the summation term is invariant with κ for a given value of N, this may be reduced to

$$F_\kappa^\pm = \mp \frac{\mu}{d} \alpha_\kappa E - F \tag{A-14}$$

Therefore, the solution may now be written as

$$\Psi_\kappa^\pm(\xi) = \frac{1}{\sqrt{\pi}} \sum_{j=1}^{N-1} \left[C_j \frac{e^{p_j \xi}}{1 \pm \sqrt{\eta_j}\, \alpha_\kappa} + D_j \frac{e^{-p_j \xi}}{1 \mp \sqrt{\eta_j}\, \alpha_\kappa} \right] + E(\xi \mp \frac{\mu}{d} \alpha_\kappa) - F \tag{A-15}$$

where the C_j, D_j, E, and F are 2N arbitrary constants which are determined by applying the boundary conditions. If the conditions of Equation (A-3) are applied, the system of equations to be solved for the arbitrary constants is

$$\frac{1}{\sqrt{\pi}} \sum_{j=1}^{N-1} \left[C_j \frac{e^{-p_j/2}}{1 + \sqrt{\eta_j}\, \alpha_\kappa} + D_j \frac{e^{p_j/2}}{1 - \sqrt{\eta_j}\, \alpha_\kappa} \right] + E(-\frac{1}{2} - \frac{\mu}{d} \alpha_\kappa) - F = -w \tag{A-16}$$

and

$$\frac{1}{\sqrt{\pi}} \sum_{j=1}^{N-1} \left[C_j \frac{e^{p_j/2}}{1 - \sqrt{\eta_j}\,\alpha_\kappa} + D_j \frac{e^{-p_j/2}}{1 + \sqrt{\eta_j}\,\alpha_\kappa} \right] + E\left(\frac{1}{2} + \frac{\mu}{d}\alpha_\kappa\right) - F = +w \quad \text{(A-17)}$$

However, from the symmetry of this flow, it can be shown that $C_j = -D_j$ and $F = 0$ by substituting these values into Equation (A-16) and (A-17). Also, note that the constant w, representative of the velocity difference between the plates, may be included in the arbitrary constants so that the solution need not be repeated for different values of w. Thus, finally, the solution may be written as

$$\frac{\psi_\kappa^+}{w} = \frac{1}{\sqrt{\pi}} \sum_{j=1}^{N-1} \bar{C}_j \left[\frac{e^{p_j\xi}}{1 + \sqrt{\eta_j}\,\alpha_\kappa} - \frac{e^{-p_j\xi}}{1 - \sqrt{\eta_j}\,\alpha_\kappa} \right] + \bar{E}\left(\xi - \frac{\mu}{d}\alpha_\kappa\right) \quad \text{(A-18)}$$

and

$$\frac{\psi_\kappa^-}{w} = \frac{1}{\sqrt{\pi}} \sum_{j=1}^{N-1} \bar{C}_j \left[\frac{e^{p_j\xi}}{1 - \sqrt{\eta_j}\,\alpha_\kappa} - \frac{e^{-p_j\xi}}{1 + \sqrt{\eta_j}\,\alpha_\kappa} \right] + \bar{E}\left(\xi + \frac{\mu}{d}\alpha_\kappa\right) \quad \text{(A-19)}$$

for $\kappa = 1,2,\ldots,N$. Here, $\bar{C}_j = C_j/w$ and $\bar{E} = E/w$ and they are determined from the conditions

$$\frac{1}{\sqrt{\pi}} \sum_{j=1}^{N-1} \bar{C}_j \left[\frac{e^{p_j/2}}{1 - \sqrt{\eta_j}\,\alpha_\kappa} - \frac{e^{-p_j/2}}{1 + \sqrt{\eta_j}\,\alpha_\kappa} \right] + \bar{E}\left(\frac{1}{2} + \frac{\mu}{d}\alpha_\kappa\right) = 1 \quad \text{(A-20)}$$

The p_j and η_j are determined from the characteristic Equation (A-7) and the relation $\eta_j = (\mu\ p_j/d)^2$.

APPENDIX B

SOLUTION OF THE LINEARIZED BOLTZMANN EQUATION FOR FULLY DEVELOPED FLOW OF A GAS BETWEEN TWO INFINITE PARALLEL PLATES

The linearized Boltzmann equation with Krook model and assuming a constant pressure gradient $\bar{\kappa}/kT$ in the z-direction takes on the form

$$\bar{\eta} + \frac{\mu}{d} c_x \frac{\partial \psi^{\pm}}{\partial \xi} = -\psi^{\pm} + \frac{1}{\sqrt{\pi}} \left[\int_0^{\infty} e^{-c_x^2} \psi^{+} dc_x + \int_{-\infty}^{0} e^{-c_x^2} \psi^{-} dc_x \right] \quad \text{(B-1)}$$

where $\bar{\eta} = \bar{\kappa}/\mu$. Applying the discrete ordinate method to the integrations over c_x gives a system of 2N ordinary differential equations of the form

$$\bar{\eta} \pm \frac{\mu}{d} \alpha_{\kappa} \frac{d\psi_{\kappa}^{\pm}}{d\xi} = -\psi_{\kappa}^{\pm} + \frac{1}{\sqrt{\pi}} \sum_{i=1}^{N} H_i (\psi_i^{+} + \psi_i^{-}) \quad \text{(B-2)}$$

for $\kappa = 1,2,\ldots,N$. The linearized boundary conditions are

$$\psi_{\kappa}^{\pm}(\xi = \mp 1/2) = 0 \; ; \qquad \kappa = 1,2,\ldots,N \quad \text{(B-3)}$$

Note that Equation (B-2) represents a nonhomogeneous system; however, the homogeneous case corresponds exactly to the governing system for steady Couette flow, Equation (A-2) of Appendix A. Since the nonhomogeneous terms are all constants and since this system results in the same

characteristic equation as that given by Equation (A-7), there results a solution of the form

$$\Psi_{\kappa}^{\pm}(\xi) = R_{\kappa}^{\pm}\xi^2 + S_{\kappa}^{\pm}\xi + T_{\kappa}^{\pm} \tag{B-4}$$

in addition to the N-1 pairs of exponential solutions.

Equation (B-4) contains too many constants for the number of boundary conditions available so it is necessary to find some relationship between them. Substituting (B-4) into (B-2) and equating the coefficients of ξ^2 gives

$$R_{\kappa}^{\pm} = \frac{1}{\sqrt{\pi}} \sum_{i=1}^{N} H_i(R_i^{+} + R_i^{-}) \tag{B-5}$$

for $\kappa = 1,2,\ldots,N$ so that all the R_{κ} must be equal. Hence, there results the relation

$$R_{\kappa}^{\pm} = R \tag{B-6}$$

Similarly, equating the coefficients of ξ gives

$$S_{\kappa}^{\pm} = \mp 2\frac{\mu}{d}\alpha_{\kappa}R + \frac{1}{\sqrt{\pi}} \sum_{i=1}^{N} H_i(S_i^{+} + S_i^{-}) \tag{B-7}$$

or, since the summation is independent of κ,

$$S_{\kappa}^{\pm} = \mp 2\frac{\mu}{d}\alpha_{\kappa} R + S \tag{B-8}$$

Finally, equating the constants gives

$$T_\kappa^{\pm} = -\bar{\eta} + 2\left(\frac{\mu}{d}\right)^2 \alpha_\kappa^2 R \mp \frac{\mu}{d}\,\alpha_\kappa\, S + T \tag{B-9}$$

Note that all the $R_\kappa^{\pm}$, $S_\kappa^{\pm}$, and $T_\kappa^{\pm}$ have been expressed in terms of known quantities and three new constants R, S, and T. However, there is still one extra constant for the number of boundary conditions available. One final substitution of the quadratic form into the original equation yields the relation

$$R = \left(\frac{d}{\mu}\right)^2 \bar{\eta} \tag{B-10}$$

Thus, the solution may be written as

$$\frac{\psi_\kappa^+}{\bar{\eta}} = \frac{1}{\sqrt{\pi}} \sum_{j=1}^{N-1} \tilde{C}_j \left[\frac{e^{p_j \xi}}{1 + \sqrt{\eta_j}\,\alpha_\kappa} + \frac{e^{-p_j \xi}}{1 - \sqrt{\eta_j}\,\alpha_\kappa} \right] + \left(\frac{d}{\mu}\right)^2 \xi^2 \tag{B-11}$$

$$- 2\alpha_\kappa \frac{d}{\mu}\,\xi + (-1 + 2\alpha_\kappa^2 + \tilde{T})$$

and

$$\frac{\psi_\kappa^-}{\bar{\eta}} = \frac{1}{\sqrt{\pi}} \sum_{j=1}^{N-1} \tilde{C}_j \left[\frac{e^{p_j \xi}}{1 - \sqrt{\eta_j}\,\alpha_\kappa} + \frac{e^{-p_j \xi}}{1 + \sqrt{\eta_j}\,\alpha_\kappa} \right] + \left(\frac{d}{\mu}\right)^2 \xi^2 \tag{B-12}$$

$$+ 2\alpha_\kappa \frac{d}{\mu}\,\xi + (-1 + 2\alpha_\kappa^2 + \tilde{T})$$

where the condition of symmetry of the problem has been applied and the perturbed distribution function has been divided by the parameter $\bar{\eta}$ so that solutions may be obtained which are independent of this quantity.

Applying the boundary conditions to these equations yields a system of N equations from which the constants $\tilde{C}_j$ and $\tilde{T}$ may be obtained,

$$\frac{1}{\sqrt{\pi}} \sum_{j=1}^{N-1} \tilde{C}_j \left[\frac{e^{-p_j/2}}{1 + \sqrt{\eta_j}\, \alpha_\kappa} + \frac{e^{+p_j/2}}{1 - \sqrt{\eta_j}\, \alpha_\kappa} \right] + \tilde{T} \approx 1 - \frac{1}{4} \left(\frac{d}{\mu}\right)^2 - \alpha_\kappa \frac{d}{\mu} - 2\alpha_\kappa^2 \qquad \text{(B-13)}$$

The p_j and η_j are determined from the characteristic equation

$$\sum_{i=1}^{N} H_i \frac{1}{1 - \eta\alpha_i^2} = \frac{\sqrt{\pi}}{2} \qquad \text{(B-14)}$$

and the relation $\eta = (\mu\, p/d)^2$.

APPENDIX C

SOLUTION OF THE TRANSIENT, COLLISIONLESS, LINEARIZED BOLTZMANN EQUATION FOR COUETTE AND RAYLEIGH FLOWS

Couette Flow

For the collisionless, transient case the one-dimensional linearized Boltzmann equation takes the form

$$\frac{\partial \Psi^{\pm}}{\partial \tau} + c_x \frac{\partial \Psi^{\pm}}{\partial \xi} = 0 \qquad \text{(C-1)}$$

where $\tau = t/\beta d$ and $\xi = x/d$ are the nondimensional time and distance coordinates. For the Couette flow problem it is convenient to transform the normal coordinate according to the relations

$$\tilde{\xi} = \xi + 1/2$$

$$\tilde{\eta} = \xi - 1/2 \qquad \text{(C-2)}$$

so that $0 \leq \tilde{\xi} \leq 1$ and $-1 \leq \tilde{\eta} \leq 0$. This coordinate system is indicated below

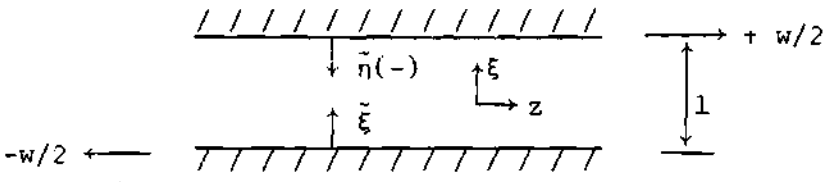

Thus, Equation (C-1) may be written as

$$\frac{\partial \Psi^+}{\partial \tau} + c_x \frac{\partial \Psi^+}{\partial \tilde{\xi}} = 0 \qquad \text{(C-3)}$$

$$\frac{\partial \Psi^-}{\partial \tau} + c_x \frac{\partial \Psi^-}{\partial \tilde{\eta}} = 0 \qquad \text{(C-4)}$$

Impulsive Acceleration

For the case of impulsive acceleration of the plates the boundary conditions are

$$\Psi^+(\tilde{\xi} = 0, \tau) = -w$$

$$\Psi^-(\tilde{\eta} = 0, \tau) = +w \qquad \text{(C-5)}$$

while the initial conditions are

$$\Psi^+(\tilde{\xi} > 0, \tau = 0) = 0$$

$$\Psi^-(\tilde{\eta} < 0, \tau = 0) = 0 \qquad \text{(C-6)}$$

Taking the Laplace transform of Equation (C-3) yields

$$c_x \frac{d\bar{\Psi}^+}{d\tilde{\xi}} + s\,\bar{\Psi}^+ = 0 \qquad \text{(C-7)}$$

where $\bar{\Psi}^+(\tilde{\xi})$ is the Laplace transform of $\Psi^+(\tilde{\xi}, \tau)$. The solution to this equation corresponding to the transformed boundary condition is

$$\bar{\Psi}^{+} = -\frac{w}{s} e^{-(s/c_x)\tilde{\xi}} \tag{C-8}$$

where s is the transformation parameter.

Similarly, the solution for $\bar{\Psi}^{-}$ is given by

$$\bar{\Psi}^{-} = \frac{w}{s} e^{-(s/c_x)\tilde{\eta}} \tag{C-9}$$

where both $\tilde{\eta}$ and c_x are non-positive. These may be inverted to yield

$$\Psi^{+} = \begin{cases} 0 & \text{for } \tilde{\xi} > \tau c_x > 0 \\ -w & \text{for } 0 < \tilde{\xi} < \tau c_x \end{cases} \tag{C-10}$$

$$\Psi^{-} = \begin{cases} 0 & \text{for } \tilde{\eta} < \tau c_x < 0 \\ +w & \text{for } \tau c_x < \tilde{\eta} < 0 \end{cases} \tag{C-11}$$

The flow velocity is obtained by performing the velocity moment integration

$$q_z(\xi,\tau) = \frac{1}{2\sqrt{\pi}} \left[\int_0^{\infty} e^{-c_x^2} \Psi^{+} dc_x + \int_{-\infty}^{0} e^{-c_x^2} \Psi^{-} dc_x\right] \tag{C-12}$$

Substituting the relations for Ψ^{+} and Ψ^{-} into this equation gives

$$\frac{q_z}{w/2} = \frac{1}{2}\left[-\operatorname{erfc}(\tilde{\xi}/\tau) + \operatorname{erfc}(|\tilde{\eta}|/\tau)\right] \tag{C-13}$$

or, in terms of the normalized space coordinate

$$\frac{q_z(\xi,\tau)}{w/2} = \frac{1}{2}\left[\operatorname{erfc}\left\{\frac{\frac{1}{2} - \xi}{\tau}\right\} - \operatorname{erfc}\left\{\frac{\frac{1}{2} + \xi}{\tau}\right\}\right] \qquad \text{(C-14)}$$

where the complementary error function is defined as

$$\operatorname{erfc}(x) = \frac{2}{\sqrt{\pi}} \int_x^\infty e^{-u^2}\, du = 1 - \operatorname{erf}(x)$$

Constant Acceleration

If the surfaces are accelerated with constant acceleration $\pm w/2$ over a period of time $0 < \tau \leq 1$ and then held at the constant velocities $\pm w/2$ for $\tau > 1$, the boundary conditions become

$$\Psi^+(\tilde{\xi} = 0,\tau) = \begin{cases} -w\tau & \text{for } 0 < \tau \leq 1 \\ -w & \text{for } \tau > 1 \end{cases}$$

$$\Psi^-(\tilde{\eta} = 0,\tau) = \begin{cases} w\tau & \text{for } 0 < \tau \leq 1 \\ w & \text{for } \tau > 1 \end{cases} \qquad \text{(C-15)}$$

while the initial conditions remain the same as for the previous case.

Since this free molecular solution is to be used as a comparison with numerical solutions reported in Chapter VI, the time period of

interest is that for which $0 < \tau \leq 1$. Only in this region can the assumption of neglecting collisions be justified for the values of d/μ which were treated numerically. Thus, the transformed equation is again the same as for the impulsive case, but the transformed boundary conditions are altered. The solutions for $\bar{\Psi}^{\pm}$ are then

$$\bar{\psi}^{+} = -\frac{w}{s^2} e^{-\frac{s}{c_x}\tilde{\xi}} \tag{C-16}$$

$$\bar{\psi}^{-} = \frac{w}{s^2} e^{-\frac{s}{c_x}\tilde{\eta}} \tag{C-17}$$

These may be inverted to give

$$\psi^{+} = \begin{cases} 0 & \text{for } 0 < \tau c_x < \tilde{\xi} \\ -w(\tau - \tilde{\xi}/c_x) & \text{for } 0 < \tilde{\xi} < \tau c_x \end{cases} \tag{C-18}$$

$$\psi^{-} = \begin{cases} 0 & \text{for } \tilde{\eta} < \tau c_x < 0 \\ +w(\tau - \tilde{\eta}/c_x) & \text{for } \tau c_x < \tilde{\eta} < 0 \end{cases} \tag{C-19}$$

for $0 < \tau \leq 1$. Recall that $\tilde{\eta}, c_x \leq 0$ in Equation (C-19).

The flow velocity is given by Equation (C-12) which may be written as

$$\frac{q_z}{w/2} = \frac{1}{\sqrt{\pi}} \left[- \int_{\tilde{\xi}/\tau}^{\infty} (\tau - \tilde{\xi}/c_x) e^{-c_x^2} \, dc_x + \int_{|\tilde{\eta}|/\tau}^{\infty} (\tau - |\tilde{\eta}|/c_x) e^{-c_x^2} \, dc_x \right] \qquad \text{(C-20)}$$

or

$$\frac{q_z}{w/2} = \frac{1}{\sqrt{\pi}} \left[\frac{\sqrt{\pi}}{2} [-\tau \operatorname{erfc}(\tilde{\xi}/\tau) + \tau \operatorname{erfc}(|\tilde{\eta}|/\tau)] \right. \qquad \text{(C-21)}$$

$$\left. + \tilde{\xi} \int_{\tilde{\xi}/\tau}^{\infty} e^{-c_x^2} / c_x \, dc_x - |\tilde{\eta}| \int_{|\tilde{\eta}|/\tau}^{\infty} e^{-c_x^2} / c_x \, dc_x \right]$$

But $\int_a^{\infty} e^{-u^2} / u \, du$ is related to the exponential-integral function [40]

$$-\mathrm{Ei}(-t) = \int_t^{\infty} e^{-y}/y \, dy = \int_1^{\infty} e^{-tx} / x \, dx \qquad \text{(C-22)}$$

so that by letting $y = u^2$ there results

$$-\mathrm{Ei}(-t) = 2 \int_{\alpha=\sqrt{t}}^{\infty} e^{-u^2} / u \, du \qquad \text{(C-23)}$$

Thus, the solution for the flow velocity may be written as

$$\frac{q_z}{w/2} = \frac{1}{\sqrt{\pi}} \left\{ \frac{\sqrt{\pi}}{2} \tau \left[\operatorname{erfc}[(1/2 - \xi)/\tau] - \operatorname{erfc}[(1/2 + \xi)/\tau] \right] \right. \qquad \text{(C-24)}$$

$$- [(\xi + 1/2)/2] \, \mathrm{Ei}[-(\xi + 1/2)/\tau] +$$

$$\left. [(1/2 - \xi)/2] \, \mathrm{Ei}[-(\xi - 1/2)^2/\tau^2] \right\}$$

for $0 < \tau \leq 1$.

Rayleigh Flow

Impulsive Acceleration

The free molecular solution for the Rayleigh problem is quite similar to that for the transient development of Couette flow. An infinite plate is impulsively accelerated in its own plane from rest to a velocity of w with the geometry and coordinate system given below

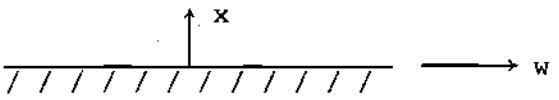

The governing equations for the collisionless, one-dimensional linearized case are

$$\frac{\partial \Psi^{\pm}}{\partial \tau_1} + c_x \frac{\partial \Psi^{\pm}}{\partial x} = 0 \qquad \text{(C-25)}$$

where $\tau_1 = t/\beta$ has the dimension of distance. Due to the condition that $\Psi^{-}(x \to \infty, \tau_1) = 0$ and the assumption that there are no molecular collisions, the solution for Ψ^{-} is

$$\Psi^{-}(x, \tau_1) = 0 \qquad \text{(C-26)}$$

Solving Equation (C-25) by using Laplace transforms as was done in the Couette flow case and applying the linearized boundary condition

that $\Psi^+(x=0,\tau_1) = 2w$ gives

$$\Psi^+ = \begin{cases} 0 & \text{for } x > \tau_1 c_x > 0 \\ 2w & \text{for } 0 < x < \tau_1 c_x \end{cases} \tag{C-27}$$

The flow velocity is then obtained by the velocity moment integration indicated in Equation (C-12) and the resulting expression is

$$\frac{q_z}{w} = \frac{1}{2} \operatorname{erfc}(x/\tau_1) \tag{C-28}$$

Constant Acceleration

If the plate is accelerated with a constant acceleration w over an interval $0 < \bar{\tau} \leq 1$ and then held constant at the velocity w for $\bar{\tau} > 1$, the boundary condition becomes

$$\Psi^+(\bar{x}=0,\bar{\tau}) = \begin{cases} 2w\bar{\tau} & \text{for } 0 < \bar{\tau} \leq 1 \\ 2w & \text{for } \bar{\tau} > 1 \end{cases} \tag{C-29}$$

where $\bar{x} = x/\mu$ and $\bar{\tau} = t/\beta\mu$ are the ratios of distance to mean free path and true time to collision time, respectively.

Again solving by Laplace transforms for the range $0 < \bar{\tau} \leq 1$ there results the solution

$$\psi^+ = \begin{cases} 0 & \text{for } \bar{x} > \bar{\tau}c_x > 0 \\ 2w(\bar{\tau}-\bar{x}/c_x) & \text{for } 0 < \bar{x} < \bar{\tau}c_x \end{cases} \tag{C-30}$$

$$\psi^- = 0 \tag{C-31}$$

The flow velocity is then given by a velocity moment integration as before and yields

$$\frac{q_z}{w} = \frac{1}{\sqrt{\pi}} \{\frac{\sqrt{\pi}}{2} \bar{\tau} \quad \text{erfc}(\bar{x}/\bar{\tau}) - \frac{\bar{x}}{2} \text{Ei}[-(\bar{x}/\bar{\tau})^2]\} \tag{C-32}$$

which is valid only if $0 < \bar{\tau} \leq 1$.

APPENDIX D

STABILITY ANALYSIS FOR THE SYSTEM OF FINITE DIFFERENCE EQUATIONS

For the stability analysis of the system of finite difference equations the form of each equation for $\Psi^{\pm}$ may be written as

$$\Psi_{\kappa}^{\hat{n}+1}(\hat{i})^{\pm} = \Psi_{\kappa}^{\hat{n}}(\hat{i})^{\pm} - \alpha_{\kappa} \frac{\delta\tau}{2h} [\Psi_{\kappa}^{\hat{n}+1}(\hat{i}+1)^{\pm} - \Psi_{\kappa}^{\hat{n}+1}(\hat{i}-1)^{\pm}] \qquad (D\text{-}1)$$

$$-\delta\tau \Psi_{\kappa}^{\hat{n}}(\hat{i})^{\pm} + \frac{\delta\tau}{\sqrt{\pi}} \sum_{j=1}^{N} H_j [\Psi_j^{\hat{n}}(\hat{i})^{+} + \Psi_j^{\hat{n}}(\hat{i})^{-}]$$

where $\Psi_{\kappa}^{\hat{n}}(\hat{i})^{\pm}$ denotes the function $\Psi_{\kappa}^{\pm}$ evaluated at space step $\hat{i}$ and time step $\hat{n}$, and h and $\delta\tau$ are the finite space and time steps, respectively. The most unstable of the $\Psi_j^{\pm}$ functions is now selected from the set for $j = 1,2,\ldots,N$ and is denoted by Ψ_{κ}^{+} (it may be shown that stability results are the same if one of the Ψ_j^{-} functions had been selected). Now following the von Neumann method for stability analyses, let

$$\Psi_{\kappa}^{\hat{n}}(\hat{i})^{+} = (\psi_{\kappa} r^{\hat{n}} e^{\hat{i}k_{\kappa}\hat{i}})_{\kappa}^{+} = \zeta_{\kappa}^{+} \qquad (D\text{-}2)$$

where $i = \sqrt{-1}$, ψ_{κ} represents a magnitude for the function Ψ_{κ}^{+}, and r represents a growth term which is indicative of the error increase as the time steps increase. The requirement for stability is that $|r| \leq 1$.

From Equation (D-2) it is seen that

$$\psi_{\kappa}^{\hat{n}+1}(\hat{i}) = \zeta_{\kappa}^{+} r \tag{D-3}$$

and

$$\psi_{\kappa}^{\hat{n}}(\hat{i+1})^{+} = \zeta_{\kappa}^{+} e^{ik_{\kappa}} \tag{D-4}$$

Substituting these relations into Equation (D-1) gives

$$\zeta_{\kappa}^{+} r = \zeta_{\kappa}^{+} - \alpha_{\kappa} \frac{\delta\tau}{2h} [\zeta_{\kappa}^{+} r e^{ik_{\kappa}} - \zeta_{\kappa}^{+} r e^{-ik_{\kappa}}] \tag{D-5}$$

$$- \delta\tau \zeta_{\kappa}^{+} + \frac{\delta\tau}{\sqrt{\pi}} \sum_{j=1}^{N} H_j(\zeta_j^{+} + \zeta_j^{-})$$

or

$$r = 1 - \alpha_{\kappa} \frac{\delta\tau}{2h} r (\cos k_{\kappa} + i \sin k_{\kappa} - \cos k_{\kappa} + i \sin k_{\kappa}) \tag{D-6}$$

$$+ \delta\tau\left(\frac{H_{\kappa}}{\sqrt{\pi}} - 1\right) + \frac{\delta\tau}{\sqrt{\pi}} \sum_{\substack{j=1 \\ j\neq\kappa}}^{N} H_j \left\{\frac{\zeta_j^{+} + \zeta_j^{-}}{\zeta_{\kappa}^{+}}\right\} + \frac{\delta\tau}{\sqrt{\pi}} \frac{H_{\kappa}\zeta_{\kappa}^{-}}{\zeta_{\kappa}^{+}}$$

Thus, the expression for r may be simplified to

$$r = \frac{1 - \delta\tau\left\{1 - \frac{H_{\kappa}}{\sqrt{\pi}}\right\} + \frac{\delta\tau}{\sqrt{\pi}} \left[\sum_{\substack{j=1 \\ j\neq\kappa}}^{N} H_j \left\{\frac{\zeta_j^{+} + \zeta_j^{-}}{\zeta_{\kappa}^{+}}\right\} + H_{\kappa} \frac{\zeta_{\kappa}^{-}}{\zeta_{\kappa}^{+}}\right]}{1 + i\,\alpha_{\kappa} \frac{\delta\tau}{h} \sin k_{\kappa}} \tag{D-7}$$

The criterion for stability is that $|r| \leq 1$ or that $|r^2| \leq 1$. Note that Equation (D-7) is of the form

$$r = \frac{K}{a + ib} \tag{D-8}$$

so that

$$|r^2| = \frac{K^2}{a^2 + b^2} \tag{D-9}$$

Applying this to Equation (D-7) gives

$$|r^2| = \frac{\left\{ 1 - \delta\tau(1 - \frac{H_\kappa}{\sqrt{\pi}}) + \frac{\delta\tau}{\sqrt{\pi}} \left[\sum_{\substack{j=1 \\ j \neq \kappa}}^{N} H_j \left\{ \frac{\zeta_j^+ + \zeta_j^-}{\zeta_\kappa^+} \right\} + H_\kappa \frac{\zeta_\kappa^-}{\zeta_\kappa^+} \right] \right\}^2}{1 + (\alpha_\kappa \frac{\delta\tau}{h})^2 \sin^2 k_\kappa} \tag{D-10}$$

But since the most unstable function was chosen

$$|\zeta_j^+| \quad \text{and} \quad |\zeta_j^-| < |\zeta_\kappa^+|$$

so that

$$|r^2| \leq \frac{\left[1 - \delta\tau(1 - \frac{H_\kappa}{\sqrt{\pi}}) + \frac{\delta\tau}{\sqrt{\pi}} (\sqrt{\pi} - H_\kappa) \right]^2}{1 + (\alpha_\kappa \frac{\delta\tau}{h})^2 \sin^2 k_\kappa}$$

or

$$|r^2| \leq \frac{1}{1 + \varepsilon^2} \leq 1 \qquad \text{(D-11)}$$

regardless of the value of $\delta\tau/h$. Thus, the stability criterion is satisfied.

BIBLIOGRAPHY

1. F. S. Sherman, "A Low Density Wind Tunnel Study of Shock Wave Structure and Relaxation Phenomena in Gases," University of California at Berkeley, Report Number HE 150-122 (1954).

2. H. Yang and L. Lees, "Rayleigh's Problem at Low Mach Number According to the Kinetic Theory of Gases," *Journal of Mathematics and Physics 35*, 195 (1956).

3. H. Yang and L. Lees, "Rayleigh's Problem at Low Reynolds Number According to the Kinetic Theory of Gases," *Proceedings of the First International Symposium on Rarefied Gasdynamics*, edited by F. M. Devienne, Pergamon Press (1960).

4. D. R. Willis, *A Study of Some Nearly Free Molecular Flow Problems*, Princeton University, Ph.D. Thesis (1958).

5. R. L. Stoy, *Rarefied Gas Flow Between Two Parallel Plates for Three Molecular Models*, Georgia Institute of Technology, Ph.D. Thesis (1966).

6. A. B. Huang and R. L. Stoy, "Rarefied Gas Channel Flows for Three Molecular Models," (submitted for publication).

7. C. Cercignani and A. Daneri, "Flow of a Rarefied Gas Between Two Parallel Plates," *Journal of Applied Physics 34*, 3509 (1963).

8. H. M. Mott-Smith, "A New Approach in the Kinetic Theory of Gases," Massachusetts Institute of Technology, Lincoln Laboratory Group Report V-2 (1952).

9. C. S. Wang Chang and G. E. Uhlenbeck, "Transport Phenomena in Very Dilute Gases," University of Michigan Engineering Research Institute, Report Number C.M. 579 (1949).

10. C. S. Wang Chang and G. E. Uhlenbeck, "The Couette Flow Between Two Parallel Plates as a Function of Knudsen Number," University of Michigan Engineering Research Institute, Report Number 199-1-T (1954).

11. C. S. Wang Chang and G. E. Uhlenbeck, "The Heat Transfer Between Two Parallel Plates as a Function of Knudsen Number," University of Michigan Engineering Research Institute, Report Number M999 (1953).

12. E. P. Gross, E. A. Jackson, and S. Ziering, "Boundary Value Problems in Kinetic Theory of Gases," *Annals of Physics 1*, 141 (1957).

13. S. Chandrasekhar, *Radiative Transfer*, Dover Publishing Company, New York (1960).

14. V. Kourganoff, *Basic Methods in Transfer Problems*, Clarendon Press, Oxford (1952).

15. M. Krook, "On the Solutions of Equations of Transfer. I," *Journal of Astrophysics 122*, 488 (1955).

16. J. E. Broadwell, "Study of Rarefied Shear Flow by the Discrete Velocity Method," *Journal of Fluid Mechanis 19*, 401 (1964).

17. B. B. Hamel and M. Wachman, "A Discrete Ordinate Technique for the Linearized Boltzmann Equation with Application to Couette Flow," General Electric Report R64SD53 (1964). Also, *Fourth International Symposium on Rarefied Gasdynamics I*, Edited by J. H. deLeeuw, Academic Press (1966).

18. P. L. Bhatnager, E. P. Gross, and M. Krook, "A Model for Collision Processes in Gases," *Physical Reviews 94*, 511 (1954).

19. A. B. Huang and D. P. Giddens, "The Discrete Ordinate Method for the Linearized Boundary Value Problems in Kinetic Theory of Gases," *Proceedings of the Fifth International Symposium on Rarefied Gasdynamics*, Academic Press (to be published in 1966).

20. A. B. Huang and D. P. Giddens, "Unsteady Linearized Boundary Value Problems in Kinetic Theory of Gases According to the Discrete Ordinate Method," (submitted for publication).

21. J. O. Hirschfelder, C. F. Curtiss, and R. B. Bird, *Molecular Theory of Gases and Liquids*, Wiley and Sons, New York (1954).

22. Z. Kopal, *Numerical Analysis*, Wiley and Sons, New York (1961).

23. A. B. Huang, "Evaluation of the Integral $\int_0^\infty u^m \exp(-u^2-x/u)du$ by the Discrete Ordinate Method," *Journal of Mathematics and Physics*, (to be published in 1966).

24. A. B. Huang and D. P. Giddens, "A New Table for a Modified (Half-Range) Gauss-Hermite Quadrature with an Evaluation of the Integral $\int_0^\infty \exp(-u^2-x/u)du$," *Journal of Mathematics and Physics*, (to be published).

25. M. T. Chahine and R. Narasimha, "Evaluation of the Integral $\int_0^\infty v^n \exp[-(v-u)^2-x/v]dv$," California Institute of Technology, Jet Propulsion Laboratory, Technical Report Number 32-459 (1963).

26. D. R. Willis, "Linearized Couette Flow for Arbitrary Knudsen Number," *Kth Aero TN52*, Royal Institute of Technology, Stockholm, Sweden (1960).

27. L. Lees, "A Kinetic Theory Description of Rarefied Gases," Heat Transfer and Fluid Mechanics Symposium, UCLA (1959).

28. I. Estermann, "Techniques of Measurement in Rarefied Gases," *First International Symposium on Rarefied Gasdynamics*, edited by F. M. Devienne, Pergamon Press (1960).

29. M. Knudsen, "Die Gesetze der Molekularströmung und der inneren Reibungsströmung der Gasedurch Röhren," *Annalen der Physik 28*, 75 (1909).

30. W. Gaede, "Die Äussere Reibung der Gase," *Annalen der Physik 41*, 289 (1913).

31. R. E. H. Rasmussen, "Über die Strömung von Gasen in engen Kanälen," *Annalen der Physik 29*, 665 (1937).

32. W. Dong, *Vacuum Flow of Gases Through Channels with Circular, Annular, and Rectangular Cross Sections*, University of California, Ph.D. Thesis (1956).

33. K. Takao, "Rarefied Gas Flow Between Two Parallel Plates," in *Second International Symposium on Rarefied Gas Dynamics*, 465, edited by Talbot, Academic Press, Inc., New York (1961).

34. S. Ziering, "Plane Poiseuille Flow," in *Second International Symposium on Rarefied Gas Dynamics*, 451, edited by Talbot, Academic Press, Inc., New York (1961).

35. C. Cercignani, "Plane Poiseuille Flow and Knudsen Minimum Effect," in *Third International Symposium on Rarefied Gasdynamics*, 92, edited by Laurmann, Academic Press, Inc., New York (1963).

36. H. Schlichting, *Boundary Layer Theory*, McGraw-Hill Book Company, Inc., New York, Fourth Edition (1962).

37. G. G. O'Brien, M. A. Hyman, and S. Kaplan, "A Study of the Numerical Solution of Partial Differential Equations," *Journal of Mathematics and Physics, 29*, 223 (1951).

38. G. G. Stokes, "On the Effect of the Internal Friction of Fluids on the Motion of Pendulums," *Cambridge Philosophical Transactions IX*, 8 (1851); *Math. and Phys. Papers III*, 1, Cambridge (1901).

39. E. P. Gross and E. A. Jackson, "Kinetic Theory of the Impulsive Motion of an Infinite Plane," *Physics of Fluids, 1*, 318 (1958).

40. R. V. Churchill, *Operational Mathematics*, McGraw-Hill Book Company, New York (1958).

VITA

Don Peyton Giddens was born on October 24, 1940 in Augusta, Georgia. He attended the elementary and secondary schools of that city and was graduated from the Academy of Richmond County in 1958.

In September of 1958 he entered the Georgia Institute of Technology as a student on the co-operative plan. Industrial periods during this time were spent at the Lockheed-Georgia Company in Marietta, Georgia. He received the Bachelor of Aerospace Engineering degree in June, 1963, and was graduated with highest honors at the head of the aerospace engineering class.

He continued his education at the Georgia Institute of Technology as a graduate student in September, 1963, and received an NDEA fellowship to study under the doctoral program. The degree of Master of Science in Aerospace Engineering was awarded in June, 1965. He is a member of Sigma Gamma Tau, Tau Beta Pi, Phi Kappa Phi, and Sigma Xi, and was selected to appear in *Who's Who Among Students in American Colleges and Universities* in the 1963-64 edition. He is co-author of a paper presented at the Fifth International Symposium on Rarefied Gasdynamics on July 4, 1966.

On November 5, 1958 he married the former Ann Hyatt of Augusta; and they have three children, Karen Lynne, Kimberly Ann, and Don Peyton, Jr.